AD _____

Award Number: W81XWH-11-1-0836

TITLE: Technologies for Hemostasis and Stabilization of the Acute Traumatic Wound

PRINCIPAL INVESTIGATOR: Carlson, Mark A.

CONTRACTING ORGANIZATION: University of Nebraska
Omaha, NE 68198-6810

REPORT DATE: October 2013

TYPE OF REPORT: Annual Report

PREPARED FOR: U.S. Army Medical Research and Materiel Command
Fort Detrick, Maryland 21702-5012

DISTRIBUTION STATEMENT: Approved for Public Release;
Distribution Unlimited

The views, opinions and/or findings contained in this report are those of the author(s) and should not be construed as an official Department of the Army position, policy or decision unless so designated by other documentation.

REPORT DOCUMENTATION PAGE

Form Approved
OMB No. 0704-0188

1. REPORT DATE	2. REPORT TYPE	3. DATES COVERED
October-2013	Annual	26September2012–26September2013

4. TITLE AND SUBTITLE
Technologies for Hemostasis and Stabilization of the Acute Traumatic Wound

5a. CONTRACT NUMBER
W81XWH-11-1-0836

5b. GRANT NUMBER
W81XWH-11-1-0836

5c. PROGRAM ELEMENT NUMBER

5d. PROJECT NUMBER

5e. TASK NUMBER

5f. WORK UNIT NUMBER

6. AUTHOR(S)
Carlson Mark A.,
Velander, William H.
Larsen, Gustavo
Nuñez, Luis
Burgess, Wilson H.
E-Mail: macarlso@unmc.edu

7. PERFORMING ORGANIZATION NAME(S) AND ADDRESS(ES)

AND ADDRESS(ES)

University of Nebraska
98735 Nebraska Medical Center
Omaha, NE 68198-6810

8. PERFORMING ORGANIZATION REPORT NUMBER

9. SPONSORING/ MONITORING AGENCY NAME(S) AND ADDRESS(ES)
U.S. Army Medical Research and Materiel Command
Fort Detrick, Maryland 21702-5012

10. SPONSOR/MONITOR'S ACRONYM(S)

11. SPONSOR/MONITOR'S REPORT NUMBER(S)

12. DISTRIBUTION/ AVAILABILITY STATEMENT
Approved for Public Release; Distribution Unlimited

13. SUPPLEMENTARY NOTES

14. ABSTRACT

The purpose of this research is to advance hemostasis technology, and to develop effective hemostatic devices for two difficult types of hemorrhage: (1) traumatic noncompressible (also known as truncal) hemorrhage; and (2) traumatic hemorrhage in the cold coagulopathic subject. The scope of this research will include both military and civilian trauma victims, particularly those suffering from hemorrhagic truncal injury and/or coagulopathic hemorrhage, from both penetrating and blunt mechanism. During the second (Y2) year of this project, we continued to generate stocks of two vitally important clotting factors (fibrinogen and Factor XIII), which we need for the development and manufacture of our hemostatic devices. In addition, we further developed prototypical methods to deliver foaming technology for the treatment of noncompressible hemorrhage. We also generated a reliable model for noncompressible torso hemorrhage. Importantly, we have continued to develop our single and dual foam technologies to treat noncompressible hemorrhage. In Y3 we will continue to perform extensive testing of these technologies.

15. SUBJECT TERMS
Trauma, hemorrhage, hemostasis, liver injury, biologics, clotting factors, biomaterial, bandage, wound, noncompressible, incompressible

16. SECURITY CLASSIFICATION OF:			17. LIMITATION OF ABSTRACT	18. NUMBER OF PAGES	19a. NAME OF RESPONSIBLE PERSON
a. REPORT	b. ABSTRACT	c. THIS PAGE			USAMRMC
U	U	U	UU	110	19b. TELEPHONE NUMBER *(include area code)*

Table of Contents

INTRODUCTION

Project Title: Technologies for Hemostasis and Stabilization of the Acute Traumatic Wound

The subject of this research project is the treatment of hemorrhagic in two difficult clinical scenarios: (1) traumatic noncompressible (also known as truncal) hemorrhage; and (2) traumatic hemorrhage in the cold coagulopathic subject. The purpose of this research is to advance the technology of hemostasis, and to use preclinical large animal models to test hemostatic technologies on the two difficult types of hemorrhage named above. The scope of this research will include both military and civilian trauma victims, particularly those suffering from hemorrhagic truncal injury and/or coagulopathic hemorrhage, from both penetrating and blunt mechanism. In addition, the technologies under development in this research should be useful in nontrauma surgical procedures, both elective and emergency, in which solid organ, coagulopathic, and/or noncompressible hemorrhage might occur.

BODY

The description of the work performed during the past year will be organized according to the Tasks delineated in the project's Statement of Work (SoW), which has been reproduced in the Appendix A. For a timeline of Task execution, refer to the Gantt chart in Appendix B. For a list of acronyms used in this report, see Appendix G.

Task 1: Purification/generation of pd-FI and rFXIIIA2-a.

During the last year of funding we have continued to purify multi-gram quantities of fibrinogen from human plasma for use in the foam studies. We use two different methods. Both start with a re-suspended cryoprecipitate of the plasma. The majority is further purified by EtOH precipitation of the solvent detergent treated cryo-supernatant. The resulting product has a protein profile and in vitro clotting properties typical of commercial preparations of fibrin sealant.

The second method utilizes ammonium sulfate to precipitate fibrinogen from the solvent detergent treated re-suspended cryoprecipitate. The resulting product contains what appears to be a one to one complex of fibrinogen and fibronectin. This observation was confirmed by size-exclusion chromatography. The complex exhibits enhanced clot strength at reduced concentrations and enhanced binding of exogenous cells. The result indicates it is possible to develop a more efficacious fibrin sealant for hemostasis and wound repair (refer to Appendices F and N).

We also have continued to produce rFXIIIA2-a in quantities sufficient to continue research and development according to methods established in the Year 1 Annual Report. Three kilograms of recombinant FXIIIA2-a yeast wet cell paste were processed with a yield of 1-2 g of rFXIIIA2-a.

Task 2: Generation of ultrafine particles for tamponade carrier foam.

Work on this task has been performed during this reporting second year. It was determined that the use of polymer ultrafine particles is beneficial for the stability of foams when they are added to the optimized liquid foaming formulation. However, mixing of these foams with the stream of blood from a severe injury compromises the foam structure and strength by dilution, washing away the foam and eventually causing its premature collapse. For this reason, formulations leading to firm foams have been explored instead (see Task 7). Ultrafine particles manufactured so far may be added to such formulations to further improve foam sturdiness.

While LNK retained and continued to research this particular matter, special emphasis, as determined by team consensus, was placed on foam formulation and delivery device and manufacturing equipment improvement (see Tasks 3, 5, and 7).

Task 3: Testing of candidate tamponade carrier & FS foams.

Exploring formulations containing gelling agents instead of particles. At the start of the research during this second year, it was noted that the use of particles did not prevent a collapse of the foam after 60 minutes. In order to keep the structural integrity of the foam, studies involving the

addition of alginic acid sodium salt (alginate) to the foaming precursor solution and subsequently contacting the foam with a $CaCl_2$ solution to create a hardened gel structure were performed. More detailed results are presented in Task 7 section.

Fibrin Sealant. Levels of pd-FI and rFXIIIA2-a were raised to 21.9 mg/ml pd-FI and 0.72 mg/ml rFXIIIA2-a from 9 mg/ml pd-FI and 0.36 mg/ml rFXIIIA2-a to investigate foam composition as part of task 3. The increased strength of the additional materials was demonstrated with TEG (Fig. 1). *In vivo* efficacy testing of this new formulation is pending.

Task 4: Testing of single foams in swine (tamponade carrier & FS foams separately).

Initial efficacy testing. Testing of single foam constructed from calcium alginate was tested in ten swine using the noncompressible injury model (see Appendix H for a description of the model). Sample datasheets and images from these subjects are shown in Appendix L. The outcomes of these ten subjects are shown in Table 1.

Table 1. Results of swine (N = 10) with noncompressible injury treated with single foam agent (calcium alginate).

Swine no.	Survival at 1 hr	Survival duration (min)	Blood loss (mL)	Final MAP (mm Hg)
143	no	27	2909	10
144	no	34	3416	10
147	yes	60	3064	21
148	no	26	3725	10
153	yes	60	3061	31
154	yes	60	633	90
157	yes	60	782	93
158	no	38	3525	10
173	yes	60	1558	52
185	yes	60	1980	39

Survival at 1 hour was 60% (6 of 10), but in four of the surviving subjects, the final MAP was ~50 or less (i.e., these animals may not have survived much beyond the 1 h observation period). The other two surviving subjects did quite well, with blood loss < 1 L and final MAP ≥ 90. We will continue to engineer the calcium alginate foam to improve efficacy and address the issues described below.

Embolism. In several subjects placed through the noncompressible injury protocol (Appendix H), there was evidence of central venous or cardiac embolism with or without foam (Fig. 2; Fig 3; Appendix L, pp. 5, 9, 10;). Given the size of the hepatic vein laceration made in these subjects (Figure 4), the occurrence of cardiac embolism would not be unexpected. In order to minimize the chance of a foam embolism, we have stopped directing the tip of the foam applicator toward the injury, but instead have directed the tip into the right colic gutter. With this technique, we have not seen any further foam emboli in the heart.

Calcium alginate foam toxicity. We have observed an apparent toxic effect of the calcium alginate that is injected into the abdomen (Fig. 5-12). This toxic effect presumably is related to free calcium left in the calcium alginate solution after the foaming process has completed (another candidate source of toxicity is the Tween detergent). We have been engineering the foam formulation and the delivery device to minimize the amount of free calcium (and Tween) that can diffuse onto the intestines and other intraabdominal organs after foam treatment. If we ultimately are not successful in removing the toxicity from the calcium alginate foam formulation, then we will pursue an alternative foaming mechanism.

In vivo alginate foam stability. One issue that presented itself with the single-foam calcium alginate treatments was the volume of foam retrieved after the 60 min observation period typically was several hundred mL, and not the several liter volume that was expected (see Fig. 13-15). The calculated *in* vivo foam stability (volume of foam removed from abdomen after 60 min ÷ initial volume of foam injected) for the calcium alginate formulations has been in the range of 10-15%. A more desired 1 h stability would be in the range of 50-60%. We will continue to engineer the foam treatment to ensure that the foam delivery will produce a several liter volume that will persist throughout the 60 min observation period (see Tasks 3, 5, and 7).

Task 5: Development & engineering of dual foam candidate devices.

Candidate Devices. Three versions of the dual foam device were tested both *in vitro* and *in vivo* using both current candidate foams. These three device designs were results of iteration between the engineering team and the surgical team. *In vitro* testing of the prototype device revealed a homogenous mixture of the applied sealant on the surface of the carrier foam (Fig. 16). The *in vivo* testing of the prototype device showed that the dual foam remained at the site of application for the duration of the procedure (Fig. 17). This prototype device was replaced by the second generation device due to clotting found when the fibrin sealant components were mixed before application to the foam (Fig. 18). A new device was engineered containing a longer barrel in order to apply the dual foam directly to the wound site (Fig. 19A). This device was designed to apply the fibrin sealant components circumferential to the carrier foam (Fig. 19B) to avoid clotting in the device. A beveled tip was also added to the device in order to help mix the carrier foam and fibrin sealant (Fig. 19C). The application of the foam was relocated to an indirect placement in the abdominal cavity due to a foam clot entering the heart (Fig. 2). The second generation device has
been tested both *in vitro* and *in vivo* at indirect sites in the abdominal cavity without issue. The third generation device was engineered to apply alginate foam using a modified second generation device (Fig. 20). The device was encapsulated in Teflon to avoid contamination of the device and for facile cleaning and sterilization. *In vitro* testing revealed consistent coating of mixed substitute fibrin sealant (Fig. 21) components and fibrin sealant (Fig. 22) onto both candidate carrier foams. *In vivo* application was successful in applying the dual foam to the application site (Fig. 23)

Task 6: Testing of dual foam in swine.

Testing of an early iteration of dual foam (calcium alginate foam + fibrin sealant foam;

please refer to Task 5) was begun in Y2. Three swine underwent a noncompressible injury followed by foam treatment; refer to Appendix L and Fig. tf28 for technical details, data, and images from these subjects. One subject died 33 min after injury with 3.5 L of blood loss and a large cardiac clot embolus. The other two subjects survived the 1 h observation period with a final MAP of ~50 and ~1.5 L of blood loss. As described under Task 4, the volume of foam retrieved at the end of observation was only several hundred mL, which was below the intended several L volume. We will continue to engineer the foam to address this problem, and obtain a foam with reasonable stability after a one hour intraabdominal incubation.

Task 7: Engineering of firm foams from alginate and alginate derivatives.

Alginate is a linear polymer comprised of two monomeric units, β -D-mannuronic acid and α -L-guluronic acid. The polymer strands are formed by joining these monomers at the C-1 and C-4 positions. It has been shown that the polymer chains are made up of three distinct regions or blocks: 1) G blocks containing only units derived from L-guluronic acid; 2) M blocks based entirely on D-mannuronic acid; and MG blocks consisting of alternating units from D-mannuronic acid and L-guluronic acid. Higher percent G-block alginate produces a more rigid and cohesive gel and foam structure in presence of calcium ions.

At the beginning of the research in the second year, alginate acquired from Sigma-Aldrich (A1112-1KG) with unspecified properties was used in the foam formulations. Two samples of sodium alginate were also acquired from FMC Biopolymer (Philadelphia, PA). In this case, sample one is a pharmaceutical grade sodium alginate with 60% to 70% G-block monomer content; sample two is a food grade sodium alginate with high viscosity and gel rigidity. Sample one was used to produce the new foam formulation.

A series of tests were performed to compare the viscosity of the FMC alginate to the previous one used in the foam formula using Sigma-Aldrich's alginate. A solution of 12% Sigma-Aldrich alginate in DI water despite high viscosity could still be poured into a mixing container (consistency of molasses) where as 8% FMC alginate in DI water formed a mixture viscous enough to have the consistency of set Jell-o gelatin. As a result a 5% workable mixture of FMC alginate in DI water was prepared to be used in the foam formulation. FMC alginate has a finer particle size and lighter color (pale yellow) in comparison to the Sigma-Aldrich alginate (color of honey).

A cream dispenser with a volume of 500 mL was used as a foaming device with some modifications. The original cream dispensing nozzle was replaced with a narrower nozzle in order to reduce the flow rate of the discharge. It was determined that a nozzle with a 1.78 mm orifice diameter is adequate to deliver the required flow rate of 4L of foam in ~ 90 seconds. For each discharge experiment the foaming solution was placed in the dispenser and, after securing the dispensing cap, the device was charged with liquid butane (Ronson butane refill canister, Zippo Manufacturing Corporation, USA) through the charging inlet on the cap. The device was shaken for 20 seconds to mix the liquid butane (propellant) with foaming solution. Before discharging the device, disposable syringes with a needle deliver aqueous solution of calcium chloride on the foam to produce the gel (Fig. 24).

A series of test were performed to examine the viability of the foaming process without the presence of the two other foam ingredients: Xanthan gum and Tween 20. Two foam formulations were prepared with one lacking Xanthan gum and the other lacking Tween 20 (the missing

ingredients were replaced with DI water). After using the two formulas in producing expanding foam it was concluded that the presence of Tween 20 is integral in the formation of expanding foam. However, Xanthan gum could be removed from the formulation without any adverse effect on the foaming process when using the FMC alginate.

A series of foam formulations were prepared with FMC alginate content ranging from 3.0% to 3.5% and 0.9% Tween 20 in DI water to examine flow characteristic through the dispensing nozzle. With 21 grams of butane as a propellant (this amount of propellant was used in all experiments), 3.1 % alginate content gave the best flow characteristic and most suitable dispensing time (1 minutes and 45 seconds).

The second most important factor controlling the rigidity of the final foam product after the molecular structure of alginate polymer is the amount of calcium available for the gelling process. Due to possible toxicity effect excess calcium produces when in contact with tissue, it was important to optimize the amount of calcium present to produce the desired foam integrity while minimizing the excess calcium.

A series of tests were performed to optimize the amount of calcium used in the gelling process when using FMC alginate. Foam formulation with 3.1% alginate content was mixed in the dispensing nozzle with calcium chloride solution of various concentration dispensed at 102 ml/min. In each test total of 180 ml of calcium chloride solution was used. The concentration of the calcium chloride solution was decreased from 2 M to 0.5 M and the rigidity of the foam was observed. A concentration of 0.6 M seemed to produce desired a desired rigidity while leaving very small amount of calcium unused. At concentrations below 0.6 M the final foam product was not rigid enough.

As a result of the experiments performed, the following composition was prepared for use in the swine surgery performed on 10-22-13: 186 mL of 5% (w/v) sodium alginate (FMC Biopolymer – Pharmaceutical grade with 60%-70% G-block content) in DI water (186 g), 43.5 mL of 6% (w/v) Tween 20 in DI water (44.4 g) and 70.5 mL of DI water were combined to form 300 mL of foaming solution. The final composition of the foaming solution is as follows: 3.1% sodium alginate and 0.87% Tween 20 in DI water.

The above formulation was mixed with 21 grams of butane and dispensed while mixing with a solution of calcium chloride in DI water with a concentration of 0.6M dispensed at a rate of 102 ml/min. in a laboratory setting the above produced ~5 liters of non-compressed foam. After mechanical stress, the foam volume was reduced to 800 ml (Fig. 25). The initial volume when dispensed into the abdominal cavity of the swine during the operation most likely is much less due to the pressure in the abdominal cavity (~19 mmHg). As a result, the final volume observed in the surgery was close to 500 ml.

Currently experiments are being performed to improve further foam rigidity and volume expansion.

Task 8: Testing of dual foam in swine noncompressible model (laparotomy with 2˚ closure).

In Y2Q1, some off-protocol studies in swine were performed in order to develop the open swine model of noncompressible hemorrhage (see Appendix H). As a result of these studies, a workable model of noncompressible torso hemorrhage was developed to address Aim 1 of this project (i.e., treatments of noncompressible torso hemorrhage); refer also to Tasks 4 and 6.

During Y2 we tested an early version of the dual foam, in which shaving-cream (Barbasol) based foam combined with clotting factors (various combinations of fibrinogen, thrombin, and Factor XIII) was used to treat hemorrhage in the noncompressible model that is described in Appendix H. Representative images from this preliminary testing is shown in Fig. 26-28. Results from the preliminary testing of the Barbasol-based FS dual foam are shown in Table 2.

Table 2. Results of swine (N = 12) with noncompressible injury treated with dual foam agent (Barbasol + FS).

Swine no.	Survival at 1 hr	Survival duration (min)	Blood loss (mL)	Final MAP (mm Hg)
115	No	31	3354	9
116	No	10	3239	8
117	No	10	3061	11
118	No	27	3710	9
119	No	8	2625	10
120	No	34	3957	8
121*	No	4	1990	12
122	Yes	70	4003	40
123	Yes	69	2583	24
124	No	40	3712	13
125	No	59	3666	10
126	No	8	2209	10

*Expiration from air/foam embolism to the heart.

The preliminary testing of this Barbasol-FS dual foam did not reveal any efficacy over the no-treatment controls. We will continue to engineer this dual-foam to improve efficacy.

Task 9: Delivery of candidate field-ready dual foam device.

This task has yet to start.

Task 10: Testing of dual foam in swine noncompressible model (closed penetrating wound).

This task has yet to start.

Task 11: Delivery of report on final recommended product description for dual foam device for treatment of noncompressible hemorrhage.

This task has yet to start.

Task 12: Delivery of resorbable bandage for final preclinical study in hypothermic coagulopathic model.

In Y2Q1, some off-protocol studies in swine were performed to obtain preliminary efficacy data on bandage configurations (see Appendix J). In Y2Q2, continued off-protocol work was performed to address the bandage adhesion issue (please see Appendix K). These appendices describe an unexpected difficulty that was encountered in the work on Aim 2 of this award. The problem consisted of inadequate adhesion of our prototype fibrin sealant bandage to the wound surface (liver injury) in the hypothermic hemodiluted swine (refer to the Y2Q1 Quarterly Report for a background discussion). After multiple discussions among the investigators, we decided that we would need to pursue detailed study of adhesion at the bandage-wound interface. A crude example of such a study is shown in Appendix K (pp. 11, 16), in which a hand-held spring gage is measuring the force required to distract the bandage from the wounded liver surface. Our intention is to perform more sophisticated studies of adhesion of the biologic-based bandage to *ex vivo* porcine liver using a high-sensitivity tensiometer. In order to do this, we have applied for DURIP funding from the DoD to obtain a tensiometer appropriate for our purpose. The DURIP application (Appendix M) contains a detailed discussion of the adhesion issue that we would like to address. If the DURIP application is funded, then we will proceed with bandage-wound adhesion studies during Y3.

Task 13: Delivery of fibrin sealant for final preclinical study in hypothermic coagulopathic model.

We will continue to generate fibrin sealant so that Tasks 12, 14, and 15 can be completed.

Task 14: Final preclinical study of resorbable bandage for the hypothermic coagulopathic model (swine).

Numerous animal studies were done in support of this Task during Y2, but these were off-protocol (see Task 12). Prior to initiating the final preclinical study of the resorbable fibrin sealant bandage in the hypothermic coagulopathic model, we will need to engineer a bandage that will have adequate adherence to the injured liver surface (see Task 12 and Appendix M).

Task 15: Delivery of report on final recommended product description for resorbable fibrin sealant bandage for treatment of compressible coagulopathic hemorrhage.

The task has yet to start.

KEY RESEARCH ACCOMPLISHMENTS

Below is a list of key research accomplishments from this past year's work:

1. Purification of pdFI from plasma and synthesis/purification of recombinant human FXIII from yeast.

2. Development of a noncompressible model of hemorrhage.

3. Identification and subsequent avoidance of cardiac embolism in the noncompressible model of hemorrhage.

4. Development of delivery system for the calcium alginate foam (a single foam formulation).

5. Development of delivery system for the calcium alginate-fibrin sealant foam (a dual foam formulation).

6. Development of delivery system for the Barbasol-fibrin sealant foam (a dual foam formulation).

7. Preliminary data on use of the three foams specified in 2-4 above in the noncompressible model of hemorrhage.

8. Identification and subsequent reduction (not elimination) of toxicity from the calcium alginate foam formulations.

9. Improvement in the *in vivo* stability of the calcium alginate foam formulation.

10. Identification of bandage adhesion problem in Aim 2, and submission of DURIP proposal (for a tensiometer) as the solution.

REPORTABLE OUTCOMES

Provide a list of reportable outcomes that have resulted from this research to include:

- manuscripts, abstracts, presentations;
- licenses applied for and/or issued;
- degrees obtained that are supported by this award;
- development of cell lines, tissue or serum repositories;
- informatics such as databases and animal models, etc.;
- funding applied for based on work supported by this award;
- employment or research opportunities applied for and/or received based on experience/training supported by this award

[Above copied from:
https://mrmc.amedd.army.mil/index.cfm?pageid=researcher_resources.technical_reporting]

1. Manuscript published in *Biomacromolecules* (Appendix C). This work was done prior to this award, but constitutes a large portion of preliminary data on which this award depends.

2. Manuscript accepted for publication in *J Surg Res* (Appendix D). This work was done off protocol, but represent important characterizations of the fibrin sealant utilized in this award.

3. Manuscript in preparation that describes the development of the noncompressible model of hemorrhage (Appendix H) in detail, for submission to *J Surg Res*.

4. Abstract accepted for presentation at the 2014 Academic Surgical Congress (San Diego CA, February 2014; Appendix E). This contribution describes the noncompressible model.

5. Abstract accepted for presentation at the 2013 Biomedical Engineering Society meeting (San Antonio TX, October 2013: Appendices F and N). This work was done off protocol, but is relevant to the interaction of recombinant fibrin sealant with wound surfaces.

6. Application for a 2013 Defense University Research Instrumentation Program (DURIP; Appendix M) to obtain a tensiometer for bandage-wound adhesion studies, relevant to Aim 2 of this award.

In addition to the above, Drs. Carlson (UNMC) and Nuñez (LNK) have been proceeding with the Phase I Program from the Department of Economic Development of the State of Nebraska for a separate (**not** funded by the DoD) but related project entitled "Hemostatic Patch," which studied elective surgical applications for the synthetic resorbable mesh devices. This program has been funded at $100,000 for the first year. Starting in late 2012, we began a comparative study with a synthetic resorbable mesh *vs.* a commercially-available product (Surgicel®). To date, the comparison has demonstrated favorable results. Survival toxicity studies will be completed by December 2013. We have initiated conversations with the state to proceed to the Phase II option ($400,000 of funding), to begin at the end of the Phase I period.

CONCLUSIONS

This overall goal of this project is to develop hemostatic technology for two severe clinical scenarios: (1) noncompressible (truncal) hemorrhage, which is the topic of Aim 1 of the original proposal; and (2) solid organ hemorrhage in a cold coagulopathic subject, which is the topic of Aim 2. Conclusions drawn from the work during the first year of this project are as follows:

1. Biologic materials have been produced in sufficient quantities to continue research and development.

2. A porcine noncompressible model of torso hemorrhage involving a hepatic laceration with open technique can produce a lethal and reproducible endpoint.

3. Our studies of the dual foam technology have produced a device capable of delivering a liquid fibrin sealant coated carrier foam into the abdominal cavity of a swine.

4. The dual foam technology minimizes the amount and therefore the cost of the biologics delivered in a closed cavity wound application.

5. Continued engineering of the foam carrier technology is needed to increase efficacy of the foam treatments in the noncompressible model.

6. The bandage-wound adhesion phenomenon in the hypothermic hemodiluted porcine subject will need extensive *ex vivo* study in order to develop an efficacious bandage whose efficacy does not depend on gram quantities of fibrinogen.

The relevance of studying hemostatic devices in the treatment of hemorrhage in the two scenarios described above is in this project is that both noncompressible and coagulopathic hemorrhage remain difficult clinical problems. Noncompressible truncal hemorrhage in particular is emerging as the leading cause of preventable hemorrhagic death in the injured warfighter (1), and coagulopathic hemorrhage remains a perennial problem (2) with imperfect solutions that is faced by surgeons during emergency and elective procedures, in both military and civilian environments.

REFERENCES

1. Kelly JF, Ritenour AE, McLaughlin DF, Bagg KA, Apodaca AN, Mallak CT, et al. Injury severity and causes of death from Operation Iraqi Freedom and Operation Enduring Freedom: 2003-2004 versus 2006. *J Trauma*. 2008 Feb;64(2 Suppl):S21-6; discussion S6-7.

2. Holcomb JB, Jenkins D, Rhee P, Johannigman J, Mahoney P, Mehta S, et al. Damage control resuscitation: directly addressing the early coagulopathy of trauma. *J Trauma*. 2007 Feb;62(2):307-10.

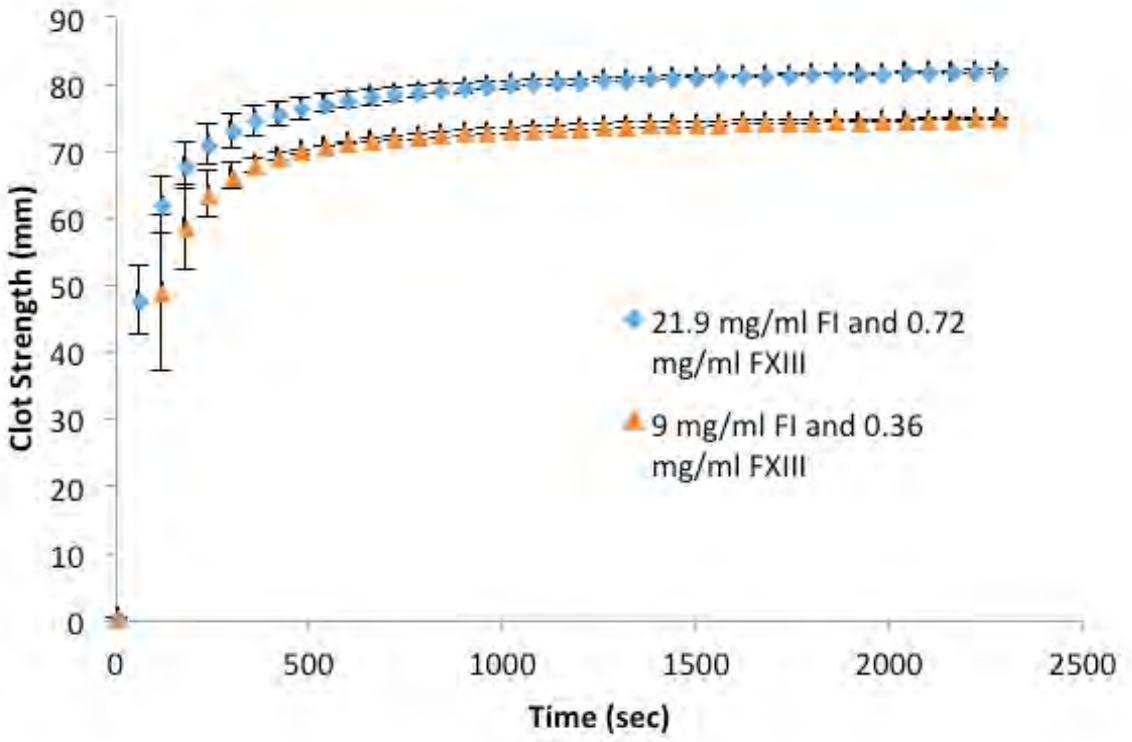

Figure 1. Thromboelastographic, quality control analysis of fibrin sealant formulation made this past funding year. The Fibrinogen made by ethanol (EtOH) formulated at 9 mg/mL FI, 0.36 mg/ml rFXIIIA2-a, and 106 U/mL rFIIa and also 21.9 mg/mL FI, 0.72 mg/ml rFXIIIA2-a, and 106 U/mL rFIIa.

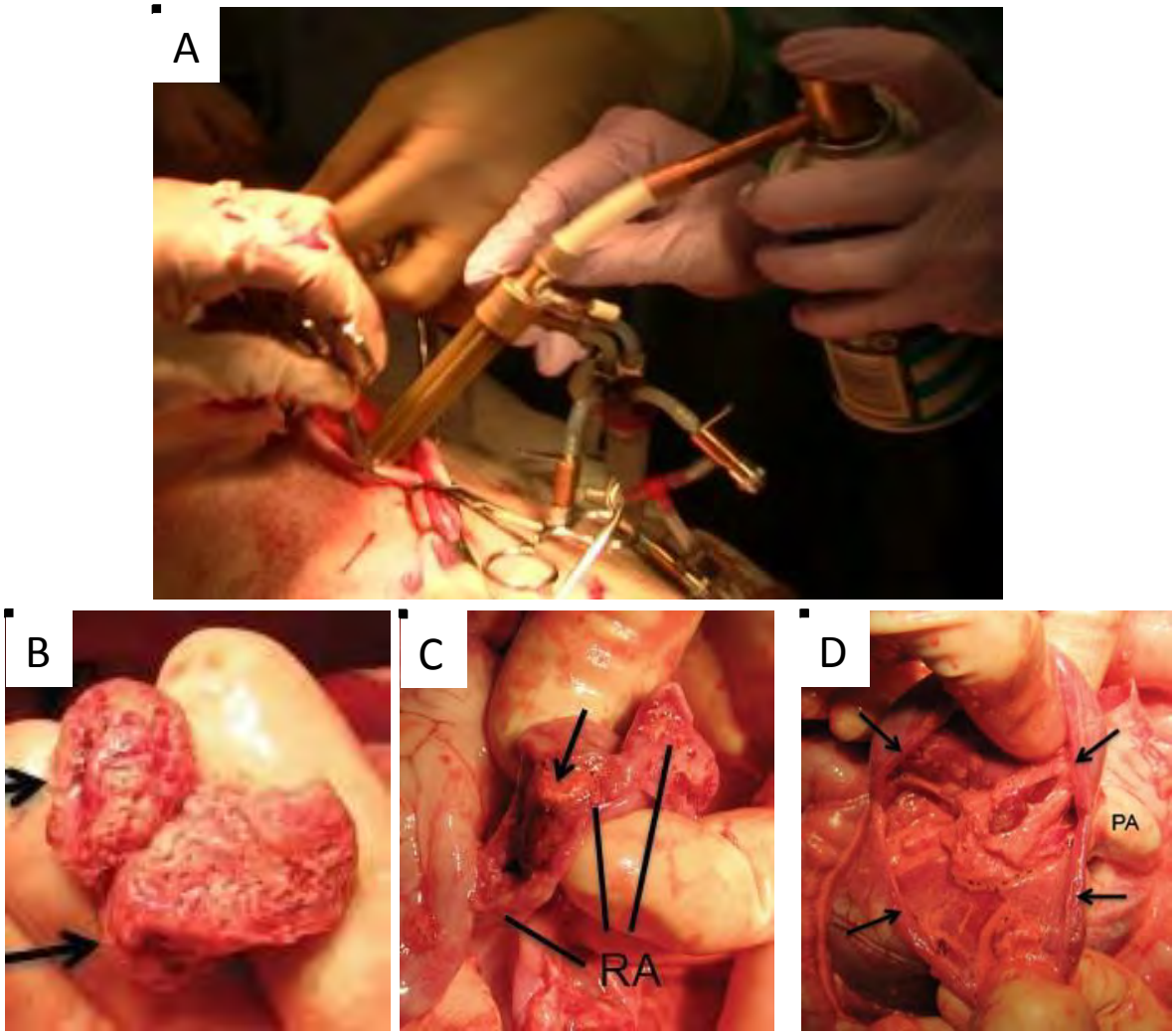

Figure 2. *In vivo* testing of the 2nd generation dual foam device. (A) Application of FS and carrier foam to a swine liver injury model. Foam clot entered the IVC (B), right atrium (C) and right ventricle (D) of the heart.

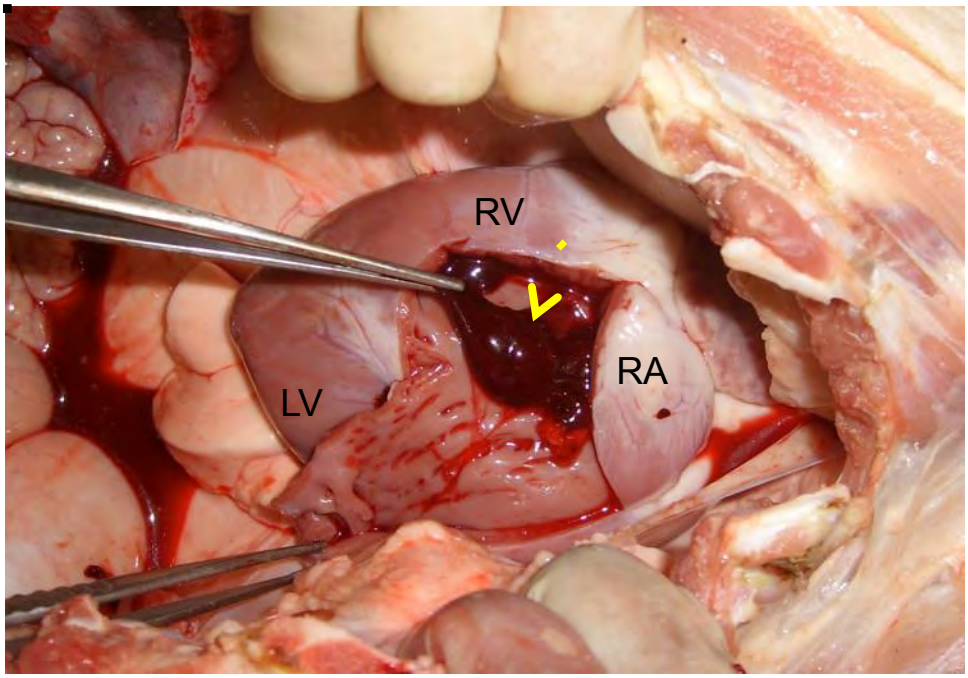

Figure 3. Swine 158. Examination of heart *in situ* at postmortem. The right ventricle (RV) has been opened along its anterior surface. There was a large red clot (arrow; extraction with forceps) without foam present in the RV. Cephalad is to the right. LV = left ventricle; RA = right atrium.

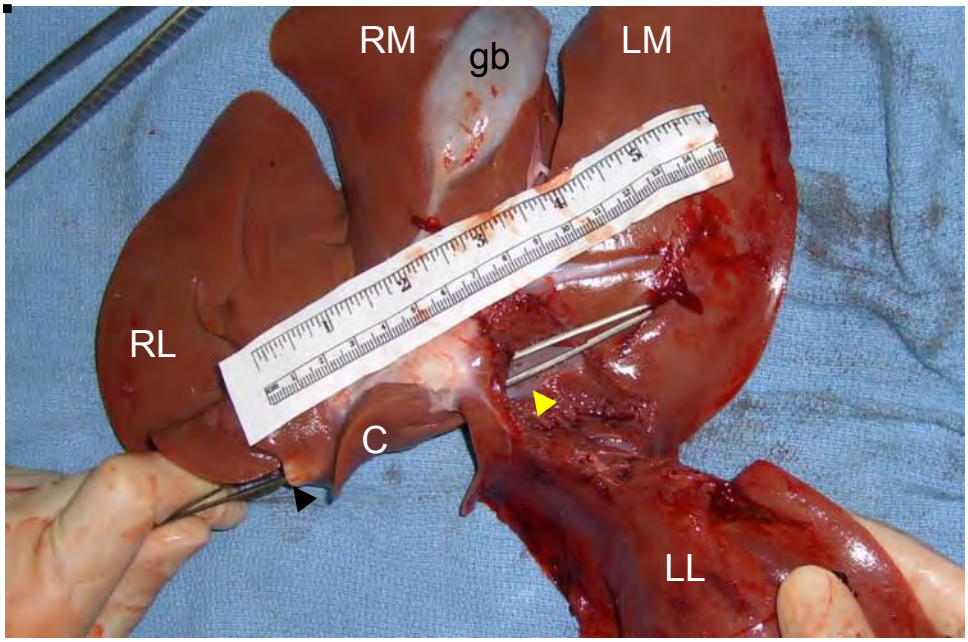

Figure 4. Swine 158. Liver ex vivo (inferior aspect). Standard injury was made at base of LL lobe. C = caudate lobe; RL = right lateral lobe; RM = right medial lobe; LM = left medial lobe; LL = left lateral lobe; gb = gallbladder. Forceps have been inserted through the infrahepatic IVC (black arrow) and have emerged out the base of the LL, indicating a hemitransection of the intrahepatic IVC (yellow arrow).

Figure 5, swine 168. Overhead view of the swine abdomen after a 1 h incubation with calcium alginate foam. The foam was injected with the closed abdominal technique (see Appendix L). The abdomen remained closed during the 1 h incubation period, and then was reopened. The foam was evacuated, and the intraabdominal organs were inspected. The intestines were diffusely dusky (i.e., purplish).

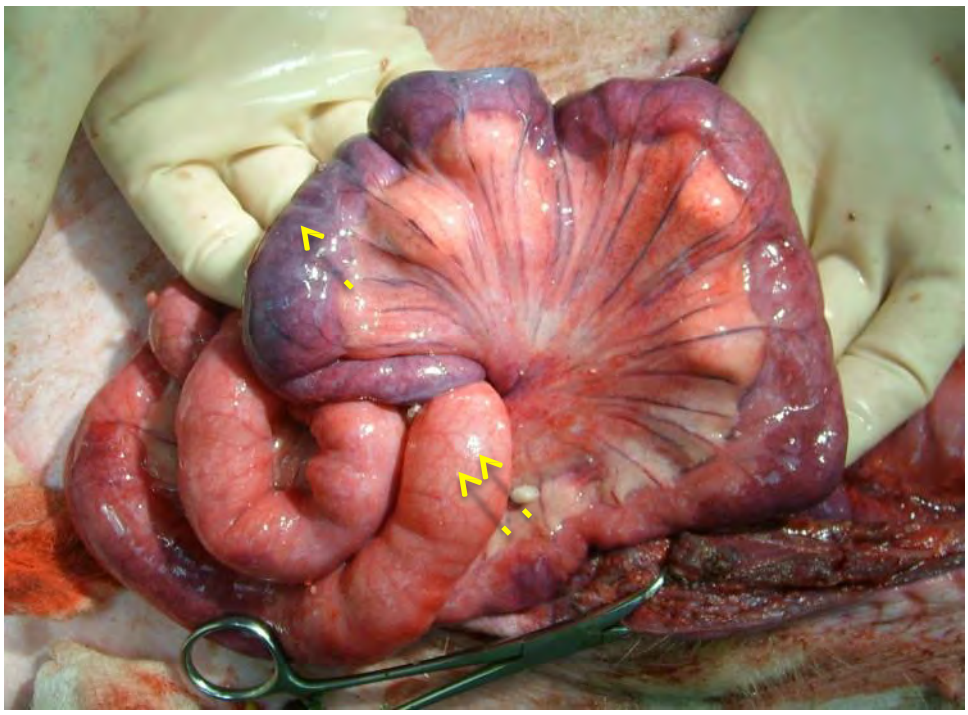

Figure 6, swine 168. Loops of small bowel from Fig. 5, showing a dusky-ischemic looking zone (single arrow) and a normal-appearing zone (double arrow).

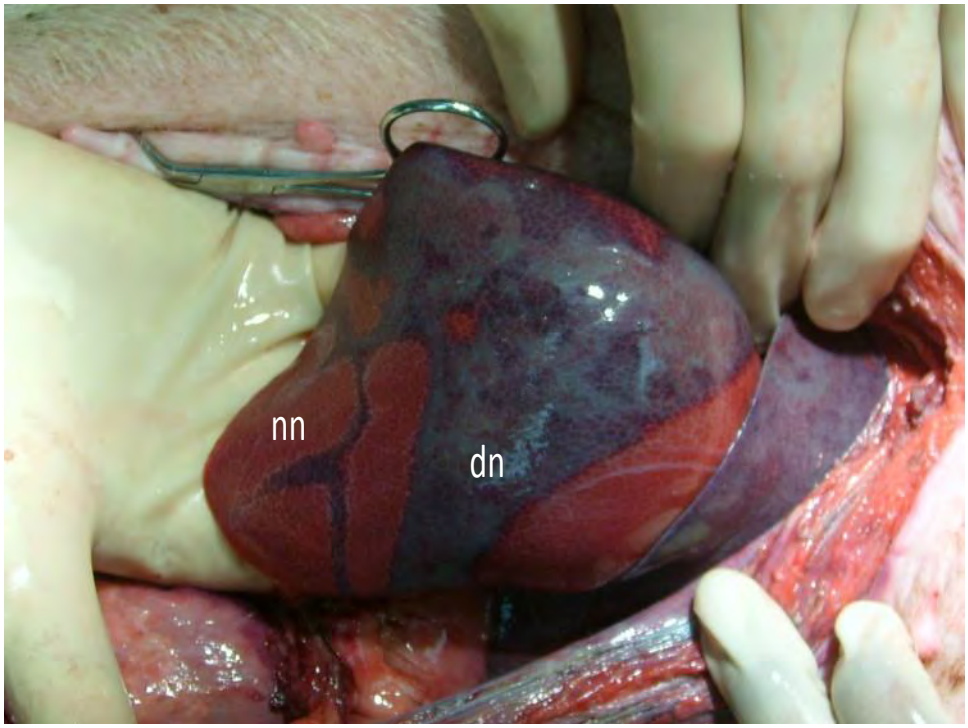

Figure 7, swine 168. Liver from from Fig. 5, showing sharply demarcated areas of darker color (duskiness, d) distinct from more normal (n) colored regions, an effect apparently produced from loops of bowel draped over the lobe.

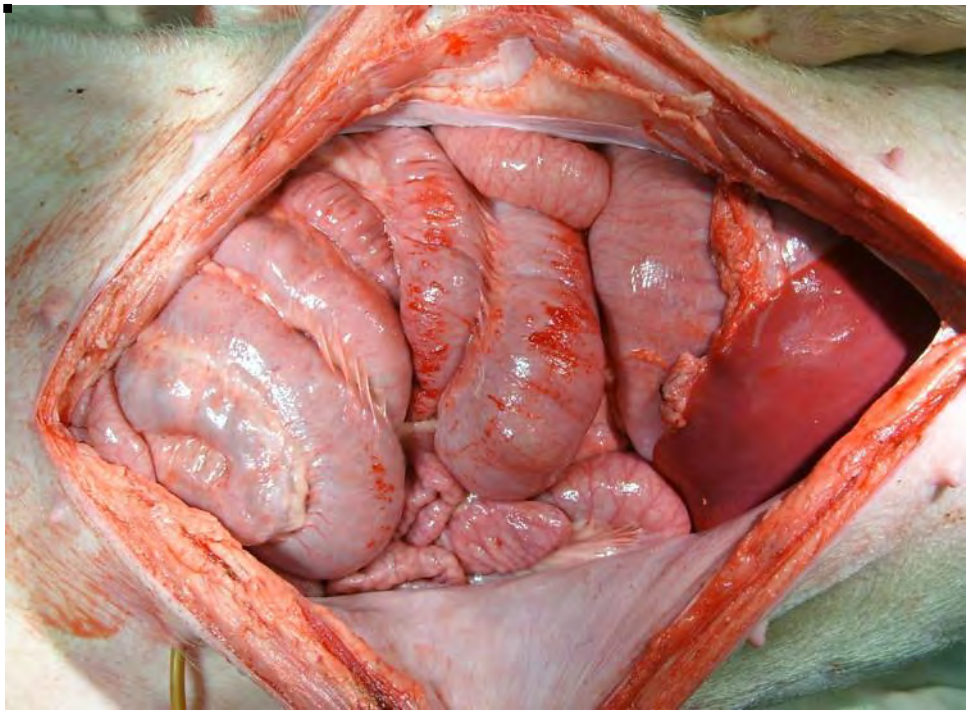

Figure 8, swine 170. Overhead view of the abdomen immediately prior to injection of foam. Midline incision is stretched open to show intraabdominal organs. Image taken to demonstrate normal appearance of intestines at beginning of procedure. Cephalad is to the right.

Figure 9, swine 170. Overhead view of the abdomen after observation period & removal of foam. Intestines that were in contact with the foam are diffusely dusky (i.e., purplish); compare with Figure 8. Cephalad is to the right.

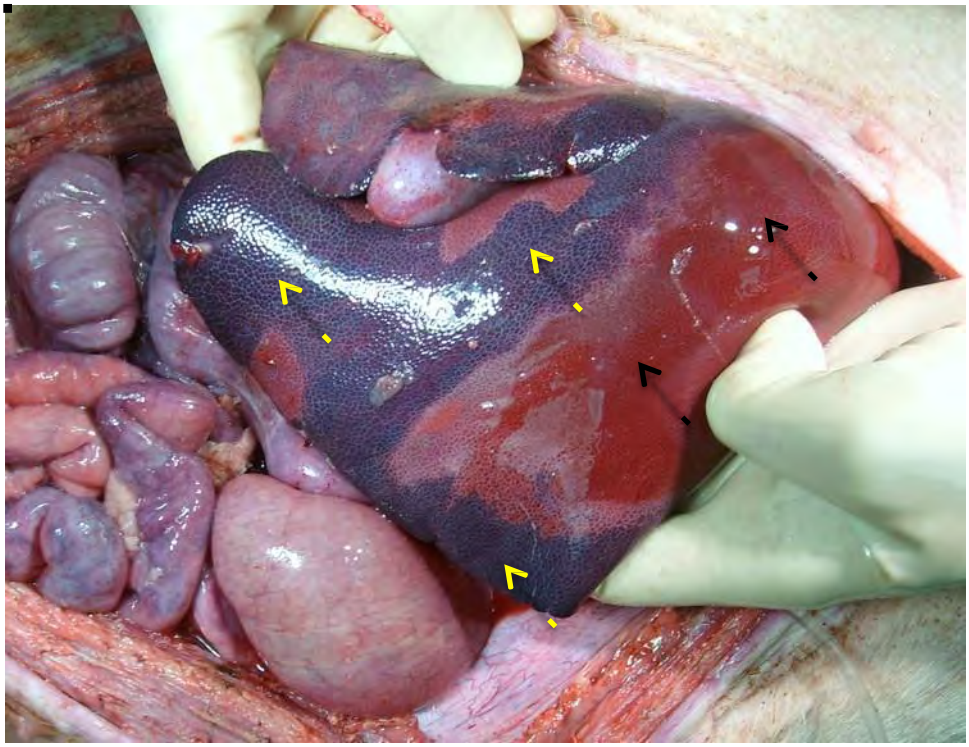

Figure 10, swine 170. Close up view of the liver from Figure 9. Yellow arrows indicate surface that was in direct contact with the foam; black arrows indicate surface not in contact with foam.

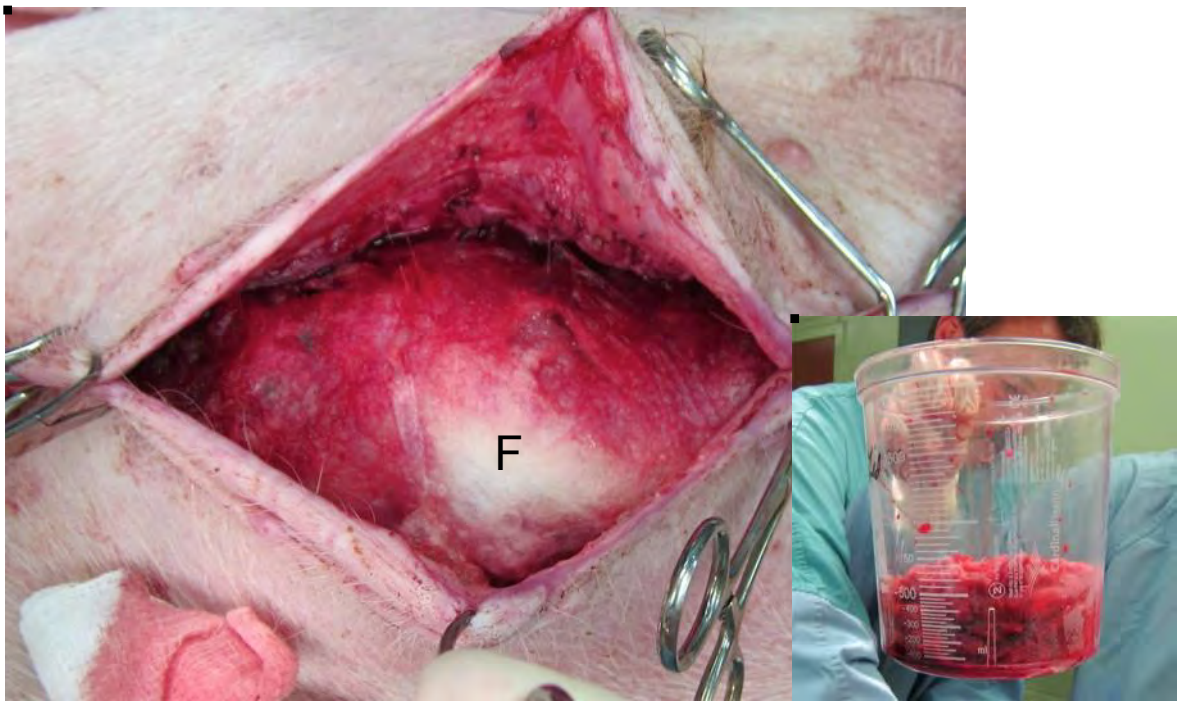

Figure 11, swine 185. Overhead view of the abdomen immediately after 1 hr observation period; swine survived. Midline incision reopened; foam (F) shown within abdomen (final volume removed ~500 mL; see inset). Cephalad is to the left.

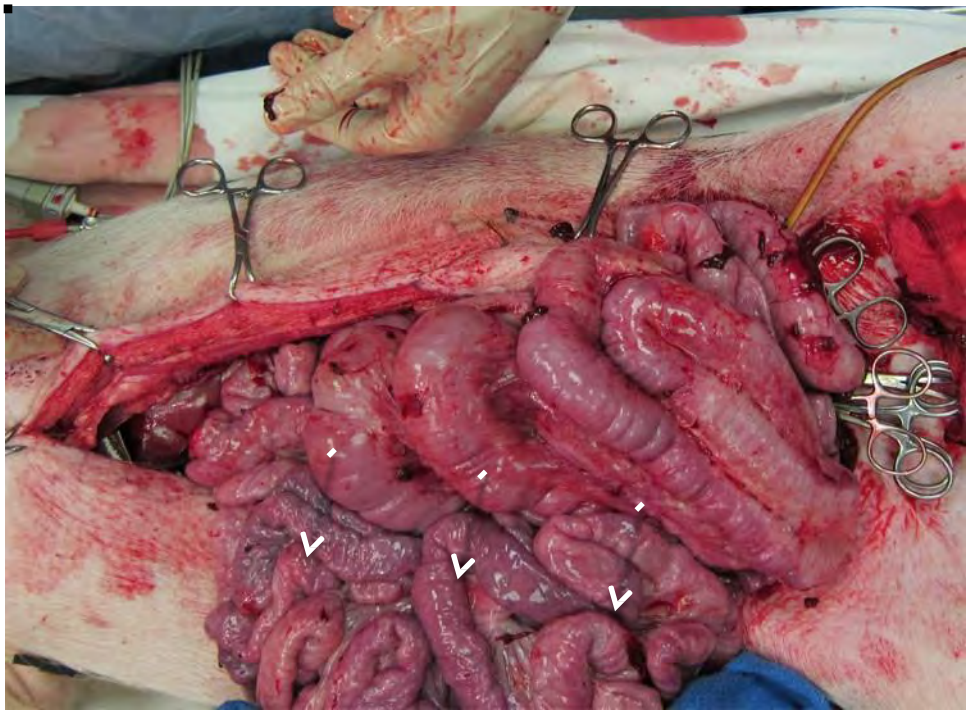

Figure 12, swine 185. Overhead view of the abdomen after observation period & removal of foam/ blood. The intestines appear somewhat dusky (arrows) Cephalad is to the left.

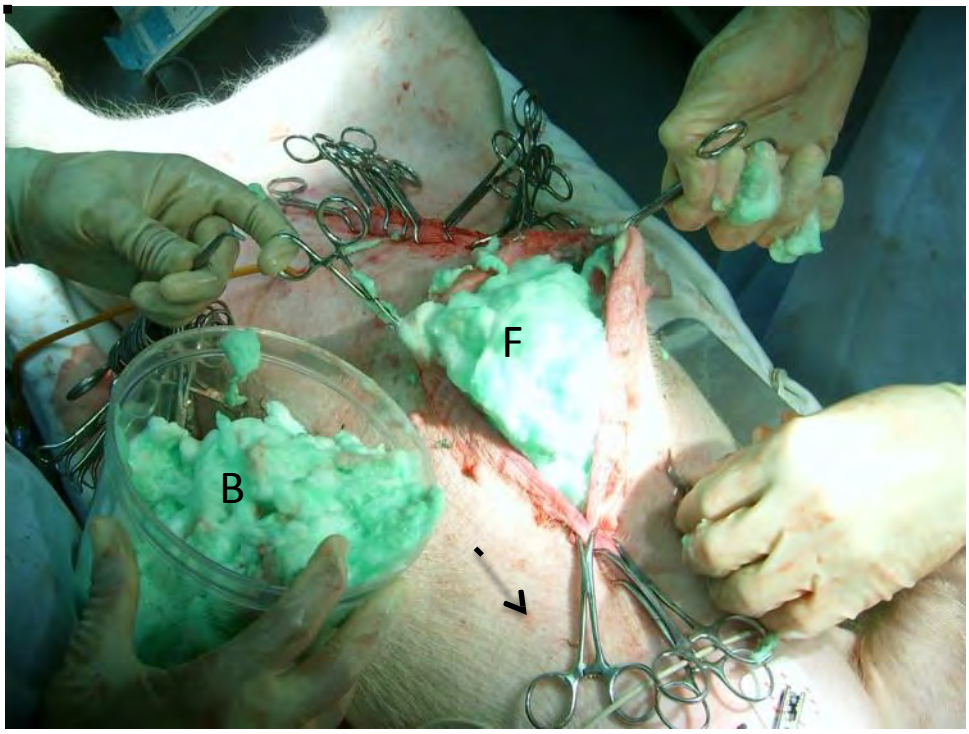

Figure 13, swine 168. Manual extraction of foam immediately after foam injection (actually about 1 min after injection of foam completed). Midline incision was closed with towel clips during the injection, and is now partially re-opened to allow egress of greenish-tinged foam (F), which then is being placed into the beaker (B) for volume measurement. Arrow = cephalad.

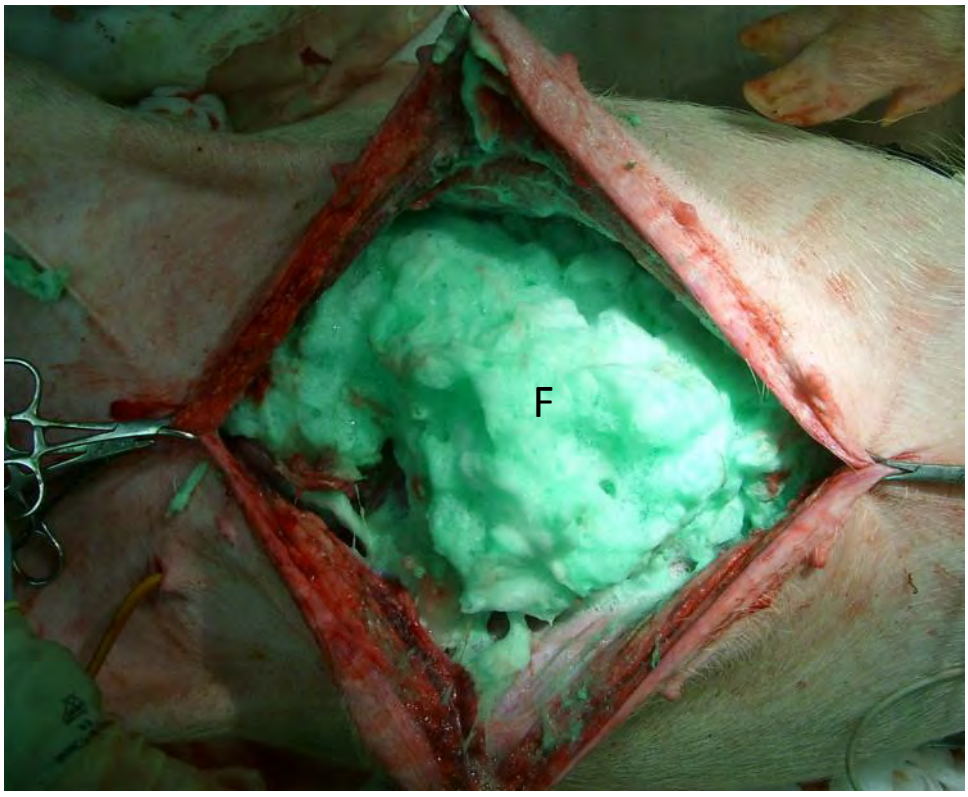

Figure 14, Swine 168. Same time point as in Fig. 13. Overhead view of incision, showing the foam (F) covering the intestines. Cephalad is to the right.

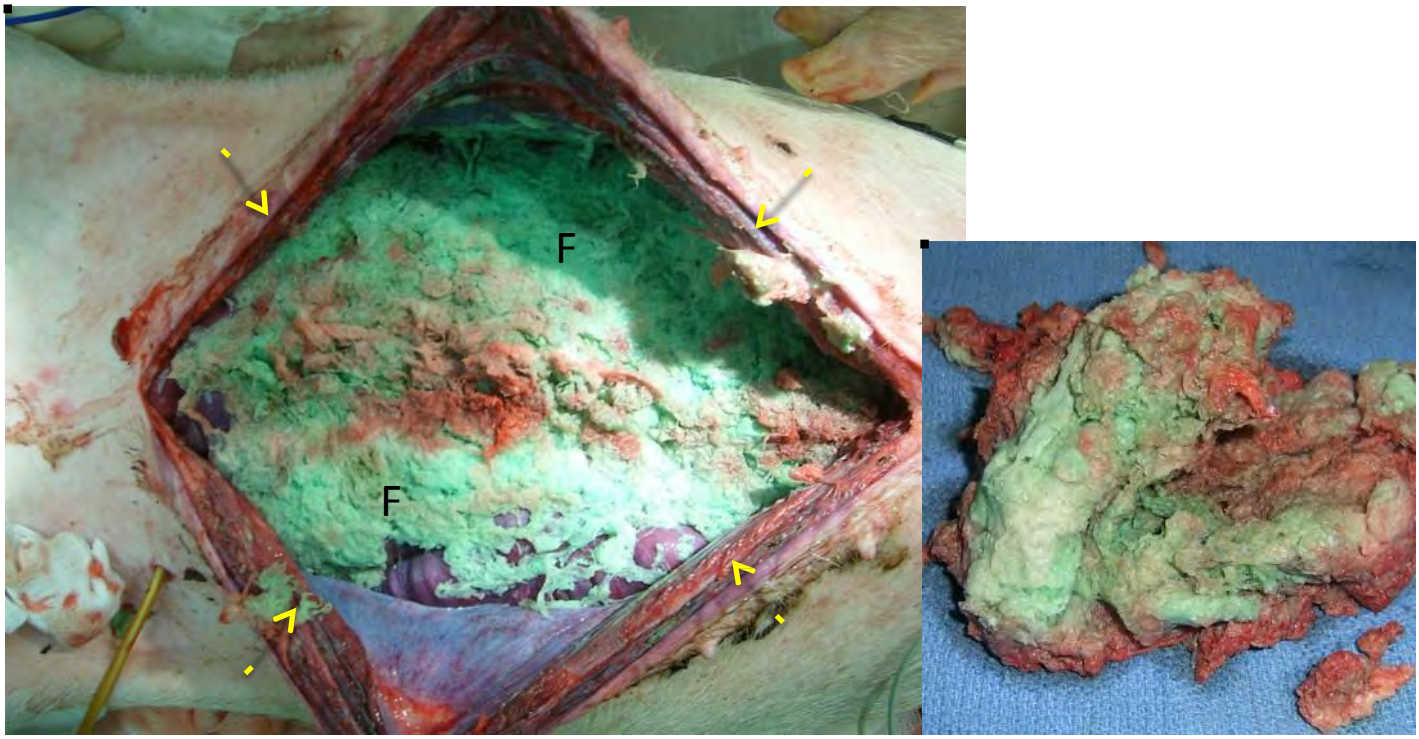

Figure 15, swine 168. Overhead view of the abdomen re-opened immediately after completion of 60 min observation period. Cephalad is to the right. Arrows = margin of incision, stretched open. F = calcium alginate foam (with color dye) covering the intestines. Inset: all foam after removal.

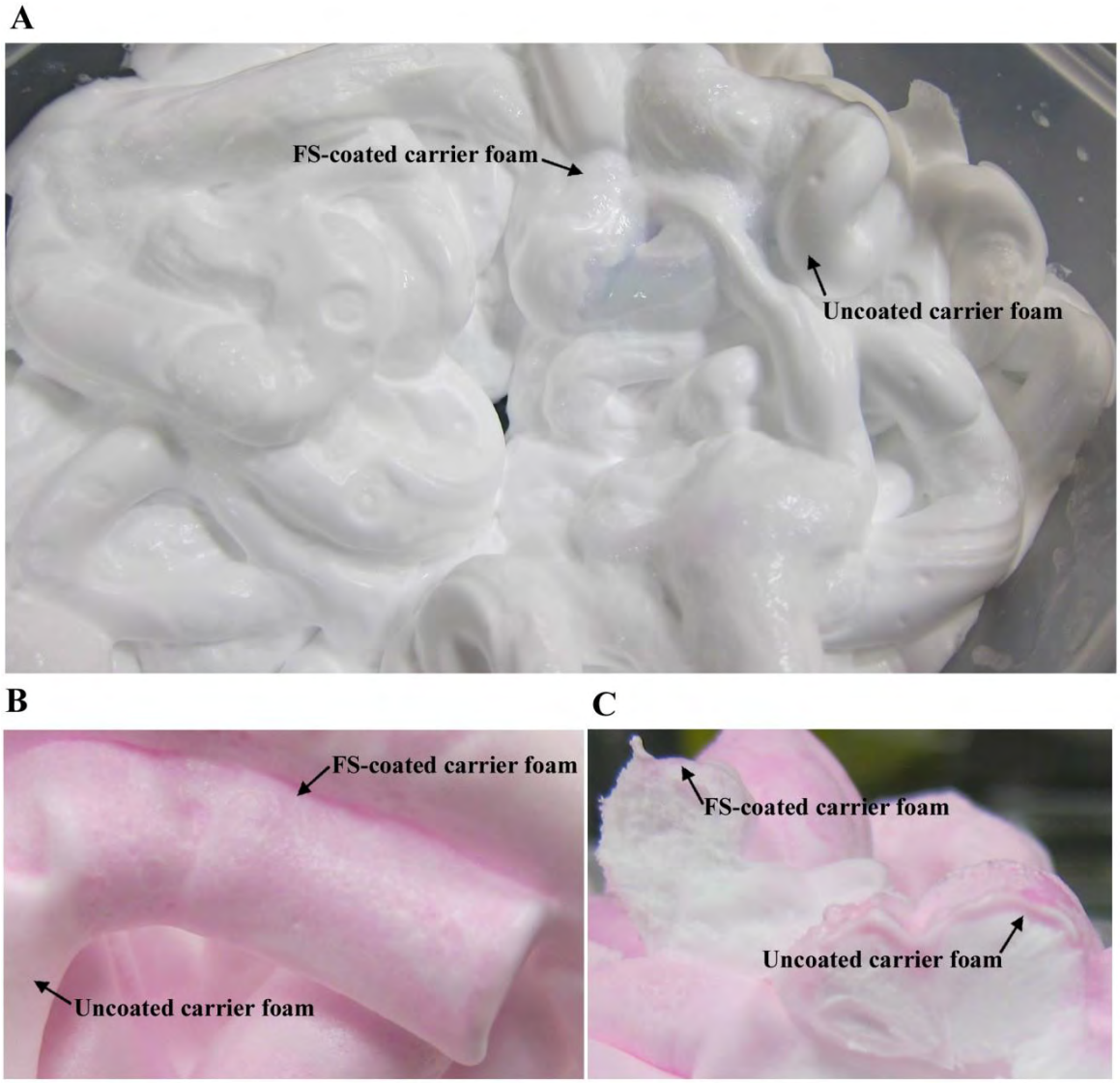

Figure 16. Images of foamed FS and carrier foam. (A) Foamed FS (rough, uneven texture with a shiny finish) coating carrier foam (seen as smooth texture with a matte finish). (B) Close-up of foamed FS (dark pink bubbles) and carrier foam (smooth light pink surface) dyed pink. (C) Cross-section of foamed FS and carrier foam after dying the external foam surface pink. Note that the dye does not absorb into the carrier foam when coated with FS.

Figure 17. *In vivo* application FS and carrier foam into a swine abdomen.

Figure 18. Clots formed by the FS components within the prototype application nozzle.

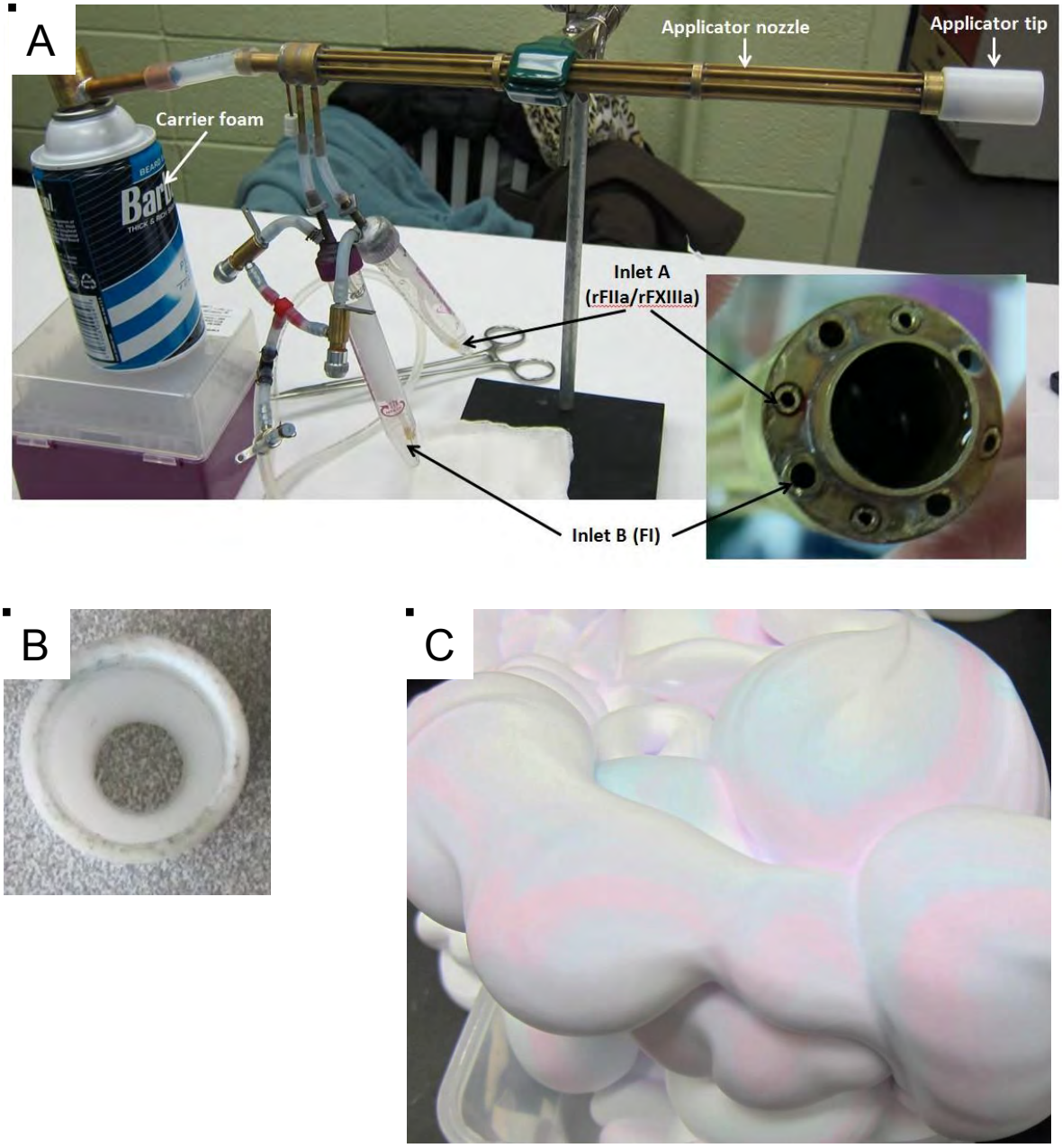

Figure 19. (A) 2nd generation dual foam device that was redesigned to circumferentially apply FS to the carrier foam, eliminate clots within the device and deliver the FS/foam to the wound surface. (B) Beveled applicator tip. (C) *In vitro* testing of the 2nd generation dual foam device with red and blue substitute FS components and the beveled applicator tip which displayed an application pattern of the red and blue FS substitutes on the white carrier foam.

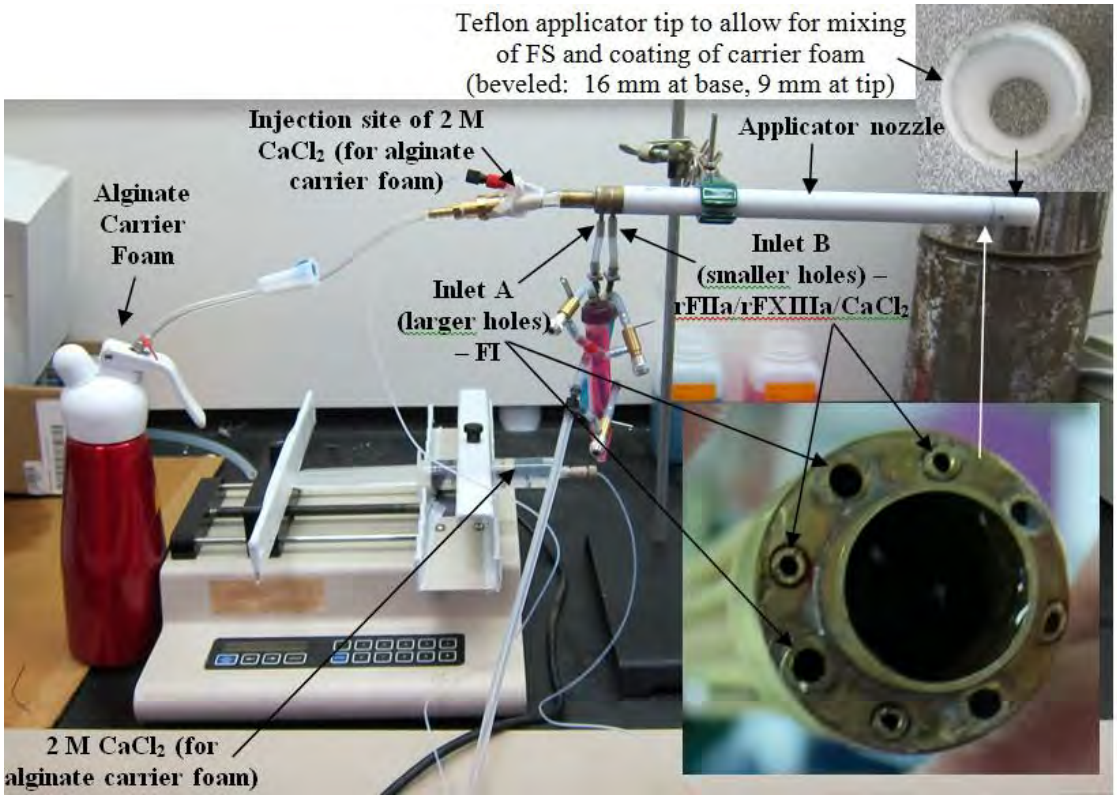

Figure 20. 3rd generation dual foam device that was redesigned to circumferentially apply FS to the alginate carrier foam and deliver the FS/foam to the wound surface. The redesign provides a facile and nonabrasive Teflon outer sleeve to minimize tissue damage during the insertion of the foam delivery device.

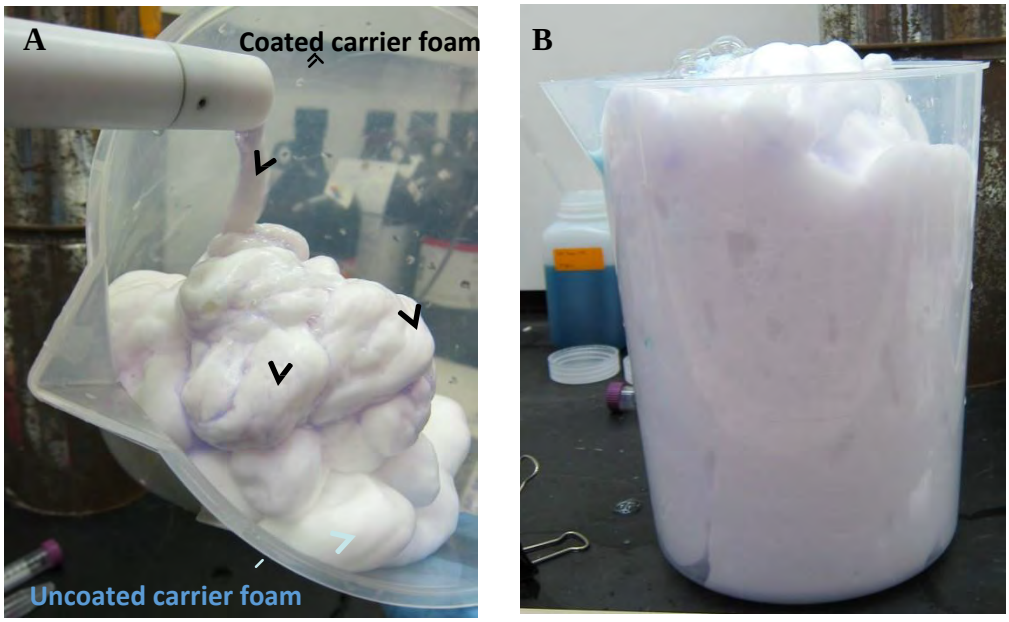

Figure 21. *In vitro* testing of fluid mixing phenomenon in the 3rd generation dual foam device with red and blue substitute FS components. (A) Carrier foam circumferentially coated by FS substitutes during application. The red and blue dyed FS substitutes mixed to make purple coating on the white carrier foam. (B) Final volume (4.5 L) of FS substitute coated carrier foam after application.

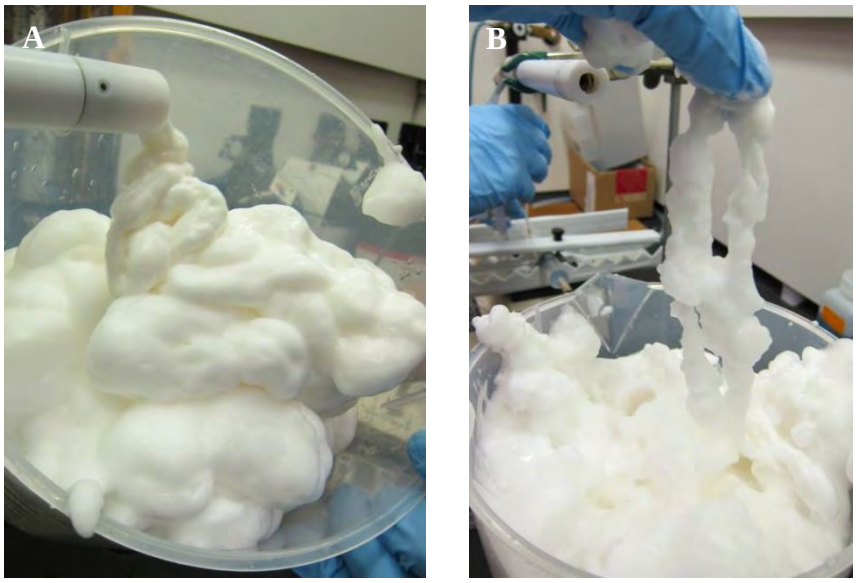

Figure 22. *In vitro* testing of fluid mixing phenomenon in the 3rd generation dual foam device with actual FS components. (A) Carrier foam circumferentially coated by FS substitutes during application. (B) Strings of FS clot in foam.

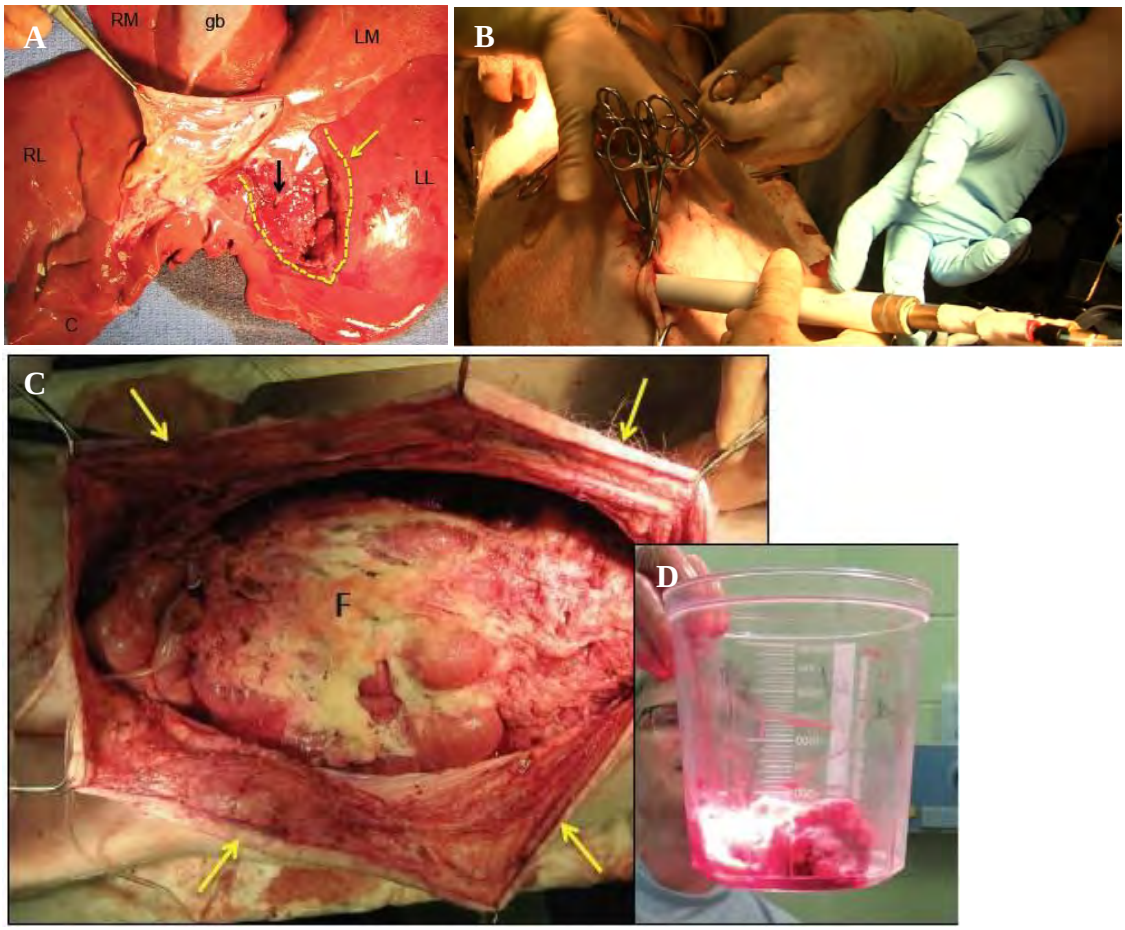

Figure 23. *In vivo* testing of the 3rd generation dual foam device in noncompressible surgical wound model. (A) Standard liver injury (dotted yellow line) made at the base of the left lateral lobe (LL) of the liver. C = caudate lobe; RL = right lateral lobe; RM = right medial lobe; LM = left medial lobe; gb = gallbladder; yellow arrow = approximate location where large portal vein branch to LL should have been (missing in this subject). (B) Application of FS coated carrier foam. (C) Overhead view of the abdomen re-opened immediately after completion of 60 min observation period; subject alive and well. Cephalad is to the right. Arrows = margin of incision, stretched open. F = calcium alginate foam coated with FS covering the intestines. (D) Total amount of foam removed from abdomen (~200 mL).

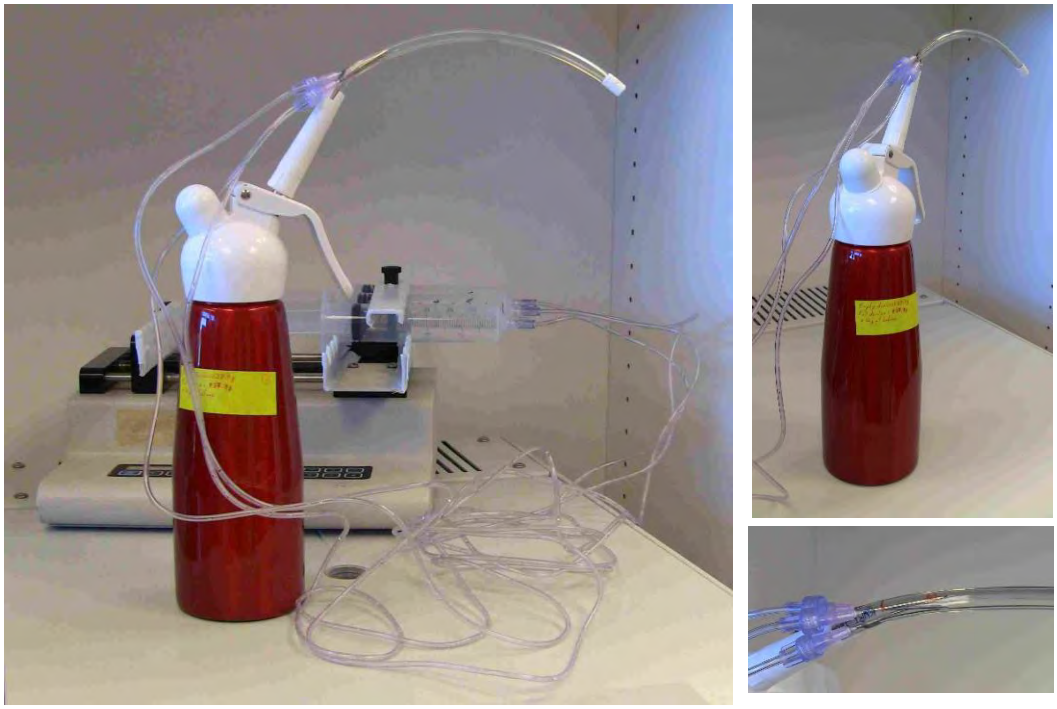

Figure 24. Foaming and delivery device.

Figure 25. Alginate foam as produced (left) and after mechanical stress (right).

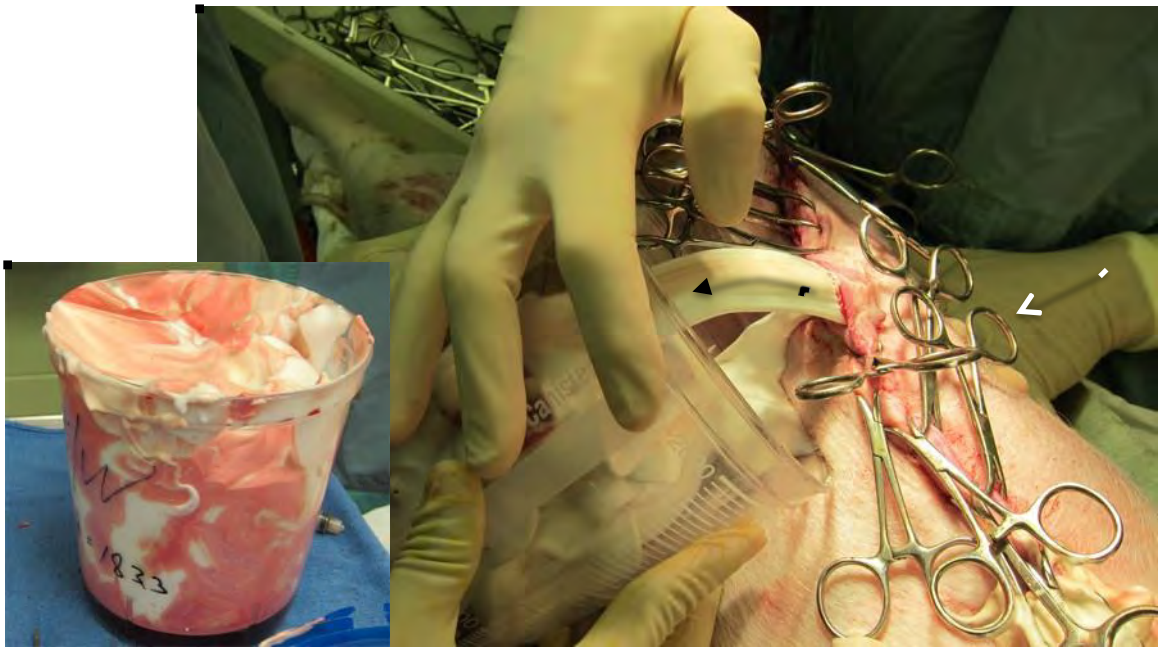

Figure 26, swine 186. Oblique view of abdomen just after expiration. Cephalad is to the lower right. Two clips have been removed from the center of the midline incision. A hand is pushing into the abdomen on the right side (white arrow). This pressure is ejecting a stream of Barbasol foam (black arrow) from the abdomen, through the gap between the clips, and into the bucket. Note absence of blood in the foam. Inset: ejected foam in bucket. Toward the end of the stream, some nonclotted blood mixed with foam (pinkish foam) emerged, giving the swirled appearance.

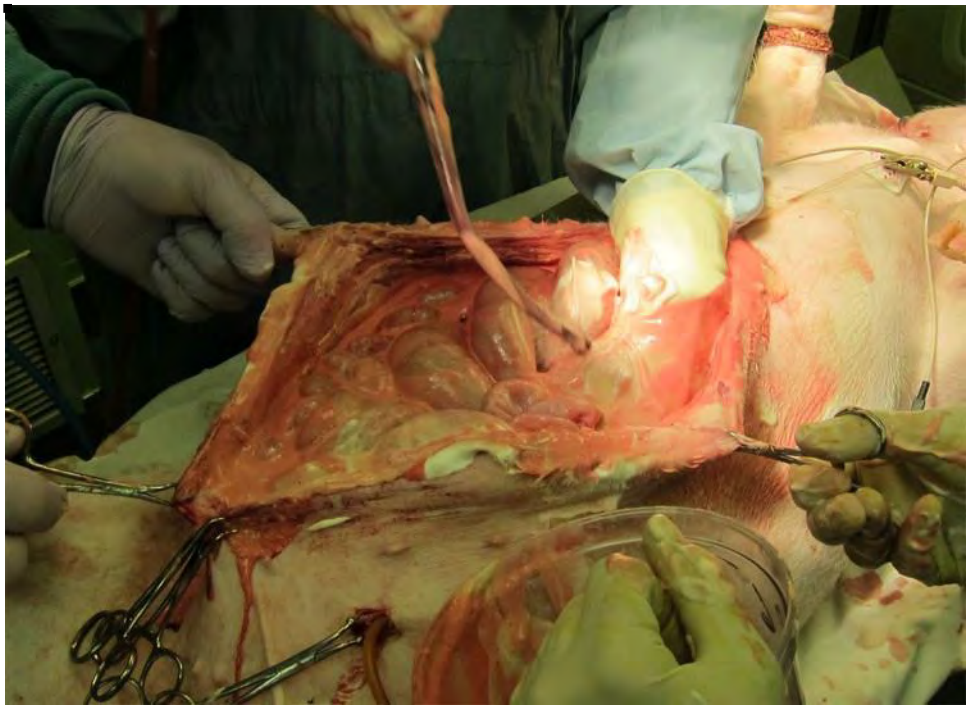

Figure 27, swine 186. Post-expiration. The midline incision has been re-opened. Most of foam has been removed, leaving a “soup” of foam mixed with nonclotted blood that was bathing the intestines. Cephalad is to the upper right.

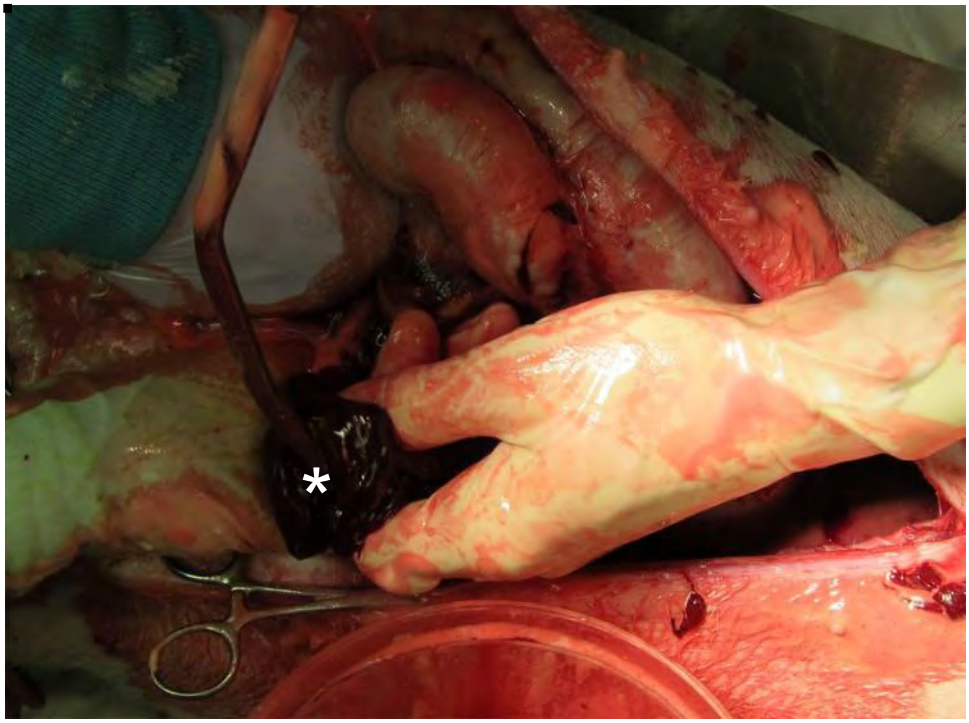

Figure 28, swine 186. View of the abdomen with incision re-opened. After “soup” in Figure 27 was evacuated, some pure red clots (*) not mixed with foam were removed from deep recesses of the abdomen mostly in the subdiaphragmatic regions, in the subhepatic space, and intermingled with the intestines. Cephalad is to the right.

LIST OF APPENDICES

2013 Annual Report, Award Number: W81XWH-11-1-0836

Item	Description
A	Statement of Work (SoW)
B	Gantt chart
C	*Biomacromolecules* 2013;14:169-178
D	*J Surg Res* accepted 26 Sep, 2013 (proofs)
E	2014 Academic Surgical Congress (ASC) abstract
F	2013 Biomedical Engineering Society (BMES) abstract
G	Acronyms
H	Model of noncompressible hemorrhage
J	Preliminary data with the hypothermic hemodilutional laceration model
K	Preliminary data with the hepatic planar resection model
L	Supplementary information with foam treatment in the noncompressible model
M	DURIP application for a tensiometer
N	Poster for the 2013 BMES meeting

Proposal Title: "Technologies for Hemostasis and Stabilization of the Acute Traumatic Wound"
USAMRMC No. 10091006
Contract No. W81XWH-11-1-0836
PI: Carlson, Mark A.
SOW version date: February 13, 2013

STATEMENT OF WORK

No.	Task description	Site	Year	Aim
1	Purification/generation of pd-FI and rFXIIIA2-a	UNL	1-3	1
2	Generation of ultrafine particles for tamponade carrier foam	LNK	1-3	1
3	Testing of candidate tamponade carrier & FS foams	LNK & UNL	1-2	1
4	Testing of single foams in swine (tamponade carrier & FS foams separately)	UNMC	2-3	1
5	Development & engineering of dual foam candidate devices	LNK & UNL	1-2	1
6	Testing of dual foam in swine	UNMC	2-3	1
7	Engineering of firm foams from alginate and alginate derivatives	LNK	2-3	1
8	Testing of dual foam in swine noncompressible model (laparotomy with 2˚ closure)	UNMC	3-4	1
9	Delivery of candidate field-ready dual foam device	UNL & LNK	3	1
10	Testing of dual foam in swine noncompressible model (closed penetrating wound)	UMM	3	1
11	Delivery of report on final recommended product description for dual foam device for treatment of noncompressible hemorrhage	LNK, UNL, UNMC, UMM	4	1
12	Delivery of resorbable bandage for final preclinical study in hypothermic coagulopathic model	LNK	1	2
13	Delivery of fibrin sealant for final preclinical study in hypothermic coagulopathic model	UNL	1	2
14	Final preclinical study of resorbable bandage in for hypothermic coagulopathic model (swine)	UNMC	1	2
15	Delivery of report on final recommended product description for resorbable fibrin sealant bandage for treatment of compressible coagulopathic hemorrhage	LNK, UNL, UNMC	2	2

Project Title: “Technologies for Hemostasis and Stabilization of the Acute Traumatic Wound”
Award Number: W81XWH-11-1-0836
Grant Number: 10091006
PI: Carlson, Mark A.
Reporting period: 09-27-2012 to 09-26-2013 (Y2 Annual Report)

Appendix B. Gantt Chart (current year in boldface). See Appendix A for definitions of Tasks.

Task	Y1Q1	Y1Q2	Y1Q3	Y1Q4	**Y2Q1**	**Y2Q2**	**Y2Q3**	**Y2Q4**	Y3Q1	Y3Q2	Y3Q3	Y3Q4	Y4Q1	Y4Q2	Y4Q3	Y4Q4	Status
1																	On schedule
2																	On schedule
3																	On schedule
4																	Delayed
5																	On schedule
6																	Delayed
7																	Delayed
8																	Yet to start
9																	Yet to start
10																	Yet to start
11																	Yet to start
12																	On schedule
13																	On schedule
14																	On schedule
15																	Yet to start

Key

- Task completed
- Task on schedule & active
- Task delayed
- Anticipated span of delayed task
- Task yet to start

Article

pubs.acs.org/Biomac

Recombinant Human Fibrinogen That Produces Thick Fibrin Fibers with Increased Wound Adhesion and Clot Density

Jennifer Calcaterra,[†] Kevin E. Van Cott,[†] Stephen P. Butler,[‡] Geun Cheol Gil,[†] Marta Germano,[§] Harrie A. van Veen,[§] Kay Nelson,[§] Erik J. Forsberg,[∥] Mark A. Carlson,[⊥] and William H. Velander*[,†]

[†]Department of Chemical and Biomolecular Engineering, University of Nebraska, Lincoln, Nebraska 68588-0643, United States

[‡]Department of Biochemistry, Virginia Polytechnic Institute and State University, Blacksburg, Virginia 24061, United States

[§]Pharming Group NV, Leiden, Netherlands 2300 AL

[∥]WiCell Research Institute (formerly Infigen, Inc., DeForest, WI), Madison, Wisconsin 53707-7365, United States

[⊥]Department of Surgery, University of Nebraska Medical Center and the Omaha VA Medical Center, Omaha, Nebraska 68105, United States

Supporting Information

ABSTRACT: Human fibrinogen is a biomaterial used in surgical tissue sealants, scaffolding for tissue engineering, and wound healing. Here we report on the post-translational structure and functionality of recombinant human FI (rFI) made at commodity levels in the milk of transgenic dairy cows. Relative to plasma-derived fibrinogen (pdFI), rFI predominately contained a simplified, neutral carbohydrate structure and >4-fold higher levels of the γ′-chain transcriptional variant that has been reported to bind thrombin and Factor XIII. In spite of these differences, rFI and pdFI were kinetically similar with respect to the thrombin-catalyzed formation of protofibrils and Factor XIIIa-mediated formation of cross-linked fibrin polymer. However, electron microscopy showed rFI produced fibrin with much thicker fibers with less branching than pdFI. In vivo studies in a swine liver transection model showed that, relative to pdFI, rFI made a denser, more strongly wound-adherent fibrin clot that more rapidly established hemostasis.

1. INTRODUCTION

Known as coagulation Factor I (FI), fibrinogen is a complex protein which polymerizes to form a wound adherent fibrin barrier that stops bleeding and acts as a scaffold for healing.[1−4] During the healing process, the fibrin clot is enzymatically digested and reabsorbed.[2,4] These characteristics make FI naturally useful as a biomaterial in surgical tissue sealants[5−7] and as an important tool in tissue engineering.[8−11] For decades, FI has been used in the treatment of hemorrhage incurred on battlefields, in civilian trauma,[12] and in surgical procedures.[13] The therapeutic transplantation of tissue made from autologous cells frequently uses a provisional matrix made of cross-linked fibrin to help culture and then deliver layers of cells into debrided wound sites.[10] Because of its role in making fibrin polymer, FI is a protein present at a high concentration of 2−4 g/L in human plasma,[14] and its clinical applications typically use large 0.1−2 g doses.[5] Unfortunately, a safe and abundant supply of plasma-derived FI (pdFI) is limited worldwide by the availability of pathogen-screened plasma.[15,16] Surgical applications for tissue sealants[13] in the United States indicate that FI would need to be manufactured at amounts greater than several metric tons per annum (Supporting Information, Table S1).

FI is a transcriptionally and post-translationally complex molecule. For example, after transcription of three separate genes, the human liver translates and assembles two Aα, two Bβ, and two γ-polypeptides into hexameric FI having a molecular weight of 340 kDa.[17,18] Assembly arises from the restrictive pooling of free chains within the endoplasmic reticulum prior to secretion as a holoprotein. In addition, there are two variations of the γ-chain. About 11% of pdFI contain a subpopulation of the γ-chain (γ′), which is a result of an alternative mRNA splicing event that replaces the four amino acid residues on the carboxy-terminal of the γ-chain with a 20 amino acid fragment.[19,20] The γ′ and γ subpopulations are both physiologically important.[21−24] The activation of FI, assembly into protofibrils and fibrin cross-linking are also affected by post-translational sulfation,[25] phosphorylation,[26] and glycosylation.[27,28] Importantly, the γ′-chain content and the post-translational modifications of FI have been associated with opposing changes in fibrin fiber diameter, porosity, and degree of branching.[27,29−31] Past reports show that the impact of increased γ′ content on fibrin formation is slowed fibrin polymerization, decreased fiber diameter with increased branching that produces smaller pores.[29−31] In contrast, in vitro deglycosylation of FI produced fibrin structure with a larger fiber diameter, decreased branching, and larger pores.

Received: October 11, 2012
Revised: November 26, 2012
Published: December 7, 2012

Deglycosylation also resulted in increased polymerization rates but no change in the activation kinetics of FI.[27] The physiologic significance of FI with an in vivo modified glycoform has not been reported. Indeed, there is currently no clear understanding between altering FI structure and the hemostatic barrier function at a wound site.

The molecular complexity of FI and commodity amounts needed for biotherapeutic applications are best addressed by the biosynthetic capabilities of mammalian cells. For example, classical large-scale suspension culture of animal cells can make hundreds of kilograms of therapeutic-grade, 2-chain assembled, humanized monoclonal recombinant antibody per year.[32] However, an impediment to higher productivity in mammalian cell culture at the metric ton per year level is the low cell density of about 10^7 cells/mL of bioreactor media.[33] As a result, the economics of scale-up necessitate large capital commitments of >$300 M in multiple bioreactors.[32,34] Alternatively, the mammary gland of transgenic livestock can potentially make complex blood proteins in milk at rates of 2000−10000 L/year per dairy animal.[35] Compared to animal cell bioreactors, the mammary gland can produce proteins at high rates of >1 g/L/h due to a high cell density of 10^9 cells/mL of mammary tissue.[36] Moreover, the cost of scale-up to add manufacturing capacity is estimated to be 10% of current bioreactor facilities.[34] However, to date, only the moderately complex human blood protein antithrombin III (ATIII) has been produced at large-scale in the milk of a transgenic livestock and received federal regulatory approval.[35,37,38]

Over the past two decades, we and other laboratories have studied the biosynthesis of recombinant human fibrinogen (rFI) made in the milk of transgenic mice.[39−42] However, the small amount of rFI produced in mice limited detailed molecular and material characterization where in vivo studies such as on fibrin tissue adhesion were not possible. Here we provide the first report on the biosynthesis and material characterization of rFI made in the milk of cloned, transgenic dairy cows. To our knowledge, rFI is one of the most challenging biomacromolecules to ever be produced in transgenic livestock. We evaluate the post-translational modifications made by the mammary epithelia relative to the human liver. The molecular function of the rFI in vitro is examined by turbidimetric and viscoelastic properties as related to the formation of fibrin protofibrils and a cross-linked fibrin clot. We also study the physical structure of rFI fibrin by electron microscopy. The hemostatic function and wound adhesion of rFI is examined in an in vivo porcine hepatic injury model and by immunohistochemistry of the fibrin−wound interface.

2. EXPERIMENTAL SECTION

2.1. Materials. All reagents were obtained from Sigma unless otherwise specified. Plasma-derived human thrombin (pdFIIa), plasma-derived FI (pdFI) depleted of plasminogen, von Willebrand factor and fibronectin, and bovine fibrinogen (bFI) was bought from Enzyme Research Laboratories (South Bend, IN). Recombinant human thrombin (rFIIa) was purchased from ZymoGenetics (Seattle, WA). Anhydrous dimethyl sulfoxide (DMSO), sodium hydroxide, and methyl iodide were obtained from Sigma (St. Louis, MO). PNGase F was purchased from New England Biolabs (Beverly, MA).

2.2. Transgene Construction. The use of bovine αS1-casein promoter to direct mammary epithelial expression has been previously described.[43] The complete 5.2 kbp human Aα, 7.6 kbp Bβ, and 8.5 kbp γ fibrinogen genes were cloned from a human genomic library contained within a P1-bacteriophage derived artificial chromosome (PAC) in Escherichia coli cells from Genome Systems, Inc. (St. Louis, MO). All three transgenes were constructed using the 6.2 kbp bovine αS1 casein 5′-upstream promoter linked to the genomic fibrinogen coding sequences followed by each chain specific 3′ UTR. The following linearized transgene constructs resulted in a: 16.7 kbp 5′-bovine αS1-casein, α fibrinogen gene (Supporting Information, Figure S1A); a 18.3 kbp 5′-bovine αS1-casein, β fibrinogen gene (Supporting Information, Figure S1B); and 21.7 kbp 5′-bovine αS1-casein, γ fibrinogen gene (Supporting Information, Figure S1C). These constructs were cotransfected into a female genital ridge cell lineage using calcium phosphate precipitation (CalPhos, Clontech, Mountain View, CA) to make founder animals by nuclear transfer.[44]

2.3. Southern Blot Analysis. Genomic cow DNA was isolated from blood using Broodram procedure and subjected to restriction enzyme digestion with either BsrGI, HindIII or BglII as per the manufacturer's instructions (New England BioLabs, Ipswich, MA). Digests were loaded on a 0.8% agarose gel and subjected to electrophoresis for 4 h at 120 V. The gel was washed in 0.25 N HCl for 15 min and then 0.5 N NaOH for 30 min before transferring to a MagnaCharge membrane (GE Healthcare, Uppsala, Sweden) using the Turbo blot system from BioRad (Hercules, CA). The αS1 casein probe was generated by PCR using Kirkegaard and Perry Laboratory's (KPL) Detector Biotinylation kit (Gaithersburg, MD). The 500 bp probe corresponding to a region from 200 to 700 bp upstream from transcriptional start in the casein gene (5′ UTR promoter region) was used to detect the endogenous αS1 gene and each fibrinogen transgene. After cross-linking, the membrane was probed and detected using the KPL AP-Chemiluminescent Blotting kit per manufacturer's instructions. Hybridization was carried out at 50 °C and high stringency wash at 60 °C.

2.4. Purification. rFI was purified from 32 L of milk collected on eight lactation days from two transgenic cows (Foxy and Fantasy) of the BFI2n8c83-EGFIneo lineage. Processed in 4L batches, rFI was purified by a two-column purification procedure using cation exchange (CIEX) and hydrophobic interaction chromatography (HIC). Transgenic milk was clarified by adding ethylene diamine tetracetic acid (EDTA) to a final concentration of 50 mM and defatted by centrifugation (1600g, 20 min, 4 °C). The clarified milk loaded on a Fractogel EMD SE (Merck, Darmstadt, Germany) column (10/20 cm) equilibrated in 20 mM sodium phosphate, pH 7.0. After loading, the column was washed with five volumes of the same buffer and bound proteins were eluted with a linear salt gradient from 0 to 0.5 M NaCl in 10 column volumes at a linear flow rate of 60 cm/h. Elution fractions containing rFI were pooled, diluted (1:1) with 1 M ammonium sulfate, and loaded on a Butyl Sepharose (GE Healthcare, Uppsala, Sweden) column (10/15 cm) equilibrated in 50 mM sodium phosphate pH 7.0 + 0.5 M ammonium sulfate. After loading and washing, the column was eluted with a linear salt gradient from 0.5 to 0 M ammonium sulfate in 10 column volumes at a linear flow rate of 60 cm/h. Elution fractions containing rFI were pooled, concentrated and buffer exchanged to 20 mM sodium citrate pH 7.0 + 0.15 M NaCl. Purified rFI from the 4L processing batches were pooled. The purified protein was subsequently filtered over 0.22 μm and stored at −70 °C until use. The step yields of the column purifications were ~60%; the overall yield of rFI was ~40%. Purity was evaluated by size exclusion chromatography. After being passed through a 0.20 μm nylon filter (Millipore, Billerica, MA), 0.5 mL of purified rFI was passed through a TSK-G3000SW$_{xL}$ (Tosoh Biosciences, South San Francisco, CA) column (14 mL, 30 cm length, 7.8 mm ID) attached to a Knauer HPLC System at 0.5 mL/min for 45 min and data were collected by a photodiode array (PDA) with a 1 mm flow cell and analyzed by EZChrom Elite software.

2.5. SDS-PAGE and Western Blot. Nonreduced and reduced FI samples of purified pdFI, rFI, and bovine fibrinogen (bFI) and transgenic and nontransgenic milks were evaluated by sodium dodecylsulfate−polyacrylamide gel electrophoresis (SDS-PAGE) on 4−12% NuPage Bis-Tris gels (Invitrogen, Carlsbad, CA). Gels were then stained with Colloidal Blue (Invitrogen, Carlsbad, CA) or electroblotted onto Immun-Blot polyvinylidene fluoride (PVDF) membranes (BioRad, Hercules, CA) for immunobloting. Blots were

probed with a polyclonal antibody for human FI (USBiological, F4200−07C, Swampscott, MA).

2.6. γ- and γ′-Chain Content. FI samples (200 μg) were deglycosylated with peptide N-glycosidase F (PNGase F, New England Biolabs, Ipswich, MA), adjusted to 3 M GuHCl, reduced for 1 h with tris(2-carboxyethyl)phosphine (TCEP, 5 mM final concentration, Pierce, Rockford, IL), alkylated for 30 min with iodoacetamide (15 mM final concentration), and then adjusted to 0.2% (v/v) formic acid. Analysis was performed on an Agilent 6210 ESI-TOF MS with an Agilent 1200 capLC using liquid chromatography coupled to electrospray time-of-flight mass spectrometry (LC-ESI-TOF-MS). The column was an Agilent Poroshell 300SB-C8 with dimensions of 0.5 mm ID and 7.5 mm L (Agilent Technologies, Santa Clara, CA). The flow rate was 20 μL/min, and the gradient program consisted of injection in 5% acetonitrile (HPLC-grade) in 0.1% formic acid followed by washing and then a linear gradient of 1%/min to 55% acetonitrile in 0.1% formic acid. MS data were acquired in positive mode. The raw data were deconvoluted with Agilent's Qualitative Analysis software (v B.01.03) to generate the zero-charge spectra. The corresponding peak abundances were used to estimate the amounts of each species.

2.7. Fibrinopeptide Phosphorylation. Fibrinopeptides A (FpA) and B (FpB) were obtained by incubating rFI and pdFI (10 mg/mL) with rFIIa (236 U/ml) at 37 °C for 60 min. Phosphorylation was identified by a LC-MS/MS system which included a Dionex U3000 nanoflow HPLC system with a UV detector and an Applied Biosystems 4000 Q-Trap triple quad/ion trap mass spectrometer. The samples were injected onto a Dionex Acclaim Pepmap C18 trap column (Thermo Scientific, Rockford, IL) and the peptides were eluted by a linear gradient of 15−40% acetonitrile in 0.1% formic acid. Data were analyzed manually to confirm phosphorylation sites using theoretical m/z values calculated from the UCSF Protein Prospector MS-Product Web site and Analyst 1.4.2. The fibrinopeptide release chromatograms showed that the FpA from pdFI consisted of two peaks: a fronting shoulder that accounted for ~20−30% of the peak area and the main peak. The fronting shoulder is the phosphorylated at Ser3. Comparison of the rFI FpA elution time indicated that the majority of rFI was phosphorylated at Ser3. This was confirmed by LC-MS/MS analysis as described in Supporting Information.

2.8. Glycosylation Analysis. Sialylation profiling of rFI N-glycans was performed by normal phase high performance liquid chromatography (NP-HPLC) using the method of Anumula and Dhume.[45] For ESI-MS/MS analysis of the glycans, rFI was incubated with PNGase F. Released N-glycans were separated from proteins using C18 Extract Clean columns (100 mg, 1.5 mL, Alltech, Deerfield, IL), eluted with 2 × 0.5 mL of solvent 0.1% (w/v) TFA in 50% acetonitrile/50% water, and dried by speed-vac (Labconco CentriVap, Kansas City, MO). The dried glycan sample was dissolved with a DMSO/NaOH suspension (100 μL) in 1.5 mL centrifuge tube and allowed to sit at room temperature for 30 min with occasional vortexing. Methyl iodide (50 μL) was added and the mixture was vortexed for 60 min. After the reaction, 100 μL of DMSO/NaOH suspension and 50 μL of methyl iodide were added again and vortexed for 60 min. A 500 μL aliquot of chloroform was added and washed repeated with ice-chilled water until the aqueous phase became neutral. The organic phase was dried under speed vac for MS analysis. MS analysis was performed on a 4000 Q-Trap hybrid triple quadruple/ion trap system (Applied Biosystems, Foster City, CA) with a MicroIon Spray II ion source. Premethylated N-glycan was prepared in 70% acetonitrile/30% water. The sample solution was directly infused using a syringe pump at 0.3 μL/min. Possible structures were proposed by analyzing MS spectra and searching theoretical precursor ion mass on web-based Glycomod. The structures were determined by analyzing the corresponding MS/MS spectra and matching with calculated fragment ion mass consistent with the precursor ion definition using Glycoworkbench.[46]

2.9. Thrombin-Catalyzed Activation. The thrombin-catalyzed release of fibrinopeptides A (FpA) and B (FpB) from rFI and pdFI (Enzyme Research Laboratories, South Bend, IN) was determined based on the method from Gorkun et al.[47] Two levels were used: (1) pdFI or rFI (0.1 mg/mL) incubated with rFIIa (0.01 U/ml) as described previously;[47] and (2) pdFI or rFI (0.5 mg/mL) incubated with rFIIa (0.05 U/mL). Reversed-phase high-performance liquid chromatography (HPLC) was used to monitor fibrinopeptides on a Waters 2695 Alliance with a Waters 2996 PDA detector using a Jupiter C18 column (300 Å, 2 × 150 mm, 5 μm particles; Phenomenex, Torrance, CA). Waters Empower software was used to generate calibration curves ($R^2 > 0.996$ for FpA and FpB) using commercial standards (Sigma, St. Louis, MO) and integrate peak areas for quantification. Data were plotted as percent release with respect to time assuming 100% release at 180 min. N = 6 for the low level condition (0.1 mg/mL FI and 0.01 U/mL thrombin) and N = 2 for the high level condition (0.5 mg/mL FI and 0.05 U/mL thrombin).

2.10. Thrombin-Catalyzed Protofibril Formation. Polymerization of pdFI and rFI after treatment with thrombin was measured by changes in turbidity over time at 350 nm with a Beckman Coulter General Purpose spectrophotometer (Brea, CA), as previously described.[47] pdFI or rFI (0.2 mg/mL) was loaded into a 10 mm optical path microcuvette. Thrombin (0.1 U/mL) was added. Samples were run in triplicate (N = 3). The change in turbidity was monitored at 350 nm for 30 min at 25 °C.

2.11. Factor XIIIa Catalyzed Molecular Cross-Linking. Activated recombinant factor XIIIA subunit (rFXIIIa) was produced in Pichia pastoris as previously described.[48] The specific activity of the rFXIIIa was measured to be 7000 U/mg using Pefakit (Pentapharm, Norwalk, CT). pdFI (Enzyme Research, South Bend, IN) was depleted of constitutive FXIII contamination by immunoaffinity purification using an anti-FXIII monoclonal antibody (Green Mountain Antibodies, Burlington, VT). Cross-linking of FI by rFXIIIa was analyzed as previously described.[47] rFI or pdFI (0.38 mg/mL) was incubated with rFIIa (1 U/mL) and four levels of rFXIIIa (1, 25, 50, and 100 U/mL) for 0, 2.5, 5, 10, and 15 min at 24 °C. FI was also incubated with thrombin without rFXIIIa for 15 min, respectively. Cross-linking was studied by reducing SDS-PAGE (4−12% Bis-Tris NuPAGE) stained with Colloidal Blue (Invitrogen, Carlsbad, CA). The pdFI and rFI samples treated with rFIIa and 25 U/mL rFXIIIa for 15 min were electroblotted onto polyvinylidene fluoride (PVDF) membrane (Millipore, Billerica, MA) by applying 30 V for 1 h and stained with Colloidal Blue. The bands at approximately 130 and 150 kDa were excised and the first 10 amino acids in the N-terminal of each were sequenced by Edman degradation with an Applied Biosystems 494 Procise automated sequencer. N-terminal sequencing was performed by the University of Nebraska Medical Center's Protein Structure Core Facility. The disappearance of the α-chain and γ-chain were analyzed by densitometry using Adobe Photoshop Elements 6.0 software.

2.12. Viscoelastic Characterization. Clot kinetics and strength were evaluated by thromboelastography (TEG) which was performed on solutions containing purified rFI or pdFI, rFXIIIa and rFIIa with a Thromboelastograph (TEG) Hemostasis System 5000 series (Haemoscope Corp., Niles, IL). rFI or pdFI (9 mg/mL) was incubated at 37 °C with rFIIa (53 U/mL), rFXIIIa (2429 U/mL), and $CaCl_2$ (12 mM). As a reference, normal citrated human blood (340 μL, N = 20 donors) was combined with 200 mM $CaCl_2$ (20 μL), as instructed by the TEG manufacturer. The TEG measured the strength of the clot as it formed. From those measurements, the TEG Analytical Software (version 4.2.2, Haemoscope, Niles, IL) calculated time to clot initiation (R), time to achieve a clot firmness of 20 mm (K), and maximal clot strength (MA), which is directly related to the shear elastic modulus strength (G).[49,50] Each sample was run in triplicate (N = 3) so mean and standard deviation could be calculated. The data were exported and analyzed in Microsoft Excel.

2.13. Scanning Electron Microscopy. Scanning electron microscopy was utilized to examine the structure of fibrin clots formed by rFI and pdFI. FI (0.5 mg/mL) was incubated with rFIIa (0.5 U/ml) for 1 h at room temperature. Samples underwent 2.5% glutaraldehyde fixation, stepwise ethanol and hexamethyldisilazane dehydration, and sputter coated with gold−palladium. Clots were imaged by a scanning electron microscope (S4700 Field-Emission SEM, Hitachi, Tokyo, Japan) at 15 kV and a magnification of 10000×. Average fiber diameters were measured from 20 fibers. The number of

branch points was determined in 10 1.4 μm^2 areas. Fiber diameters and branch points were statistically compared by t test with an α of 0.05.

2.14. Tissue Sealant Function. Crossbred commercial (domestic) swine obtained from UNL Agricultural Research and Development Center (Mead, NE) were anesthetized with isoflurane (1−2%) supplemented with oxygen (1−2 L/min) throughout the procedure. A carotid arterial catheter for pressure monitoring and blood sampling and a jugular venous catheter for fluid and medication administration were placed via surgical cutdown in the left neck. Blood samples from each pig were drawn before, during and after surgery and tested by thromboelastography (TEG) to identify and select pigs with normal clotting parameters and to monitor changes in endogenous coagulation parameters throughout surgery due to blood loss or hemodilution by Lactated Ringers solution. The liver was exposed through a midline incision. A scissoring injury clamp[51−53] with X-shaped blades (5 cm width and breadth) was applied through the central portion of the liver, adjacent to the vena cava, as described previously.[12] The resultant injury was a jagged, stellate laceration 8−10 cm in diameter, completely through the organ. Such injuries were treated in 10 pigs with LFS (7 mg/mL pdFI or rFI (N = 1 and 9, respectively), 1740 U/mL rFXIIIa, 85 U/mL rFIIa, 12 mM $CaCl_2$; total of 6 mL) applied with a Tisseel Duploject dual-syringe system (Baxter Healthcare Corporation) over 30 s to several minutes followed by 3−5 min of manual compression. Euthanasia was performed while the animal was under deep isoflurane anesthesia. Sodium pentobarbital (380 mg/mL, 10 mL IV) was administered, and 1 min later the animal underwent bilateral diaphragm incisions with transection of the supradiaphragmatic vena cava and aorta. All procedures performed during this research were approved by the Institutional Animal Care and Use Committee of the Omaha VA Medical Center.

2.15. Immunohistochemistry. Adherence of the human fibrin made from rFI and pdFI to wounded tissue was examined by immunohistochemistry. Wedge-shaped hepatic excisions (base of 1 cm and height of 1 cm) were made along a lobar edge. Fibrin sealant (FS), consisting of 9 mg/mL FI (pdFI or rFI), 2460 U/mL rFXIII, 106 U/mL rFIIa, and 12 mM $CaCl_2$, was applied by spray device to the wound for about 35 s. Approximately 18 mg FI, 5000 U rFXIIIa, and 210 U rFIIa was applied to each wedge. Liver sections from untreated and rFI and pdFI sealant-treated wedge excisions were fixed in 10% neutral-buffered formalin, dehydrated, and embedded in paraffin. Specimens were sliced (5 μm), mounted on slides, dewaxed, and processed with Dako TRS antigen retrieval solution (Dako, Carpentaria, CA). After blocking endogenous alkaline phosphatase and peroxidase activity, the specimens were incubated with an antiporcine fibrinogen antibody (Kamiya Biomedical Company, Seattle, WA) and exposed with HRP/DAB+. After blocking remaining peroxidase activity associated with the antiporcine fibrinogen antibody, specimens were incubated with an antihuman fibrinogen antibody (Abcam, Inc., Cambridge, MA) and exposed by alkaline phosphatase-based Permanent Red (Dako, Carpentaria, CA). The specimens were subsequently conterstained with Mayer's hematoxylin. DAKO EnVision G|2 Doublestain System (Dako, Carpentaria, CA) was used for signal detection.

3. RESULTS

3.1. Somatic Cell Transfection and Nuclear Transfer. The characterization of the transgenic cow clonal lineage BFI2n8c83-EGFIneo (termed "Fancy") is presented here as an example of a stable, cloned α-S1 casein-FI genotype. Using Southern analysis, we characterized the presence of each of the three α-S1 casein-FI transgenes (Supporting Information, Figure S1D) in Fancy's DNA isolated from leukocytes harvested from whole blood. Three restriction endonuclease digestions were chosen to yield fragments containing a common element of the α-S1 casein promoter while having differently sized sequences unique to each fibrinogen gene. The specificity of the probes for each of the BsrGI, HindIII, and BglII digests of Fancy's and control bovine DNA was demonstrated by the presence of endogenous casein signals in both. The control DNA lacked signals associated with the human FI sequences of the reference transgene mixture. In contrast, Fancy's DNA contained hybridization signals specific to the digests of the reference α-S1 casein rFI transgene mixture and eight or more copies of each Aα-, Bβ-, and γ-transgene. Two other cows of the Fancy clonal lineage (Foxy and Fantasy) showed similar copy numbers and Southern analysis results.

3.2. rFI Assembly, Concentration, and Purification. Fancy's milk was collected and skimmed, and the resulting skimmed milk was examined using Colloidal blue stained SDS-PAGE and Western analysis under nonreducing (Figure 1A,B, lane 8) and reducing (Figure 1C,D, lane 8) conditions. We estimated the concentration of assembled rFI in the milk to be 2−4 g/L in three cows of the Fancy clonal lineage using densitometric analysis of Western blots with human pdFI as a reference. This level of production was stable for a lactation study conducted over a period of 200 days. Western analysis using a polyclonal antibody confirmed the identity of the main 340 kDa species as assembled human FI. The M_r of Aα-, Bβ-, and γ-chains of pdFI and rFI were nearly identical at about 66.5, 52.0, and 46.5 kDa, respectively (Figure 1C,D) with a stoichiometric presence of 1:1:1, as analyzed by SDS-PAGE.

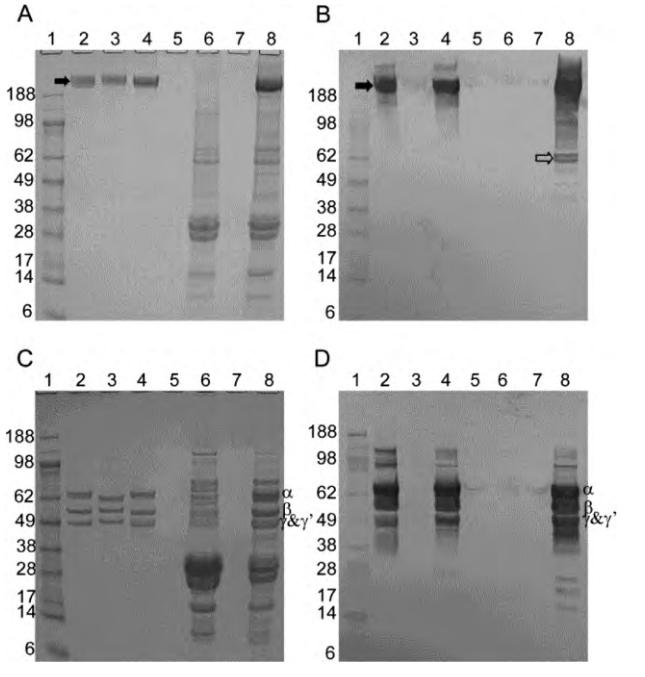

Figure 1. Expression of rFI in bovine milk. rFI expressed in the milk of transgenic cows was evaluated by SDS-PAGE gel electrophoresis under (A) nonreducing and (C) reducing conditions and Western Blot probed with goat polyclonal antibody for human FI under (B) nonreducing and (D) reducing conditions. Each panel contains a molecular weight marker (lane 1), purified, human pdFI (lane 2), bovine pdFI (lane 3), transgenic human rFI (lane 4), a blank lane (lane 5), nontransgenic skimmed cow milk (lane 6), a blank lane (lane 7), and transgenic skimmed cow milk (lane 8). The M_r of the assembled fibrinogen (340 kDa) is indicated by closed arrows in the upper panels and each individual Aα, Bβ, and γ-chains of FI are indicated by α, β, γ, and γ′, in the lower panels. The open arrow indicates free Aα.

The Aα-chain of pdFI and rFI appeared as doublet bands, which has been reported previously for pdFI.[54] SDS-PAGE partially resolved γ- and γ′-chains (Figure 1C, lane 4). The hexameric nature of pdFI and rFI was corroborated by the 340 kDa M_r under nonreducing conditions. Some smaller amounts of FI reactive species with higher and lower M_r than the 340 kDa band were present in the skimmed milk (Figure 1B, lane 8). Some of these species were similar to those found in pdFI (Figure 1B, lane 2) and thus could have been unassembled Aα-chains.

For the analysis presented here, approximately 38 g of rFI was purified from 32 L of milk from eight lactation days of two transgenic cows (Foxy and Fantasy). As detected by electrophoresis, rFI was purified to a single species using a two-step sequence of cation exchange (CIEX) and hydrophobic interaction chromatography (HIC). The purity was estimated to be >98% (Figure 1A,C, lane 4 and Figure S2, Supporting Information) with a yield of >40%. Purified rFI was examined for the presence of bovine fibrinogen (bFI). Differences in the molecular size of assembled pdFI, bFI and rFI samples were readily discriminated from each other using SDS-PAGE under reducing conditions (Figure 1C). The side-by-side comparison of the individual FI chains using electrophoresis and LC-ESI-TOF-MS showed no discernible contamination of bFI in the rFI sample. The bFI content in this sample is likely to be <2%. Taken together, rFI was sufficiently isolated from other milk proteins enabling the characterization of its structure and related biological activity in vitro and in vivo.

3.3. γ- and γ′-Chain Content. The γ′ content of rFI was investigated using mass spectrometry on deglycosylated, reduced, and alkylated samples. The theoretical molecular weight (MW_{avg}) for the γ and γ′ chains after this sample treatment is 47040 and 49054 Da, respectively, with each sulfation adding 80 Da to the γ′-chain. In both pdFI (Figure 2A) and rFI (Figure 2B), the γ-chain was the major translated species (extra carbamidomethylation of the γ-chain, an artifact of the sample processing, is seen in both pdFI and rFI). The γ′-chain of pdFI is sulfated at Tyr418 and/or Tyr422.[25] The C-terminal γ′ peptide has two potential sites of Tyr-sulfation. pdFI essentially had all doubly sulfated γ′ (theoretical molecular weight 49214 Da). We observed evidence of partial sulfation within the γ′-chain of rFI (theoretical molecular weight 49134 Da). Accounting for all observed forms of the γ- and γ′-chains in the deconvoluted spectra, there was >4-fold higher γ′ in rFI than the pdFI reference.

3.4. rFI Biochemical Features. Phosphorylation, sulfation, and glycosylation of rFI were analyzed by HPLC and LC-MS. The degree of phosphorylation of fibrinopeptide A (FpA) of rFI and reference pdFI after treatment with thrombin was evaluated by reverse phase C-18 HPLC (Figure 3A) and confirmed by LC-MS/MS (Figure 3B). Greater than 90% of the transgenic FpA was phosphorylated in contrast to 20−30% phosphorylation of FpA from the pdFI reference.

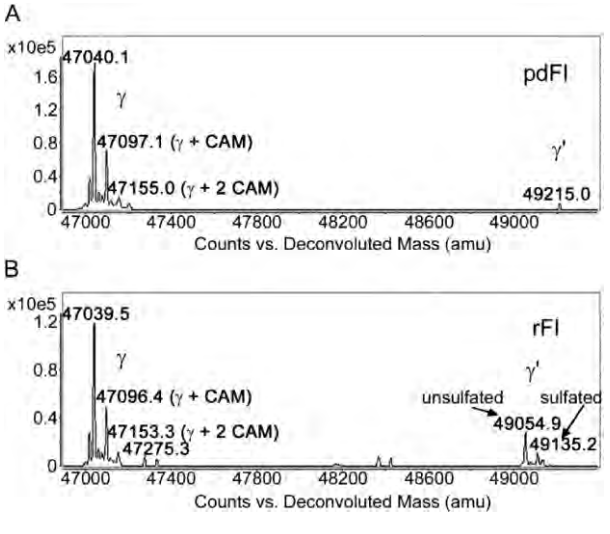

Figure 2. LC-ESI-TOF-MS analysis of γ′ content. pdFI (A) and rFI (B) were treated with PNGase F, reduced, and alkylated. The total γ- vs γ′-chain analysis indicated a >4-fold higher γ′ content in rFI compared to pdFI. Extra alkylation of γ resulting from carbamidomethylation is annotated as γ + CAM.

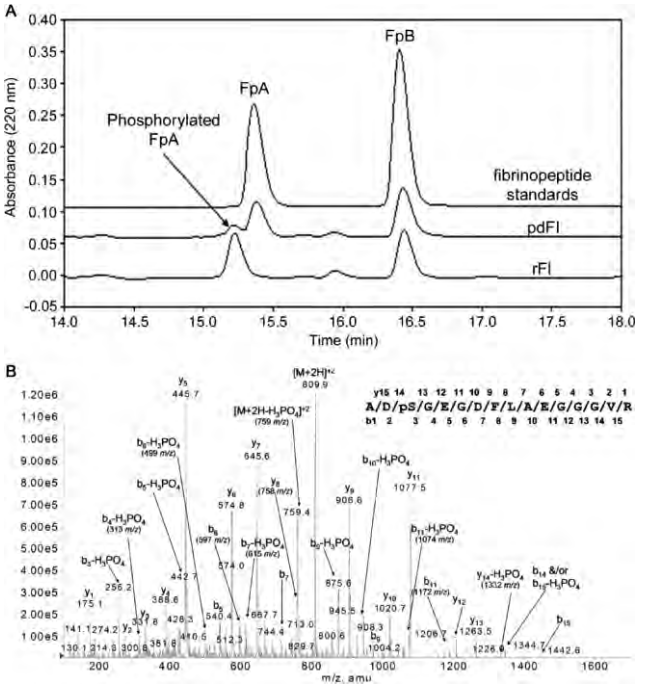

Figure 3. Fibrinopeptide phosphorylation of rFI. (A) Phosphorylation of fibrinopeptides. FpA and FpB released into the supernatant from fibrin clots formed by the treatment of pdFI and rFI (10 mg/mL) with thrombin (236 U/mL) were analyzed by C-18 HPLC and LC-MS as described in the experimental protocol. Synthetic FpA and FpB peptides were used as nonphosphorylated reference standards. Peak assignment is indicated above the corresponding peaks. (B) MS/MS spectrum of FpA released from thrombin treatment of rFI, confirming phosphorylation at Ser3. In CID, phosphorylated serine residues undergo a characteristic neutral loss of H_3PO_4 (98 amu). This characteristic loss is evident for the precursor ion ($[M + 2H - H_3PO_4]^{+2}$ = 759 m/z), the b fragment ions starting with b_3 ($b_3 - H_3PO_4$ = 256 m/z), and the $y_{14} - H_3PO_4$ (1332 m/z). These results lead to the conclusion that Ser3 is phosphorylated.

Glycosylation is a primary determinant of the clearance of glycoproteins in circulation by the liver.[55] Potential sites of N-glycosylation in pdFI and rFI are at Asn364 of the Bβ-chain and Asn42 of the γ-chain where the glycans in pdFI are biantennary complex glycans with one or two sialic acids.[56] Glycosylation of the purified rFI samples was investigated by normal phase HPLC profiling and mass spectrometry. The results of the HPLC profiling for pdFI were consistent with biantennary

complex glycans with one or two sialic acids (Figure 4A); however, the majority of the N-linked glycans in rFI were

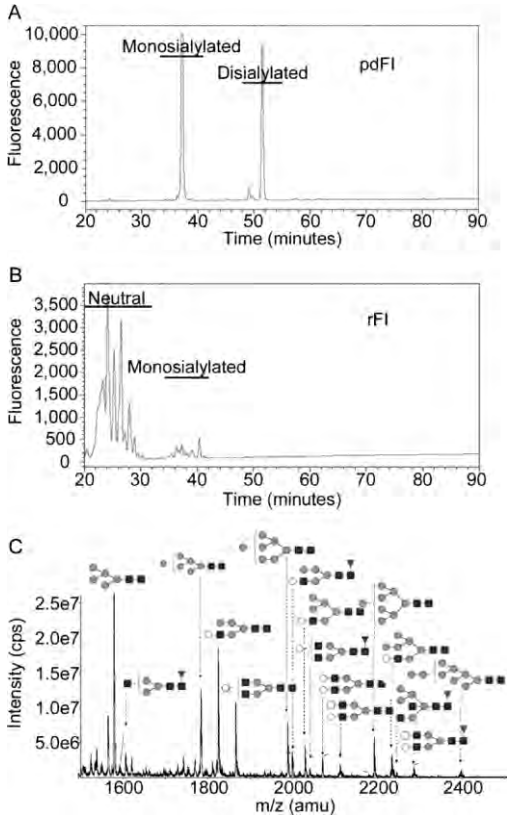

Figure 4. Biochemical features of rFI. N-glycans released by PNGase F from purified samples of pdFI and rFI were analyzed by HPLC (A, B) and mass spectrometry (C). (B, C) Elution times of neutral, monosialylated, and disialylated species are indicated.

neutral structures (Figure 4B). N-glycans were enzymatically released from rFI and permethylated for MS and MS/MS analysis. The N-glycans of rFI were a mixture of high mannose, neutral complex, and hybrid glycans (Figure 4C). These structures displayed a whey protein glycan signature similar to those observed with bovine lactoferrin.[57] A small amount of rFI N-glycans containing one sialic acid likely were degraded during permethylation. In summary, the post-translational modifications of rFI displayed a milk protein signature which was different than that of pdFI.

3.5. Activation Kinetics. The thrombin-catalyzed release of fibrinopeptides A (FpA) and B (FpB) was monitored by HPLC. We studied FpA and FpB release using previously reported FI and thrombin concentrations[47] (Figure 5A) and at 5-fold higher FI and thrombin concentrations (Figure 5B) to compare pdFI and rFI activation kinetics. At both levels, FpA and FpB release kinetics were similar for pdFI and rFI in that both showed the slower release of FpB relative to FpA. Hence, the activation of rFI and pdFI were similar.

3.6. Fibrin Protofibril Formation. The rates of protofibril formation of pdFI and rFI activated by thrombin in the absence of added FXIIIa were measured by the change in turbidity (Figure 6). At 0.2 mg/mL FI and 0.1 U/mL recombinant thrombin (rFIIa), the initiation of protofibril formation as measured by the time to initial onset of turbidity was slightly faster for pdFI than rFI. The rate of increase in turbidity, which

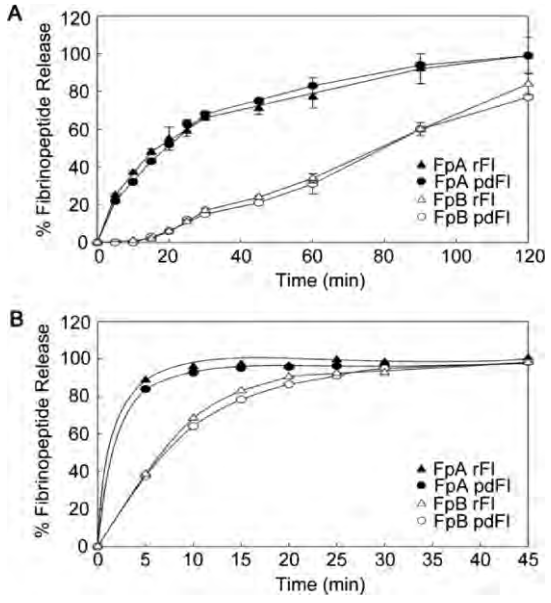

Figure 5. Activation kinetics of pdFI and rFI. The time course of the release kinetics of FpA and FpB was analyzed by HPLC at two levels: (A) rFI and pdFI (0.1 mg/mL) incubated with thrombin (0.01 U/mL), and (B) rFI and pdFI (0.5 mg/mL) incubated with thrombin (0.05 U/mL); N = 6 (A) and N = 2 (B).

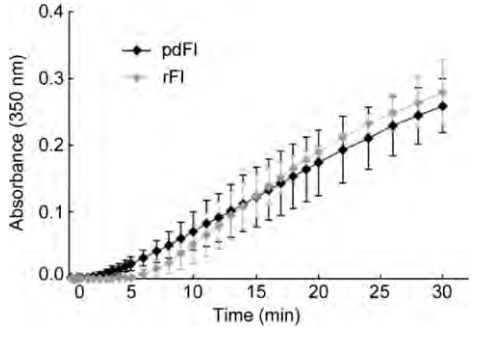

Figure 6. Fibrin protofibril formation of pdFI and rFI. Polymerization of pdFI and rFI at 0.2 mg/mL, initiated at time 0 with thrombin 0.1 U/mL, was monitored as the change in turbidity at 350 nm for 30 min (N = 3).

is indicative of protofibril assembly,[47] and final absorbance, which is indicative of fiber diameter,[29,30] were similar for pdFI and rFI.

3.7. Molecular Cross-Linking. We investigated the time course of polymerization of rFI and pdFI (0.38 mg/mL) treated with rFIIa (1 U/mL) and rFXIIIa (25 U/mL) by SDS-PAGE analysis under reducing conditions. An insoluble fibrin clot, which dissolved after treatment with reducing agent and SDS at 74 °C, was observed in all samples treated with rFXIIIa. The normal constitutive level of FXIII contamination present in pdFI preparations was observable by the appearance of γ−γ dimers after treatment by rFIIa alone (Figure 7A, lane 8).[58] In contrast, the absence of FXIIIa activity in the rFI was evident as no γ−γ dimers were formed after the addition of rFIIa alone (Figure 7B, lane 8). A total of 2.5 min after treatment of pdFI or rFI with rFIIa, we observed a 1.5 kDa shift to lower M_r of the Aα- and Bβ-chains, indicating a nearly complete conversion to their activated counterparts resulting from the release of FpA and FpB (pdFI, Figure 7A; rFI, Figure 7B). Densitometric

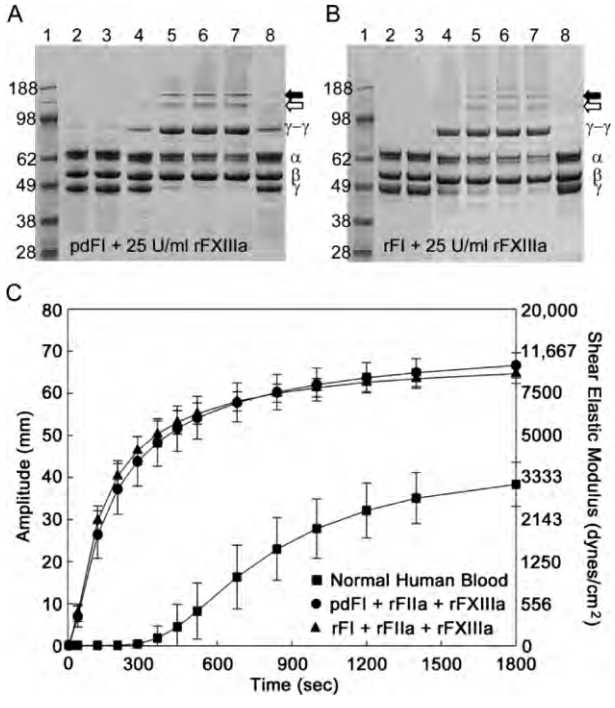

Figure 7. Cross-linking and viscoelastic characteristics of pdFI- and rFI-based tissue sealants. Purified samples of pdFI and rFI (0.38 mg/mL) were treated with rFIIa (1 U/mL) and rFXIIIa at 25 U/mL (A and B, respectively). Reactions were quenched and then analyzed by SDS-PAGE under reducing conditions. Each panel has a molecular weight marker (lane 1). Lane 2 contains pdFI (A) or rFI (B) prior to rFXIIIa and rFIIa treatment; lanes 3−7: FI, rFXIIIa, and rFIIa incubated for 0, 2.5, 5, 10, and 15 min; lane 8: FI incubated with rFIIa only for 15 min. The Aα-, Bβ-, and γ-chains (66, 52, and 46 kDa, respectively) of pdFI or rFI are indicated by α, β, and γ, and γ−γ indicates the cross-linked γ-chains. As detected by N-terminal sequencing, the open arrow indicates an α-chain multimer and the closed arrow indicates a γ-chain multimer. Thromboelastographic comparison of rFI- and pdFI-based tissue sealants (C). TEG analysis of the kinetics of clot initiation and clot strength over time for pdFI and rFI (9 mg/mL) after treatment with rFIIa (53 U/mL) and rFXIIIa (2429 U/mL). N = 20 for normal human blood and N = 3 for the pdFI and rFI treatment groups.

analysis indicated that the rates of disappearance of the γ-chain were similar for pdFI and rFI (−0.16/min and −0.15/min, respectively; Supporting Information, Figure S3A) when rFXIIIa was added exogenously. Over the initial 5 min incubation period, the rate of α-chain polymerization was slightly faster for rFI than pdFI as shown by densitometry (−0.03/min and −0.06/min, respectively; Supporting Information, Figure S3B). Similar multimerization patterns were observed for pdFI and rFI. N-terminal sequencing indicated that the band at approximately 130 kDa was an α-chain multimer (Figure 7A,B, open arrow) and the band at approximately 150 kDa was a γ-chain multimer (Figure 7A,B, closed arrow). Thus, rFI was kinetically similar to pdFI with respect to its molecular processing to a cross-linked fibrin clot.

3.8. Viscoelastic Properties. The function of fibrin as a barrier to bleeding can be related to its viscoelastic strength. The evolution of viscoelasticity during the formation of a cross-linked fibrin clot from rFI and pdFI were compared by TEG (Figure 7C). We used an optimized tissue sealant formulation of rFIIa, rFXIIIa, and rFI or pdFI to study the differences in clot strength and viscoelastic kinetics. The average viscoelastic behavior of 20 individual human blood samples strongly contrasts the rapid clotting behavior and high strength of both rFI and pdFI. The time to clot initiation was similar for rFI (18 ± 6 s) and pdFI (20 ± 0 s) ($p = 0.64$, $\alpha = 0.05$). The maximum viscoelastic strength of the developing clot was about 65 mm (9573 ± 1115 dyn/cm^2) for pdFI and about 63 mm (8637 ± 867 dyn/cm^2) for rFI ($p = 0.32$, $\alpha = 0.05$). In summary, both the kinetics of cross-linked fibrin clot formation and the clot strengths were equivalent for rFI and pdFI.

3.9. Scanning Electron Microscopy. The structure of clots formed by pdFI and rFI were compared by scanning electron microscopy (Figure 8). The fibrin from rFI had thicker fibers with larger pores and less branching than the fibrin from pdFI (Table 1). The average fiber diameter of the pdFI clot (0.10 ± 0.02 μm) was similar to diameters measured previously.[30,31] The average fiber diameter of the rFI clot (0.19 ± 0.04 μm) was significantly greater than that of pdFI ($p < 0.001$, $\alpha = 0.05$). In contrast, the rFI fibrin clot had a significantly lower proportion of branch points per area than the pdFI fibrin clot (3.0 ± 1.4 vs 6.0 ± 1.9; $p < 0.001$, $\alpha = 0.05$).

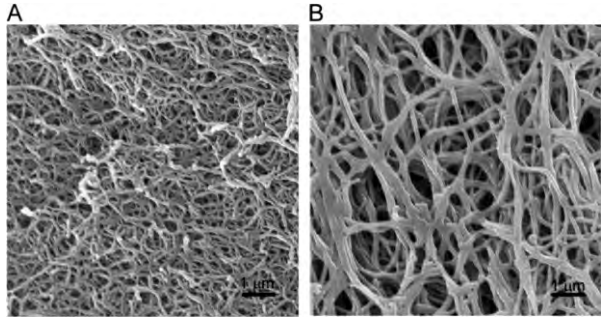

Figure 8. Scanning electron micrographs of fibrin made by pdFI and rFI. Fibrin clots were made by incubating thrombin (0.5 U/mL) with pdFI (A) or rFI (B; 0.5 mg/mL). Scale bars represent 1 μm.

Table 1. Analysis of Fiber Diameter and Number of Branch Points from SEM

	pdFI mean (SD)	rFI mean (SD)
fiber diameter (μm) n = 20	0.10 ± 0.02	0.19 ± 0.04[a]
No. of branch points/1.4 μm^2 n = 10	6.0 ± 1.9	3.0 ± 1.4[a]

[a]$p < 0.001$ vs pdFI.

3.10. Tissue Sealant Function. Because rFI had molecular and coagulation properties in vitro, similar to those of pdFI, we evaluated the wound adherence properties of fibrin made by rFI applied to a wound in vivo. All of the pigs maintained similar thromboelastographic clotting parameters before, during, and after surgery. rFI or pdFI was applied as a tissue sealant to a severe hemorrhage model generated from a grade V liver laceration involving the central hepatic veins.[12] The grade V liver laceration generated a jagged wound topography with severed veins up to 8 mm in diameter (Figure 9A). Untreated, this wound is a lethal, exsanguinating injury.[51] The pdFI and rFI tissue sealant was applied subsurface into the pool of blood which obscured the wound. Even in the presence of diluting amounts of blood, the tissue sealant rapidly formed an adherent clot after five minutes of manual compression. While both the pdFI-based (Figure 9B) and rFI-based (Figure 9C) tissue

dx.doi.org/10.1021/bm301579p | Biomacromolecules 2013, 14, 169−178

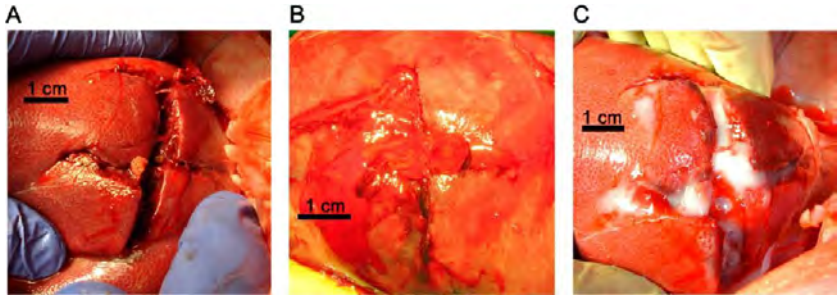

Figure 9. Evaluation of hemostatic and wound adhesive properties of rFI in a grade V central liver laceration model in swine. (A) Laceration without fibrin sealant. (B) Laceration after application of pdFI-based tissue sealant. (C) Laceration after application of rFI-based tissue sealant. Scale bars represent 1 cm.

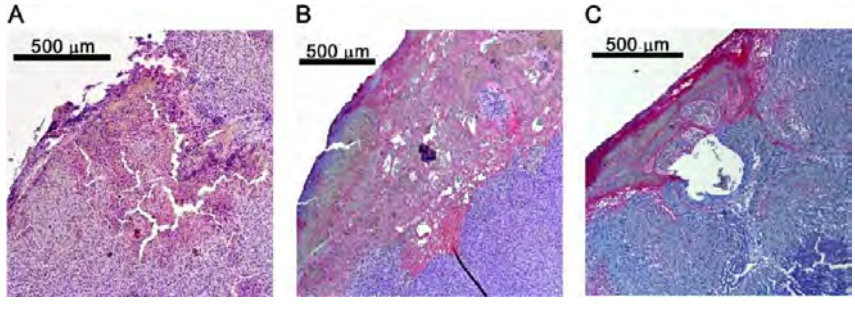

Figure 10. Histologic evaluation of the fibrin−wound interface in a liver lobe wedge excision model in swine. No fibrin sealant (A) and pdFI (B) and rFI (C) sealant treated wedge excisions were incubated with antiporcine FI antibody stained with DAB+ (brown) and antihuman FI antibody stained with Permanent Red (pink). Scale bars represent 500 μm.

sealant rapidly formed an adherent barrier that stopped bleeding, qualitatively we observed that treatments with pdFI sealant became permeated with porcine blood and formed translucent clots, whereas the rFI treatments were less permeable and formed more opaque clots.

3.11. Immunohistochemistry. We examined the clotted wound surfaces by histological cross-sectioning and immunostaining for human and porcine FI (Figure 10A−C). While the human fibrin from pdFI was well intermixed with porcine fibrin (Figure 10B), the fibrin from rFI created well delineated layers alternated with porcine fibrin (Figure 10C). We observed a relatively uniform, 100 μm thick human fibrin layer on the outer surface of the rFI sealant treated tissue. Thus, both gross visual and histological observation of the wound treated with rFI-based sealant confirmed that the resulting fibrin clot was wound adherent and intercalated with blood-borne fibrin to produce a sufficiently strong barrier to bleeding.

4. DISCUSSION

Our studies provide the first illumination of the in vivo adhesive structure and hemostatic behavior of recombinant fibrin. Importantly, the molecular complexity of FI dictates that any rFI will be a facsimile and not an exact copy of the structure and function of pdFI. For example, our rFI is perturbed by increased γ′-chain content as well as differences in the carbohydrate structure at native sites within its α-chain. Importantly, these two particular structural determinants of FI have been associated with opposing changes in fibrin fiber diameter, porosity, and degree of branching.[27,29−31] Past reports showed that increased γ/γ′ heterodimer content slowed fibrin polymerization, decreased fiber diameter, and increased branching resulting in smaller pores.[29−31] In contrast, deglycosylation of pdFI produced fibrin structures with larger fiber diameter, decreased branching, and larger pores. Deglycosylation also resulted in increased polymerization rates but no change in the activation kinetics of pdFI.[27] Prior to this work, the physiologic significance of a post-translationally modified glycoform structure has not been reported. In addition, past work has provided no clear understanding between altering FI structure and the hemostatic barrier function that occurs at a wound site. Our work shows that changes in rFI structure might result in fibrin with improved hemostatic properties achieved without adverse effects on the speed of fibrin formation.

Our studies of rFI made in the milk of cows perturbs opposing determinants of fibrin hemostatic structure and function while making sufficient amounts for preclinical studies. We observed that the bovine mammary gland performed the same alternative mRNA splicing of the FI γ gene as the human liver resulting in the expression of the γ′ variant.[19] However, the level of the γ′-chain population in rFI was strikingly higher than in pdFI. In addition, the mammary tissue also glycosylated the rFI with a neutral carbohydrate that resembled those of whey and casein milk proteins but not the ionically more bulky moiety displayed by FI made in the human liver. Surprisingly, in spite of its >4-fold higher γ′ content, the resulting rFI produced fibrin with thicker fibers, less branching, and larger pores compared to pdFI. Importantly, this was accompanied by no observable slowing in the molecular kinetics of fibrin assembly. This is a similar result for fibrin made from deglycosylated pdFI having much lower levels of γ/γ′. This prior work showed that removing the charged and branched carbohydrate structure sterically affected individual profibril alignment during the assembly into fibers.[27,28] Thus, we conclude that the perturbation to a less bulky glycoform made by the mammary gland biochemistry more strongly

influenced fibrin structure over that of the γ/γ′ heterodimer content.

Previous studies have given conflicting data on the effect of changes in the overall phosphorylation of pdFI where both increased and decreased phosphorylation of pdFI were correlated with increased fiber thickness.[26] However, these early studies did not elucidate the location of the phosphorylation within the pdFI and whether it occurred on the FpA activation peptide and at other alternate phosphorylation sites that may affect fibrin structure. Here, the phosphorylation of the rFI was 3-fold higher than pdFI and it occurred exclusively from increased phosphorylation of the FpA activation peptide, which is removed upon activation. The higher FpA phosphorylation in rFI likely reflects the very efficient phosphorylation of these same motifs in milk caseins.[59] Perhaps more importantly, both FpA/FpB release kinetics and early phase turbidity kinetics were similar for pdFI and rFI. These kinetics are associated with the start of protofibril formation and are in agreement with past studies. Thus, we conclude that there was little observable impact by the higher phosphorylation that occurred in rFI.

Our porcine hepatic injury model consisted of a stellate laceration[51] imposed under normal coagulation potential. It produced severe solid organ hemorrhage primarily from venous blood flow and a rough wound topography of exposed collagen surfaces to examine fibrin adherence. While having equivalent thromboelastic kinetics and strength, as measured in vitro, the pdFI-based tissue sealant made a translucent and less hemostatic clot than the rFI when applied to a wound surface. In contrast, the fibrin generated from rFI made an opaque white and adherent clot that more rapidly resulted in hemostasis. Furthermore, the histology of the wounds treated by pdFI and rFI showed a strong contrast in clot structure leading to hemostasis: the fibrin from the rFI was adherent as a dense stratum less than 100 μm thick while the pdFI was well mixed into the wound and diluted with endogenous pig fibrin to a depth of about 300 μm or more. This is consistent with our macroscopic observation that the rFI clot was not permeated by red blood cells, while the pdFI clot was blood red in color. This reflects the different fiber structure seen in our SEM results and is likely caused by the presence of the sterically less bulky carbohydrate that is the signature glycosylation pattern of mammary tissue.[57] Based on the wound adherence and hemostatic characteristics of rFI, we are currently conducting preclinical studies that will statistically compare the efficacy of a rFI-based tissue sealant to commercial-grade tissue sealant in a cold hemodilution, hypocoagulopathic grade V+ porcine liver injury model.[12] With respect to the potential impact of the rFI fibrin matrix on healing and reabsorption, these future in vivo studies will include the examination of clot stability during the healing process in a swine liver injury survival model. The potential for the future production of a first generation tissue sealant engineered to have improved hemostatic behavior is shown by our estimates of the commodity scale production of rFI by the cows of this study (Supporting Information, Table S2). We estimate that fewer than 300 cows can translate to the production of one metric ton of purified rFI that would help meet clinical needs worldwide.

5. CONCLUSION

This study describes the production, purification, and molecular characterization of large amounts of rFI produced in the milk of transgenic dairy cows. The rFI produced by transgenic cows was fully assembled and produced at 2−4 g/L for a lactation study conducted over a period of 200 days. Despite differences in γ′ content, glycoform, and phosphorylation content of FpA, the kinetic and viscoelastic attributes of fibrin formation by rFI were similar to those by pdFI. The fibrin from rFI had significantly thicker fibers and a lower proportion of branching than clots from pdFI. We then used this material as a tissue sealant to study the function of fibrin made from rFI in a porcine hepatic injury model. In two different swine liver surgical trauma models, rFI formed a more opaque, histologically dense, wound-adherent fibrin clot that more rapidly stopped bleeding than pdFI.

ASSOCIATED CONTENT

Supporting Information

(1) Schematic illustrations of the three separate FI transgenes used in making the transgenic cows and a corresponding southern blot; (2) flow diagram of the purification process of rFI from milk and purity of rFI by size exclusion chromatography. This material is available free of charge via the Internet at http://pubs.acs.org.

AUTHOR INFORMATION

Corresponding Author

*E-mail: wvelander2@unl.edu. Phone: (402) 472-3697. Fax: (402) 472-6989.

Notes

The authors declare the following competing financial interest(s): The academic institution of W.H.V. has licensed recombinant fibrinogen technology to Pharming Group NV. W.H.V. has no financial interest in Pharming Group NV. M.G., H.V.V. and K.N. are employees of Pharming Group NV.

ACKNOWLEDGMENTS

We are grateful to Dr. Jason Johanning and Dr. Iraklis Pipinos for their assistance in the surgical procedures. Thanks to Dr. Mehmet Inan for the production of rFXIIIa and L. Smoyer of the University of Nebraska for technical assistance. We would like to acknowledge Dr. Roman Drews and the late Dr. William Drohan and Dr. Henryk Lubon for their contributions while at the American Red Cross Jerome Holland Laboratory. This research was primarily supported by a U.S.A. Medical Material Development Activity of the Army Grant (W81XWH-05-1-0527) to W.H.V, the American Red Cross and Pharming Group NV. This study is the result of work supported in part with resources and the use of facilities at the Omaha VA Medical Center.

REFERENCES

(1) Ferry, J. D. Proc. Natl. Acad. Sci. U.S.A. 1952, 38, 566−9.
(2) Mosesson, M. W. J. Thromb. Haemost. 2005, 3, 1894−904.
(3) Ariens, R. A.; Lai, T. S.; Weisel, J. W.; Greenberg, C. S.; Grant, P. J. Blood 2002, 100, 743.
(4) Laurens, N.; Koolwijk, P.; De Maat, M. P. M. J. Thromb. Haemost. 2006, 4, 932.
(5) Spotnitz, W. D.; Burks, S. Transfusion 2008, 48, 1502−16.
(6) Achneck, H. E.; Sileshi, B.; Jamiolkowski, R. M.; Albala, D. M.; Shapiro, M. L.; Lawson, J. H. Ann. Surg. 2010, 251, 217−28.
(7) Elvin, C. M.; Brownlee, A. G.; Huson, M. G.; Tebb, T. A.; Kim, M.; Lyons, R. E.; Vuocolo, T.; Liyou, N. E.; Hughes, T. C.; Ramshaw, J. A. M.; Werkmeister, J. A. Biomaterials 2009, 30, 2059−2065.
(8) Gray, J. L.; Kang, S. S.; Zenni, G. C.; Kim, D. U.; Kim, P. I.; Burgess, W. H.; Drohan, W.; Winkles, J. A.; Haudenschild, C. C.; Greisler, H. P. J. Surg. Res. 1994, 57, 596−612.

(9) Pellegrini, G.; Ranno, R.; Stracuzzi, G.; Bondanza, S.; Guerra, L.; Zambruno, G.; Micali, G.; De Luca, M. Transplantation 1999, 68, 868−79.
(10) Linnes, M. P.; Ratner, B. D.; Giachelli, C. M. Biomaterials 2007, 28, 5298−5306.
(11) Dainiak, M. B.; Allan, I. U.; Savina, I. N.; Cornelio, L.; James, E. S.; James, S. L.; Mikhalovsky, S. V.; Jungvid, H.; Galaev, I. Y. Biomaterials 2009, 31, 67−76.
(12) Delgado, A. V.; Kheirabadi, B. S.; Fruchterman, T. M.; Scherer, M.; Cortez, D.; Wade, C. E.; Dubick, M. A.; Holcomb, J. B. J. Trauma: Inj., Infect., Crit. Care 2008, 64, 75−80.
(13) Spotnitz, W. D.; Prabhu, R. J. Long-Term Eff. Med. Implants 2005, 15, 245.
(14) Fenger-Eriksen, C.; Lindberg-Larsen, M.; Christensen, A. Q.; Ingerslev, J.; Sorensen, B. Br. J. Anaesth. 2008, 101, 769−773.
(15) Burnouf, T.; Goubran, H. A.; Radosevich, M.; Sayed, M. A.; Gorgy, G.; El-Ekiaby, M. Vox Sang. 2006, 91, 56−62.
(16) Horowitz, B.; Busch, M. Transfusion 2008, 48, 1739−53.
(17) Doolittle, R. F. Annu. Rev. Biochem. 1984, 53, 195.
(18) Weisel, J. W. Adv. Protein Chem. 2005, 70, 247.
(19) Chung, D. W.; Davie, E. W. Biochemistry (N.Y.) 1984, 23, 4232−6.
(20) Fornace, A. J., Jr.; Cummings, D. E.; Comeau, C. M.; Kant, J. A.; Crabtree, G. R. J. Biol. Chem. 1984, 259, 12826−30.
(21) Uitte de Willige, S.; de Visser, M. C. H.; Houwing-Duistermaat, J. J.; Rosendaal, F. R.; Vos, H. L.; Bertina, R. M. Blood 2005, 106, 4176−4183.
(22) Mosesson, M. W.; Cooley, B. C.; Hernandez, I.; Diorio, J. P.; Weiler, H. J. Thromb. Haemost. 2009, 7, 102−10.
(23) Cheung, E. Y. L.; Uitte de Willige, S.; Vos, H. L.; Leebeek, F. W. G.; Dippel, D. W. J.; Bertina, R. M.; de Maat, M. P. M. Stroke 2008, 39, 1033−1035.
(24) Lovely, R. S.; Falls, L. A.; Al-Mondhiry, H. A.; Chambers, C. E.; Sexton, G. J.; Ni, H.; Farrell, D. H. Thromb. Haemost. 2002, 88, 26−31.
(25) Farrell, D. H.; Mulvihill, E. R.; Huang, S. M.; Chung, D. W.; Davie, E. W. Biochemistry (N.Y.) 1991, 30, 9414−20.
(26) Martin, S. C.; Ekman, P.; Forsberg, P. O.; Ersmark, H. Thromb. Res. 1992, 68, 467−73.
(27) Langer, B. G.; Weisel, J. W.; Dinauer, P. A.; Nagaswami, C.; Bell, W. R. J. Biol. Chem. 1988, 263, 15056−63.
(28) Marchi, R.; Arocha-Pinango, C. L.; Nagy, H.; Matsuda, M.; Weisel, J. W. J. Thromb. Haemost. 2004, 2, 940−8.
(29) Gersh, K. C.; Nagaswami, C.; Weisel, J. W.; Lord, S. T. Thromb. Res. 2009, 124, 356−363.
(30) Cooper, A. V.; Standeven, K. F.; Ariens, R. A. Blood 2003, 102, 535−40.
(31) Siebenlist, K. R.; Mosesson, M. W.; Hernandez, I.; Bush, L. A.; Di Cera, E.; Shainoff, J. R.; Di Orio, J. P.; Stojanovic, L. Blood 2005, 106, 2730−2736.
(32) Thiel, K. A. Nat. Biotechnol. 2004, 22, 1365−1372.
(33) Wurm, F. M. Nat. Biotechnol. 2004, 22, 1393−1398.
(34) Powell, K. Nat. Biotechnol. 2003, 21, 965−967.
(35) Echelard, Y.; Ziomek, C. A.; Meade, H. M. BioPharm Int. 2006, 19, 36−40 42, 44, and 46..
(36) Morcol, T.; Akers, R. M.; Johnson, J. L.; Williams, B. L.; Gwazdauskas, F. C.; Knight, J. W.; Lubon, H.; Paleyanda, R. K.; Drohan, W. N.; et al. Ann. N.Y. Acad. Sci. 1994, 721, 218−33.
(37) Edmunds, T.; Van Patten, S. M.; Pollock, J.; Hanson, E.; Bernasconi, R.; Higgins, E.; Manavalan, P.; Ziomek, C.; Meade, H.; McPherson, J. M.; Cole, E. S. Blood 1998, 91, 4561−4571.
(38) Adiguzel, C.; Iqbal, O.; Demir, M.; Fareed, J. Clin. Appl. Thromb./Hemostasis 2009, 15, 645−651.
(39) Prunkard, D.; Cottingham, I.; Garner, I.; Bruce, S.; Dalrymple, M.; Lasser, G.; Bishop, P.; Foster, D. Nat. Biotechnol. 1996, 14, 867.
(40) Butler, S.; O'Sickey, T.; Lord, S.; Lubon, H.; Gwazdauskas, F.; Velander, W. Transgenic Res. 2004, 13, 437.
(41) Lubon, H.; Paleyanda, R. K.; Velander, W. H.; Drohan, W. N. Transfus. Med. Rev. 1996, 10, 131−43.
(42) Butler, S. P.; Van Cott, K.; Subrumanian, A.; Gwazduaskas, F. C.; Velander, W. H. Thromb. Haemost. 1997, 78, 537.
(43) Platenburg, G. J.; Kootwijk, E. P. A.; Kooiman, P. M.; Woloshuk, S. L.; Nuijens, J. H.; Krimpenfort, P. J. A.; Pieper, F. R.; de Boer, H. A.; Strijker, R. Transgenic Res. 1994, 3, 99−108.
(44) Forsberg, E. J.; Strelchenko, N. S.; Augenstein, M. L.; Betthauser, J. M.; Childs, L. A.; Eilertsen, K. J.; Enos, J. M.; Forsythe, T. M.; Golueke, P. J.; Koppang, R. W.; Lange, G.; Lesmeister, T. L.; Mallon, K. S.; Mell, G. D.; Misica, P. M.; Pace, M. M.; Pfister-Genskow, M.; Voelker, G. R.; Watt, S. R.; Bishop, M. D. Biol. Reprod. 2002, 67, 327−333.
(45) Anumula, K. R.; Dhume, S. T. Glycobiology 1998, 8, 685−694.
(46) Ceroni, A.; Dell, A.; Haslam, S. M. Source Code Biol. Med. 2007, 2, DOI: 10.1186/1751-0473-2-3.
(47) Gorkun, O. V.; Veklich, Y. I.; Weisel, J. W.; Lord, S. T. Blood 1997, 89, 4407.
(48) Park, D.-S.; Kim, J.-H.; Lee, S. W.; Jeong, J.-M. Biotechnol. Lett. 2002, 24, 97−101.
(49) Chandler, W. L. Semin. Thromb. Hemost. 1995, 21 (Suppl 4), 1.
(50) Prasad, S.; Lillicrap, D.; Labelle, A.; Knappe, S.; Keller, T.; Burnett, E.; Powell, S.; Johnson, K. W. Blood 2008, 111, 672−679.
(51) Holcomb, J. B.; Pusateri, A. E.; Harris, R. A.; Charles, N. C.; Gomez, R. R.; Cole, J. P.; Beall, L. D.; Bayer, V.; MacPhee, M. J.; Hess, J. R. J. Trauma 1999, 46, 49−57.
(52) Holcomb, J. B.; Pusateri, A. E.; Harris, R. A.; Reid, T. J.; Beall, L. D.; Hess, J. R.; MacPhee, M. J. J. Trauma 1999, 47, 233−40 discussion 240−2..
(53) Pusateri, A. E.; Modrow, H. E.; Harris, R. A.; Holcomb, J. B.; Hess, J. R.; Mosebar, R. H.; Reid, T. J.; Nelson, J. H.; Goodwin, C. W., Jr.; Fitzpatrick, G. M.; McManus, A. T.; Zolock, D. T.; Sondeen, J. L.; Cornum, R. L.; Martinez, R. S. J. Trauma: Inj., Infect., Crit. Care 2003, 55, 518−526.
(54) McDonagh, R. P., Jr.; McDonagh, J. M.; Blomback, M.; Blomback, B. FEBS Lett. 1971, 14, 33−6.
(55) Morell, A. G.; Gregoriadis, G.; Scheinberg, I. H.; Hickman, J.; Ashwell, G. J. Biol. Chem. 1971, 246, 1461−7.
(56) Townsend, R. R.; Hilliker, E.; Li, Y. T.; Laine, R. A.; Bell, W. R.; Lee, Y. C. J. Biol. Chem. 1982, 257, 9704−10.
(57) Spik, G.; Coddeville, B.; Mazurier, J.; Bourne, Y.; Cambillaut, C.; Montreuil, J. Adv. Exp. Med. Biol. 1994, 357, 21−32.
(58) Siebenlist, K. R.; Meh, D. A.; Mosesson, M. W. Biochemistry (N.Y.) 1996, 35, 10448−53.
(59) Bingham, E. W.; Farrell, H. M., Jr. J. Biol. Chem. 1974, 249, 3647−51.

journal of surgical research xxx (2013) 1–9

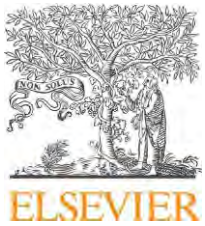

Available online at www.sciencedirect.com

ScienceDirect

journal homepage: www.JournalofSurgicalResearch.com

A totally recombinant human fibrin Sealant

Mark A. Carlson, MD,[a,c,*] Jennifer Calcaterra, PhD,[d] Jason M. Johanning, MD,[b,c] Iraklis I. Pipinos, MD,[b,c] Crystal M. Cordes, PhD,[e] and William H. Velander, PhD[d]

[a] Department of Surgery, University of Nebraska Medical Center, Omaha, Nebraska
[b] Department of Vascular Surgery, University of Nebraska Medical Center, Omaha, Nebraska
[c] VA Nebraska–Western Iowa Health Care System, Omaha, Nebraska
[d] Department of Chemical and Biomolecular Engineering, University of Nebraska–Lincoln, Lincoln, Nebraska
[e] Department of Obstetrics and Gynecology, University of Nebraska Medical Center, Omaha, Nebraska

article info

Article history:
Received 10 June 2013
Received in revised form
25 September 2013
Accepted 26 September 2013
Available online xxx

Keywords:
Fibrin sealant
Hemostasis
Hemorrhage
Swine
Fibrinogen
Factor XIII
Thrombin
Recombinant
Human

abstract

Background: Applications of plasma-derived human fibrin sealants (pdhFS) have been limited because of cost, limited supply of pathogen-screened plasma, the need for bioengineering improvements, and regulatory issues associated with federal approval. We describe a totally recombinant human fibrin sealant (rhFS), which may engender an abundant, safe, and cost-effective supply of efficacious fibrin sealant.

Materials and methods: A first-generation rhFS made from recombinant human fibrinogen (rhFI; produced in the milk of transgenic cows), activated recombinant human factor XIII (rhFXIIIa; produced in yeast), and recombinant human thrombin (rhFIIa; purchased, made in animal cell culture) was formulated using thromboelastography (TEG). The hemostatic efficacy of rhFS versus commercial pdhFS was compared in a nonlethal porcine hepatic wedge excision model.

Results: The maximal clot strength of rhFS measured in vitro by TEG was not statistically different than that of pdhFS. TEG analysis also showed that the rhFS gained strength more quickly as reflected by a steeper α angle; however, the rhFS achieved this clot strength with a 5-fold lower factor I content than the pdhFS. When these fibrin sealants were studied in a porcine hepatic wedge excision model, the hemostatic scores of the rhFS were equivalent or better than that of the pdhFS.

Conclusions: The bioengineered rhFS had equivalent or better hemostatic efficacy than the pdhFS in a nonlethal hemorrhage model, despite the factor I concentration in the rhFS being about one-fifth that in the pdhFS. Because the rhFS is amenable to large-scale production, the rhFS has the potential to be more economical and abundant than the pdhFS, while having a decreased risk of blood-borne pathogen transmission.

1. Introduction

The use of dried plasma as a topical hemostatic aid was documented in 1909 [1]. The combination of relatively pure fibrinogen (factor I or FI) with thrombin to make fibrin glue or foam was described in 1944 [2], but it was not until improved purification technology became available that fibrin sealants (FS) became commercially available in the 1970s [1]. Since that time, the efficacy of FS products as a topical hemostat or tissue adhesive has been demonstrated in numerous elective clinical

Presented in part at the 6th Annual Academic Surgical Congress; February 3, 2011; Huntington Beach, California.

* Corresponding author. Surgery 112, VA Medical Center, 4101 Woolworth Ave, Omaha, NE 68105. Tel.: þ1 402 995 5371; fax: þ1 402 995 5370.
E-mail address: carlson.mark.a@gmail.com (M.A. Carlson).

0022-4804/$ – see front matter
http://dx.doi.org/10.1016/j.jss.2013.09.039

scenarios, including peripheral vascular procedures [3], total knee arthroplasty [4], reoperative cardiac procedures [5], pulmonary resection [6], bleeding duodenal ulcer [7], and partial nephrectomy [8]. FS alone was not useful during hepatectomy [9], but FS combined with a collagen matrix applied during liver resection reduced blood loss and/or postoperative drainage compared with standard operative care [10]. Examples of currently available FS formulations that use plasma-derived fibrinogen include Evicel (Ethicon, Inc) and Tisseel (Baxter Healthcare).

The United States Department of Defense has maintained an interest in the development of hemostatic devices using FS for control of traumatic hemorrhage [11]. There has been particular interest in hemostatic FS devices for use under coagulopathic conditions [12]. Topical hemostatic treatments that incorporate FS have been successfully used in porcine trauma models, including femoral vessel injury [13], aortic injury [14], and hepatic injury [15]. One notable FS-containing device for traumatic hemorrhage was the Dry Fibrin Sealant Dressing, produced by the American Red Cross [16]. The Dry Fibrin Sealant Dressing was efficacious in porcine models of lethal hemorrhage [12,17] and was anecdotally successful in military trauma but was discontinued due to fragility and cost issues [18].

The availability of a relatively abundant FS might increase innovation into FI-based hemostatic devices for the treatment of severe hemorrhage. The essential components of FS are: FI, the biomonomer from which fibrin polymer is made [19]; activated thrombin (factor IIa or FIIa), which catalyzes the formation of soluble fibrin from FI and also activates factor XIIIa [20]; and activated factor XIII (FXIIIa), which cross-links the fibrin polymer to itself (rendering it insoluble) and to the wound surface [21]. One abundant source for these clotting factors can be large-scale recombinant protein production.

The complexity of FI and FIIa necessitates that recombinant versions of these proteins be made in animal cells [22]. We recently reported the production of recombinant human FI (rhFI) made at high concentrations in the milk of dairy cows [23]. Recombinant human FIIa (rhFIIa) already is commercially available (Recothrom; ZymoGenetics, Inc, Seattle, WA) and has been approved for topical hemostatic therapy in the United States and in Europe [24]. In contrast to FI and FIIa, FXIIIa is less complex; its core catalytic unit (FXIIIA2), which is kinetically faster than the more complex tetrameric plasma-borne FXIII [21], has been produced at large scale in yeast. FXIII nomenclature and specific activity are summarized in Table 1. Recombinant FXIIIA2 (rFXIIIA2) currently is in clinical studies of FXIII replacement therapy [25]. In the present study, we used a porcine hepatic wedge resection model to compare the hemostatic efficacy of a fully recombinant human FS (rhFS), containing rhFI, rhFIIa, and recombinant human FXIIIa (rhFXIIIa), against a commercially available, plasma-derived human FS (pdhFS).

2. Materials and methods

2.1. Animal studies

The use of swine was approved by the Subcommittee of Animal Studies and by the Research and Development Committee at the Omaha VA Medical Center. The number of swine (n ¼ 6) used for each group in the two-group comparison of rhFS versus pdhFS (with hemostatic score as the outcome measurement) was determined with a statistical power analysis [26], using D/s (Cohen d, in which D is the desired difference in means set by the observer and s is the estimated standard deviation) ¼ 2.0, false-positive rate (a) ¼ 0.05, false-negative rate (b) ¼ 0.2, and power (p, or 1 e b) ¼ 0.8.

Table 1 e Sources of factor XIII activity.

Factor XIII species	Abbreviation	Activity (U/mg)
Plasma-derived tetrameric factor XIII	FXIII	40[*]; 6e8[y]
Plasma-derived, dimeric, catalytic subunit factor XIII	FXIIIA2	N/A
Recombinant dimeric catalytic subunit factor XIII	rFXIIIA2	140[z]
Plasma-derived, activated, dimeric factor XIII	FXIIIA2a	N/A
Recombinant human, activated factor XIII	rhFXIIIa	7000[x]

N/A ¼ not applicable.
[*] Activity based on normal plasma pool, which by definition is 1 U/mL.
[y] Reported activity of plasma FXIII [37].
[z] Reported activity of FXIIIA2 made in Saccharomyces cerevisiae [25].
[x] Reported activity of rFXIIIa made in Pichia pastoris [23].

2.2. Clotting factor sources

rhFI was produced in the milk of transgenic cows by inserting the primary sequence of the human transgenes for the a-, b-, and g-chains of fibrinogen into the cow genome by nuclear transfer [23]. Southern blot analysis confirmed the presence of the three transgenes. The rhFI expressed in the milk of the transgenic cows was characterized by sodium dodecyl sulfate-polyacrylamide gel electrophoresis (SDS-PAGE), Western blot, g and g′-chain content, fibrinopeptide phosphorylation, glycosylation, thrombin-catalyzed activation, thrombin-catalyzed protofibril formation, factor XIIIa-catalyzed molecular cross-linking, viscoelasticity, scanning electron microscopy, and tissue sealant function [23]. The main differences between rhFI made in transgenic cow milk and pdFI was the g′-chain content [23].

The human FXIIIA1 gene was expressed in Pichia pastoris [23,27]. The expressed rhFXIIIa was characterized by SDS-PAGE, Western blot, Pefakit FXIII incorporation assay, FXIIIa-catalyzed molecular cross-linking of fibrin, and viscoelasticity [27]. Human rhFIIa (Recothrom) was purchased from ZymoGenetics, Inc. Human pdFI depleted of plasminogen, von Willebrand factor, and fibronectin was purchased from Enzyme Research Laboratories (South Bend, IN). Commercial human pdhFS (Tisseel, unless otherwise specified) was purchased from Baxter BioSurgery (Deerfield, IL).

2.3. Determination of clotting factor concentration and activity

The concentrations of the purified stocks of rhFI, pdFI, and rFXIIIa were determined by OD_{280} and the bicinchoninic acid

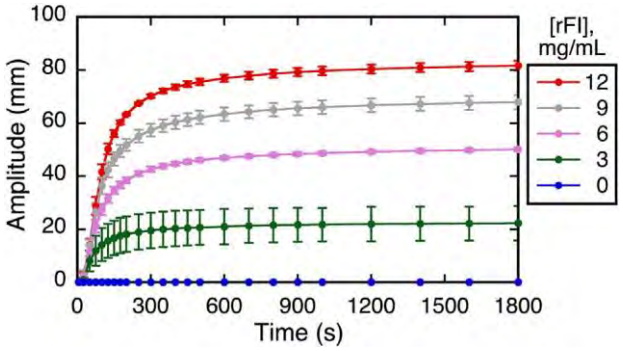

Fig. 1 e Thromboelastographic dose-response analysis of rhFI. Samples with constant concentrations of pdFIIa (53 U/mL) and rFXIIIa (2400 U/mL) were tested with varying concentrations of rhFI (0e12 mg/mL). Shown are the results from a single experiment with triplicate tubes; data are expressed as mean ± standard deviation.

assay [28]. The specific activity of rFXIIIa was estimated to be 7000 U/mg using the Pefakit FXIII Incorporation Assay (Pentapharm, Norwalk, CT).

2.4. Thromboelastography

The effect of rhFI concentration on clot formation kinetics and strength (Fig. 1) was determined with thromboelastography (TEG), using a TEG 5000 Thrombelastograph (Haemonetics Corp, Braintree, MA). rhFI (0e12 mg/mL) was incubated at 37°C with rhFIIa (53 U/mL), rFXIIIa (2400 U/mL), and $CaCl_2$ (12 mM). For the comparison of rhFS versus pdhFS, the latter was prepared as per the manufacturer's instructions by mixing the sealant and thrombin solutions in equal proportions in the TEG assay cup at 37°C. For the rhFS, rhFI (9 mg/mL) was incubated at 37°C in the cup with rhFIIa (106 U/mL), rFXIIIa (2500 U/mL), and $CaCl_2$ (12 mM). The thromboelastograph was calibrated each day of use; each time point of each analysis was run in triplicate. TEG Analytical Software (version 4.2.2) was used to calculate the time to clot initiation (R), time to clot firmness of 20 mm (K), alpha angle (a), maximal clot strength (maximal amplitude [MA], which was directly related to the shear elastic modulus strength, G), and percent lysis 60 min after MA (LY60) [29]. A single-factor analysis of variance was performed to compare the effect of plasmin on pdhFS and rhFS. The Student t-test (two-tailed, with unequal variances) was used to compare rhFS and pdhFS, with alpha set at 0.05.

2.5. Immunoblotting

Immunoblotting was used to estimate the mass concentrations of FXIII in the commercial pdhFS (Tisseel). Reduced samples were resolved with SDS-PAGE on 4%e12% NuPage Bis-Tris gels (Invitrogen, Carlsbad, CA) and then transferred onto polyvinylidene fluoride membranes (Millipore, Billerica, MA). Blots were probed with polyclonal antibodies for FXIII (F0019-46; United States Biological, Swampscott, MA) or FIIa (T5045-10B; United States Biological).

2.6. Swine hepatic injury models

Domestic swine (castrated males, aged 3 mo, weight 33e36 kg) were purchased from the Agricultural Research and Development Center (Mead, NE) of the University of NebraskaeLincoln. Each subject was fasted for 12 h before surgery, but with free access to water. Each subject was premedicated with Telazol (4.4 mg/kg; Zoetis, Madison, NJ), ketamine (2.2 mg/kg), and xylazine (2.2 mg/kg) as a single intramuscular injection. An intravenous line was established in an auricular vein, oral endotracheal intubation was performed, and anesthesia was maintained with 0.5%e1.5% isoflurane using a Matrx VMS veterinary anesthesia machine (Midmark Corp, Versailles, OH). Mechanical ventilation was maintained at 12e15 breaths/min with a tidal volume of 10e15 mL/kg, to keep the end-tidal pCO_2 at 30e35 mm Hg. A heating pad was under each subject to support body temperature. A carotid arterial catheter was placed for pressure monitoring and blood sampling, and a jugular venous catheter was placed for isotonic fluid and medication administration, all via a surgical cutdown in the left neck. Arterial pressure, end-tidal pCO_2, rectal temperature, cardiac electrical activity, and pulse oximetry were continuously recorded with a Bionet BM5 Veterinary Monitor (Bionet America, Inc, Tustin, CA) interfaced to a laptop computer. Each swine subject was maintained under an appropriate level of isoflurane anesthesia (indicated by the absence of corneal reflex) for the duration of the experiment; before euthanasia, the isoflurane was increased (see the following sections).

The porcine normothermic nondilutional stellate liver laceration model was adapted from a previous description [17]. After the above initial setup, a ventral midline incision was made, splenectomy was performed, and a transabdominal cystostomy tube was placed. Splenectomy generally has been performed in severe porcine hemorrhage models to eliminate the confounding effects of splenic autotransfusion [30]. A liver laceration was created with a custom-built liver injury clamp (Fig. 2A, inset), which consisted of tines in an X-configuration (5 cm diameter) on one arm of the clamp, and a base plate on the other arm onto which the tines seat. The base plate was placed on the inferior surface of the liver against the quadrate lobe, between the cystic duct and the portal vein. The tines were positioned over the liver dome, 4e5 cm anterior to the vena cava at the base of the left medial hepatic segment. The clamp then was closed, forcing the tines through the liver dome and onto the base plate. The test sealant (10 mL) then was applied immediately into the laceration, and the edges of the laceration were held together with manual compression for 5 min. Only one clamp application per subject was performed. No other hemostatic maneuver (e.g., cotton gauze, laparotomy packs, Pringle maneuver) was used other than sealant with manual compression. This model was intended for preliminary qualitative observation of sealant efficacy only. Quantitative data (blood loss volume, mean arterial pressure, and so forth) was not recorded for the stellate laceration model.

For the wedge excision model, a ventral midline incision was made and a cystostomy tube was placed. The left lobe of

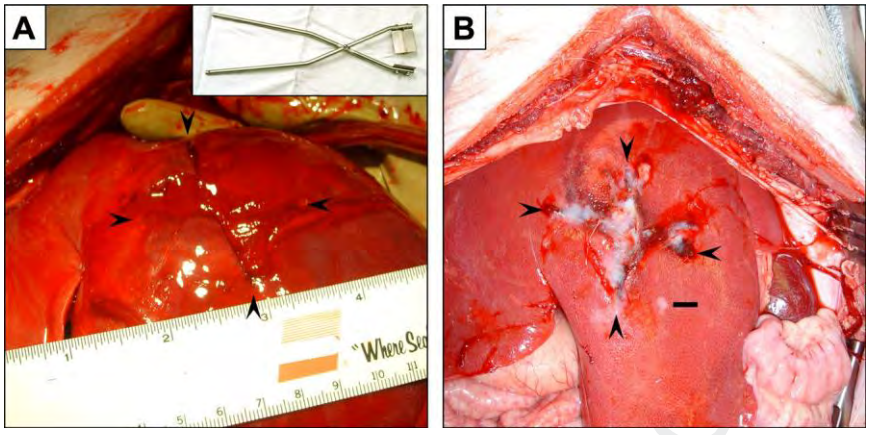

Fig. 2 e Treatment of porcine hepatic stellate laceration with human FS. The liver is shown in situ exposed through a ventral midline incision, immediately after FS application to the injury; top of each image is cephalad. (A) pdhFS treatment; the liver injury clamp is shown in the inset. (B) rhFS treatment (Table 2 formulation). Bar ▮ 1 cm; arrowheads indicate peripheral extent of the stellate hole made by the clamp tines.

the liver was exteriorized, and sites for wedge-shaped ("pie-slice") hepatic excisions were lightly scored with electrocautery on the liver capsule (Fig. 3A) along the anterior edge of both the left medial and left lateral segment (two separate but identical series of wedge excisions per subject). The base of each excision (i.e., distance along the lobar edge) was maintained constant at 1 cm. The excision depth (i.e., distance from lobar edge to apex of excision; Fig. 3A) of each series ranged from 0.5 to 3.0 cm, in crescendo fashion using 0.5 cm increments, for a total of six excisions per series, all cut with scissors (Supplementary Video File). Two such series of excisions were performed per subject, for a total of 12 excisions per subject. Only one type of sealant (either the rhFS or pdhFS) was used in any given subject.

Each excision was treated immediately with up to 1 mL of FS without digital or gauze compression or other adjunct (Supplementary Video File). pdhFS (Tisseel) was administered with the double-barrel common-channel syringe system (Duploject; Fig. 3C) provided by the manufacturer, as per the user instructions. The rhFS (as defined in Table 2) was administered using two 1 mL syringes taped together, with 30 gauge needles bent into convergence (Fig. 3D). One syringe contained the rhFI and rFXIIIa, and the other syringe contained the rhFIIa and calcium.

Hemostasis 30 s after treatment of each excision was scored as follows: 0 ¼ failure/minimal hemostasis; 1 ¼ decreased but steady bleeding; 2 ¼ oozing; and 3 ¼ hemostasis. Quantification of the small amount of blood loss, which occurred during the treatment phase, did not produce reliable data, so the above visual analog score of hemostasis was used. If an excision was not hemostatic 30 s after application of 1 mL of the test sealant, then the excision was packed with cotton gauze before performing the next excision, to minimize the ongoing blood loss. Excisions were performed during a single nonsurvival anesthetic, which lasted for 30e45 min. After completion of the two series of excisions, each subject was administered 5% isoflurane for 3 min, the supradiaphragmatic IVC then was transected, and each subject was allowed to expire from exsanguination while under deep isoflurane anesthesia.

2.7. Fibrinogen immunohistochemistry

Liver specimens were fixed in 10% neutral-buffered formalin, dehydrated, and then embedded in paraffin blocks. Paraffin sections (5 mm) underwent antigen retrieval with Target Retrieval Solution (Dako North America, Carpinteria, CA) as per the manufacturer's instructions. The presence of both human and swine fibrinogen were detected by sequential dual-immunohistochemical staining followed by a hematoxylin counterstain. Signal detection was performed using the Dako EnVision G/2 Doublestain System, as per the manufacturer's instructions. Briefly, endogenous peroxidase and alkaline phosphatase activity present in the tissue were blocked and then the swine fibrinogen antibody (Kamiya Biomedical Company, Seattle, WA) was applied and visualized using the horseradish peroxidase/3,3′-diaminobenzidine tetrahydrochloride reagents from the Dako system. A second blocking step was performed before incubation with the human fibrinogen antibody (Abcam, Inc, Cambridge, MA). The human fibrinogen antibody was visualized using alkaline phosphataseebased Permanent Red (Dako North America), as per the manufacturer's instructions.

3. Results

3.1. Effect of FI on clot formation

The effect of rhFI concentration (0e12 mg/mL) on the kinetics and strength of clot formation with rhFS was analyzed by TEG (Fig. 1). The speed of clot formation, as measured by clot initiation time (R), time to clot firmness (K), and angle (a), increased as the rhFI concentration was increased to 6 mg/mL but remained constant >6 mg/mL of rhFI (R ¼ 17 s, K ¼ 50 s, a ¼ 82°). The maximal clot strength (MA) continued to increase with each increase of rhFI concentration (up to 80 mm with rhFI ¼ 12 mg/mL). For further in vivo studies, we targeted an rhFI concentration of 9 mg/mL in the rhFS, which generated MA >50 mm. At constant rhFI concentration, the calcium

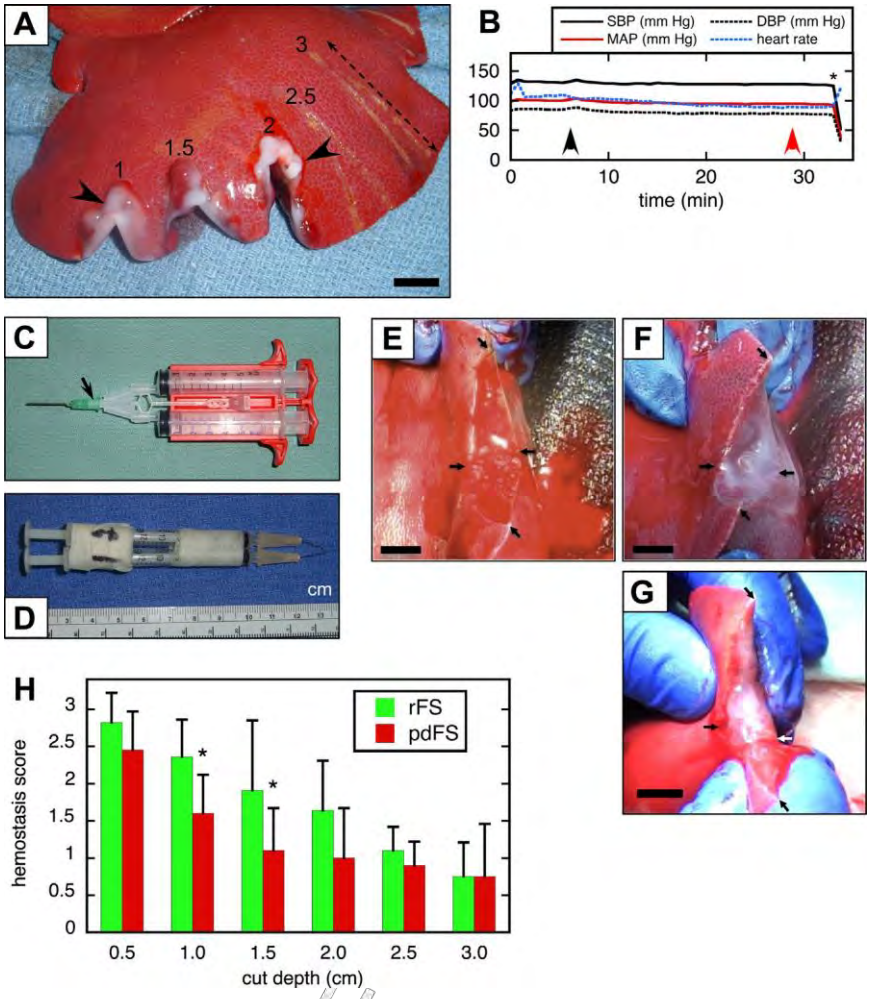

Fig. 3 e Porcine hepatic wedge excision model. (A) Intraoperative view of anterolateral edge of left lateral liver lobe during an excision procedure; top of picture is cephalad. The numbers above each excision indicate cut depth in centimeters. Excisions 1, 1.5, and 2 already were cut and treated with rhFS (arrowheads indicate white clot of sealant); excisions 2.5 and 3 were scored with cautery but had not yet been cut. Excision "depth" is dimension indicated by dashed line. (B) Vital sign recording during a typical procedure. DBP [diastolic blood pressure; MAP [mean arterial pressure; SBP [systolic blood pressure; black arrowhead [start of procedure; red arrowhead [completion of procedure; *euthanasia (IVC transection). (C) Proprietary dual-chamber syringe device (Duploject) for administration of the commercial pdhFS. Arrow indicates common mixing channel. (D) Improvised double syringe assembly for administration of the rhFS. (E) Individual wedge cut of 2 cm depth, immediately before treatment. Arrows indicate corners of excision (excision depth may appear >2 cm because some distraction occurs during handling). (F) Wedge cut in (B) immediately after treatment with rhFS. (G) A separate 1-cm deep wedge cut, immediately after treatment with commercial pdhFS. Bars [1 cm. (H) Hemostasis scores of hepatic wedge excisions treated with rhFS (Table 2 formulation) versus commercial pdhFS. Each bar represents mean score ± standard deviation of 10e12 excisions; taller bar [better hemostasis. *P < 0.05, Wilcoxon signed-rank test. Q14

concentration (3e15 mM) did not affect the thromboelastographic parameters of the rhFS (data not shown).

3.2. Thromboelastography of pdhFS versus rhFS

The formulation of the first-generation rhFS formulation is compared with commercial pdhFS (Tisseel) in Table 2. The concentration of fibrinogen was about 5-fold greater in the pdhFS with respect to the rhFS. Furthermore, the pdhFS contained ~2-fold higher level of FIIa than the rhFS. The rhFS, however, had ~50-fold higher FXIII activity compared with the pdhFS. When evaluated by TEG (Table 3), the rhFS had significantly faster clotting kinetics compared with pdhFS, as measured by the angle of clot development (a) (Table 3); the maximal clot strength (MA) was not statistically different (P ¼ 0.059) nor were the R and K values.

3.3. Treatment of stellate liver laceration with rhFS versus pdhFS

Preliminary experiments with the sealants in a porcine liver laceration model suggested that the rhFS had better

Table 2 e Comparison of component concentration and activity in pdhFS versus rhFS.

Component	pdhFS	rhFS
Fibrinogen (FI)	34e53 mg/mL	9 mg/mL
Thrombin (FII)	200e313 U/mL*	106 U/mL
Factor XIII/XIIIa		
Concentration	<0.1 mg/mL[y]	0.36 mg/mL
Activity	10e50 U/mL[z]	2475 U/mL
$CaCl_2$	18e22 mM	12 mM
Fibrinolysis inhibitor	2250e3750 KIU/mL	0

KIU ¼ Kallikrein Inhibitor Unit.
* Tisseel package insert information.
[y] Based on immunoblot analysis (data not shown).
[z] As reported on www.rxmed.com [38].

hemostatic efficacy compared with the commercial pdhFS (Fig. 2). Injection of 10 mL of pdhFS into a stellate laceration of the liver dome followed by 5 min of manual compression resulted in persistent hemorrhage (Fig. 2A); on the other hand, hemostasis was achieved with the rhFS treatment (Fig. 2B; N ¼ 2 swine per sealant). Subjectively, the white clot generated by the rhFS set up quicker, appeared more opaque, and felt more adherent than the clot generated by the pdhFS. Postmortem examination of the liver ex vivo demonstrated that one large hepatic vein was injured in each subject; there were no major portal, biliary, or hepatic artery injuries.

3.4. rhFS versus pdhFS in the hepatic wedge excision model

To determine whether there were differences in hemostatic efficacy between rhFS and pdhFS, the hemostasis assay in Figure 3, involving small hepatic wedge excisions, was devised expressly for this study. The primary determinant in this assay was the hemostatic action of the sealant alone; that is, there would be no external compression of the bleeding surfaces by the surgeon. In brief, wedges cut were made along the edge of a liver lobe (Fig. 3A), treated with a defined amount of sealant, and then a visual analog hemostasis score was assigned. Preliminary work with this model demonstrated that bleeding from an excision with a 0.5-cm cut depth was easy to control with sealant alone, whereas bleeding from 3-cm excision was quite difficult to control. So a range of excisions with a stepwise increase in cut depth (0.5e3 cm) was chosen as a discriminator of hemostatic efficacy. This range (or series) of excisions was performed twice in each subject, on separate liver lobes during the same anesthetic. Each subject tolerated these procedures well with <150 mL blood loss and minimal to no perturbation in vital signs (Fig. 3B). TEG of blood drawn immediately before versus after procedure completion did not demonstrate any deterioration of clotting during the excisions (done in all subjects; data not shown). Q11

Table 3 e TEG parameters of pdhFS (commercial) and rhFS.

Fibrin sealant	R (s)	K (s)	a (°)	MA (mm)
rhFS	10.33 ± 0.75	50 ± 0.0	85.07 ± 1.12*	63.15 ± 12.12
pdhFS	9.44 ± 1.36	54.45 ± 8.67	81.66 ± 2.93	77.41 ± 5.49

a ¼ kinetics of clot development; K ¼ achievement of 20 mm clot strength (amplitude); MA ¼ maximal amplitude (maximum clot strength); R ¼ reaction time (first evidence of clot formation).
Values are mean ± standard deviation of five and six separate experiments on multiple batches of rhFS (formulation in Table 2) and commercial pdhFS (Tisseel), respectively.
* P ¼ 0.034 compared with pdhFS, unpaired t-test.

The intended technique of FS delivery was to use a double-chamber single-channel syringe (a proprietary device for delivery of the pdhFS; Fig. 3C) in all subjects. This device keeps the fibrinogen and the activated thrombin in separate chambers; when the operator depresses the linked syringe plungers, the protein solutions are mixed in a common channel and then ejected from the syringe tip. Use of this device with the proprietary pdhFS produced a reasonably consistent stream of sealant with occasional clogging of the tip. Initial attempts at delivery of the rhFS with this proprietary double-chamber single-channel syringe, however, resulted in tip clogging before adequate rhFS could be delivered to the wound. To deliver the rhFS to the wound, the improvised delivery system shown in Figure 3D was used. Two tuberculin-type syringes were taped together, and the needles were bent to produce a convergent stream. This syringe setup moved the mixing of the rhFS components from inside the syringe assembly to outside on the wound surface, which enabled rhFS delivery at a volume and flow subjectively equivalent to that obtained with the pdhFS.

The subjective impression from treating hepatic wedge excisions with rhFS versus pdhFS confirmed the earlier observation from the hepatic laceration model, that is, the clot produced by the rhFS set up quicker, was more opaque, and was more tenacious/adherent than the clot produced by the pdhFS (Fig. 3A,F,G). A comparative analysis of hemostatic efficacy of these two sealants in the hepatic wedge excision model is shown in Figure 3H. Overall, the hemostatic scores of the rhFS were equivalent or better than those of the pdhFS. Q12 At cut depths of 1.0 and 1.5 cm, the rhFS had greater hemostatic efficacy than the pdhFS; there was a nonsignificant trend of greater efficacy at the 2.0 cm depth. At cut depth ≥2.5 cm, the hemorrhage mostly was too brisk to control with either sealant in the absence of any extrinsic compression (Fig. 3H).

3.5. Immunohistochemistry

Double immunohistochemistry of porcine and human FI in treated wedge excisions is shown in Figure 4. The fibrin cap over the hepatic wound surface typically was thicker in the rhFS sections compared with the pdhFS sections. These double-stained sections also demonstrated the mixing of the native porcine fibrin (brown color) with human (plasma-derived or recombinant) fibrin (red color) over the surface of the wound. In both the pdhFS- and rhFS-treated samples, the predominant FI in the clot appeared to be endogenous in origin (i.e., porcine). Additional images of hepatic wedge excisions treated with rhFS have been supplied in Supplementary Figure S1.

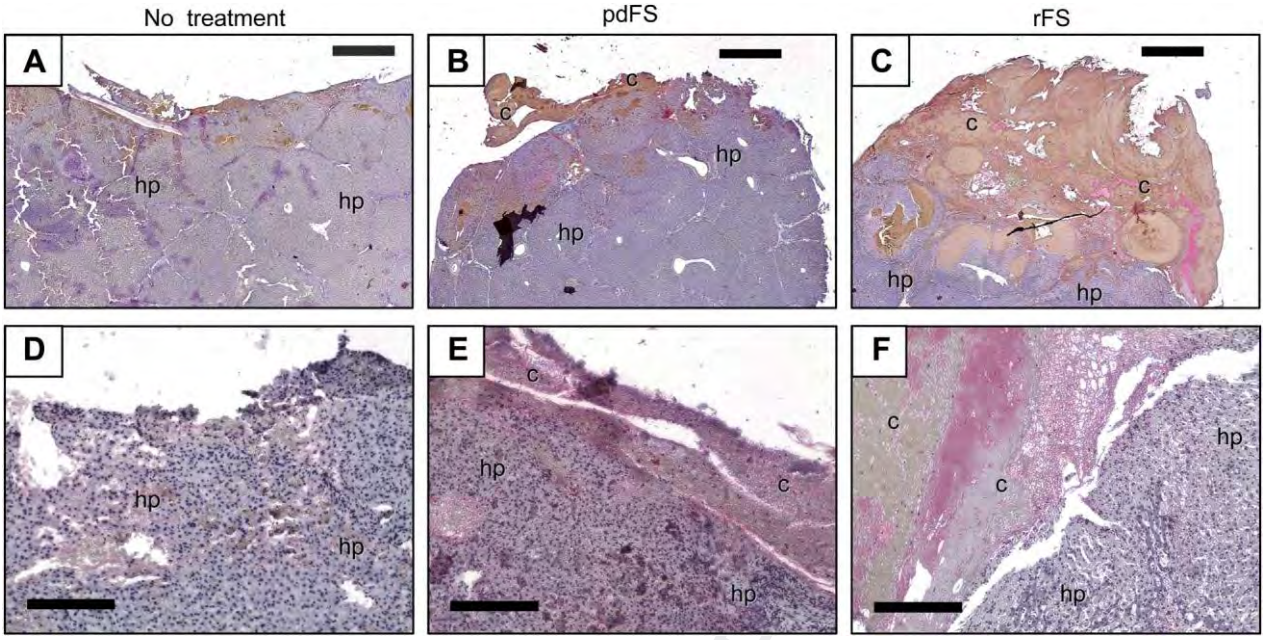

Fig. 4 e Factor FI immunohistochemistry of porcine hepatic wedge excision ± human FS treatment. Liver sections were double-stained for porcine (brown) and human (red) fibrinogen, with hematoxylin counterstain. (A and D) No treatment. (B and E) pdhFS treatment. (C and F) rhFS treatment. Bars: AeC [1 mm, DeF [200 mm; c [clot; hp [hepatic parenchyma. (For interpretation of the references to color in this figure legend, the reader is referred to the web version of this article.)

4. Discussion

Our intention in the design of this first-generation rhFS was to achieve clotting speed and strength comparable with an available pdhFS formulation, as determined by TEG. The commercial pdhFS used in this report had a clot onset of <10 s and maximal clot strength of 50e70 mm displacement. To obtain a clot onset of <10 s, 106 U/mL of rhFIIa was used (somewhat less than the level of FIIa contained in the pdhFS; Table 2). To obtain a maximal clot strength of >50 mm, 2500 U/mL of rFXIIIa were used. We believe that by providing a relatively large amount of rFXIII in its activated form, we produced higher rates of cross-linked fibrin formation and focused rhFIIa activity on conversion of fibrinogen to fibrin.

We were able to decrease the fibrinogen content of rhFS (9 mg rhFI/mL) relative to pdhFS (>50 mg pdFI/mL), while achieving the same in vitro clotting speed and strength. A typical dose of pdhFS applied to the stellate liver laceration model contained >340 mg of pdFI, whereas the typical dose of rhFS contained 90 mg of rhFI. The rhFS contained 3.6 mg per dose of rFXIIIa, whereas pdhFS contained a constitutive level of <1 mg FXIII. Importantly, when the rhFS and pdhFS were studied in the porcine hepatic wedge resection model, the rhFS had equivalent or greater hemostatic efficacy than commercial pdhFS, despite the fibrinogen concentration in the rhFS being only one-fifth that in the pdhFS.

The hemostatic potential of FS has been shown to be dependent on the degree of cross-linking achieved by FXIII [21]. Prior studies reported that depletion of FXIII in a commercial FS (Beriplast P; Aventis Behring, Marburg, Germany) decreased the ability of that sealant to control hemorrhage in porcine vascular procedures [31] and that the relative hemostatic efficacy of FS was dependent on the concentration of FXIII [32]. These previous data suggested that the optimal FXIII concentration in pdhFS was in the range of 40e80 U/mL when the pdFI concentration was 50e100 mg/mL. The data from the present study suggested that the use of rFXIIIa could produce an rhFS that had equivalent or better hemostatic properties than the pdhFS, even when the fibrinogen content of the former was relatively low.

For posttranslationally complex proteins, the signature of the host cells on the recombinant human protein potentially can cause immunologic and biologic activity issues. In the case of rhFI, the N-linked glycosylation added to the human protein sequence of the recombinant fibrinogen was the only notable posttranslational difference between pdhFS and rhFS [23]. We have seen no issues with the biologic activity of any of the recombinant proteins used in the rhFS. Definitive studies of immunologic effects would require human clinical trials.

We did not intend our hepatic wedge excision model to be a surrogate for more lethal models of traumatic hemorrhage [18], and we have not implied that rhFS or any other sealant might be useful as a stand-alone treatment for severe traumatic hemorrhage. The wedge excision model developed for this study was intended to quantify and compare the hemostatic efficacy of sealants acting without any other adjunct (such as manual compression) at the wound surface. We wanted to minimize variables that might have influenced or confounded the hemostatic activity of a sealant acting alone. We also did not intend to analyze the tissue fixation (welding or "glue") properties of the sealants, for example, for skin

grafting [33], reinforcement of gastrointestinal anastomosis [34], or sutureless anchorage of prosthetic mesh [35].

We previously estimated that it would require approximately 300 transgenic cows to produce 1 metric ton of purified rhFI per year [23]. An abundant source of rhFS might lead to increased innovation in traumatic hemostasis, acute wound stabilization, hernia surgery, and other biomaterial fields. In addition, an abundant source of recombinant fibrinogen for intravenous administration also could impact the treatment of hypofibrinogenemic conditions, such as the dilutional/consumptional state that can occur during resuscitation from traumatic hemorrhage [36]. Further studies on this condition using a hypothermic, hemodiluted swine model [12] are planned.

Acknowledgment

This was supported by grants from the United States Department of Defense W81XWH-11-1-0836 to M.A.C. and W81XWH-05-1-0527 to W.H.V. This study is the result of work supported in part with resources and the use of facilities at the VA Nebraska-Western Iowa Health Care System. The authors would like to acknowledge the anesthesia expertise of John Cavanaugh, and the technical assistance Chris Hansen and Dean Heimann. The authors declare that they have no financial relationships or conflicts of interest to disclose.

Appendix. Supplementary data

Supplementary data related to this article can be found at http://dx.doi.org/10.1016/j.jss.2013.09.039.

references

scientific rationale, production methods, properties, and current clinical use. Vox Sang 1997;72:133.

[2] Bering EA Jr. Chemical, clinical, and immunological studies on the products of human plasma fractionation. XX. A development of fibrin foam as a hemostatic agent and for use in conjunction with human thrombin. J Clin Invest 1944;23:586.

[3] Chalmers RTA, Darling RC III, Wingard JT, et al. Randomized clinical trial of tranexamic acid-free fibrin sealant during vascular surgical procedures. Br J Surg 2010;97:1784.

[4] Levy O, Martinowitz U, Oran A, Tauber C, Horoszowski H. The use of fibrin tissue adhesive to reduce blood loss and the need for blood transfusion after total knee arthroplasty. A prospective, randomized, multicenter study. J Bone Joint Surg 1999;81:1580.

[5] Rousou J, Levitsky S, Gonzalez-Lavin L, et al. Randomized clinical trial of fibrin sealant in patients undergoing resternotomy or reoperation after cardiac operations. A multicenter study. J Thorac Cardiovasc Surg 1989;97:194.

[6] Moser C, Opitz I, Zhai W, et al. Autologous fibrin sealant reduces the incidence of prolonged air leak and duration of chest tube drainage after lung volume reduction surgery: a prospective randomized blinded study. J Thorac Cardiovasc Surg 2008;136:843.

[7] Rutgeerts P, Rauws E, Wara P, et al. Randomized trial of single and repeated fibrin glue compared with injection of polidocanol in treatment of bleeding peptic ulcer. Lancet 1997;350:692.

[8] Siemer S, Lahme S, Altziebler S, et al. Efficacy and safety of TachoSil as hemostatic treatment versus standard suturing in kidney tumor resection: a randomized prospective study. Eur Urol 2007;52:1156.

[9] Figueras J, Llado L, Miro M, et al. Application of fibrin glue sealant after hepatectomy does not seem justified: results of a randomized study in 300 patients. Ann Surg 2007;245:536.

[10] Briceno J, Naranjo A, Ciria R, et al. A prospective study of the efficacy of clinical application of a new carrier-bound fibrin sealant after liver resection. Arch Surg 2010;145:482.

[11] Baer DG, Dubick MA, Wenke JC, et al. Combat casualty care research at the U.S. Army Institute of Surgical Research. J R Army Med Corps 2009;155:327.

[12] Holcomb JB, Pusateri AE, Harris RA, et al. Dry fibrin sealant dressings reduce blood loss, resuscitation volume, and improve survival in hypothermic coagulopathic swine with grade V liver injuries. J Trauma 1999;47:233.

[13] Larson MJ, Bowersox JC, Lim RC Jr, Hess JR. Efficacy of a fibrin hemostatic bandage in controlling hemorrhage from experimental arterial injuries. Arch Surg 1995;130:420.

[14] Kheirabadi BS, Acheson EM, Deguzman R, et al. The potential utility of fibrin sealant dressing in repair of vascular injury in swine. J Trauma 2007;62:94.

[15] Pusateri AE, Modrow HE, Harris RA, et al. Advanced hemostatic dressing development program: animal model selection criteria and results of a study of nine hemostatic dressings in a model of severe large venous hemorrhage and hepatic injury in swine. J Trauma 2003;55:518.

[16] Pusateri AE, Kheirabadi BS, Delgado AV, et al. Structural design of the dry fibrin sealant dressing and its impact on the hemostatic efficacy of the product. J Biomed Mater Res Part B 2004;70B:114.

[17] Holcomb JB, Pusateri AE, Harris RA, et al. Effect of dry fibrin sealant dressings versus gauze packing on blood loss in grade

[18] Pusateri AE, Holcomb JB, Kheirabadi BS, Alam HB, Wade CE, Ryan KL. Making sense of the preclinical literature on advanced hemostatic products. J Trauma 2006;60:674.

[19] Mosesson MW. Fibrinogen and fibrin structure and functions. J Thromb Haemost 2005;3:1894.

comparison of fibrin sealants in relation to their in vitro and in vivo properties. Thromb Res 2003;112:73.

[21] Ariens RA, Lai TS, Weisel JW, Greenberg CS, Grant PJ. Role of factor XIII in fibrin clot formation and effects of genetic polymorphisms. Blood 2002;100:743.

[22] Wurm FM. Production of recombinant protein therapeutics in cultivated mammalian cells. Nat Biotechnol 2004;22:1393.

[23] Calcaterra J, Van Cott KE, Butler SP, et al. Recombinant human fibrinogen that produces thick fibrin fibers with increased wound adhesion and clot density. Biomacromolecules 2013;14:169.

[24] Singla NK, Foster KN, Alexander WA, Pribble JP. Safety and immunogenicity of recombinant human thrombin: a pooled analysis of results from 10 clinical trials. Pharmacotherapy 2012;32:998.

[25] Lovejoy AE, Reynolds TC, Visich JE, et al. Safety and pharmacokinetics of recombinant factor XIII-A2 administration in patients with congenital factor XIII deficiency. Blood 2006;108:57.

[26] Neter J, Wasserman W, Kutner MH. Applied Linear Statistical Models. 3rd ed. Boston: Irwin Publishing Co.; 1990.

[27] Park D-S, Kim J-H, Lee SW, Jeong J-M. Secretory expression of the a-subunit of human coagulation factor XIII in the yeast Pichia pastoris. Biotechnol Lett 2002;24:97.

[28] Olson BJSC, Markwell J. Assays for determination of protein concentration. Curr Protoc Pharmacol 2007;Appendix 3:3A.
[29] Chandler WL. The thromboelastography and the thromboelastograph technique. Semin Thromb Hemost 1995;21(Suppl 4):1.
[30] Devlin JJ, Kircher SJ, Littlejohn LF. Swine models of hemorrhagic shock: to splenectomize or not to splenectomize, that is the question. J Trauma 2009;67:895.
[31] Dickneite G, Metzner H, Nicolay U. Prevention of suture hole bleeding using fibrin sealant: benefits of factor XIII. J Surg Res 2000;93:201.
[32] Dickneite G, Metzner HJ, Kroez M, Hein B, Nicolay U. The importance of factor XIII as a component of fibrin sealants. J Surg Res 2002;107:186.
[33] Foster K, Greenhalgh D, Gamelli RL, et al. Efficacy and safety of a fibrin sealant for adherence of autologous skin grafts to burn wounds: results of a phase 3 clinical study. J Burn Care Res 2008;29:293.
[34] Silecchia G, Boru CE, Mouiel J, et al. The use of fibrin sealant to prevent major complications following laparoscopic gastric bypass: results of a multicenter, randomized trial. Surg Endosc 2008;22:2492.
[35] Eriksen JR, Bisgaard T, Assaadzadeh S, Jorgensen LN, Rosenberg J. Randomized clinical trial of fibrin sealant versus titanium tacks for mesh fixation in laparoscopic umbilical hernia repair. Br J Surg 2011;98:1537.
[36] Hess JR, Lawson JH. The coagulopathy of trauma versus disseminated intravascular coagulation. J Trauma 2006;60:S12.
[37] Balogh I, Szoke G, Karpati L, et al. Val34Leu polymorphism of plasma factor XIII: biochemistry and epidemiology in familial thrombophilia. Blood 2000;96:2479.
[38] Tisseel® Kit VH Baxter Fibrin Sealant Prescribing Information. http://www.rxmed.com/b.main/b2.pharmaceutical/b2.prescribe.html. Accessed May 1, 2013.

Development of a porcine model of severe noncompressible truncal hemorrhage

U. R. Yanala, J. M. Johanning, I. I. Pipinos, W. H. Velander , M. A. Carlson
University of Nebraska Medical Center and VA Nebraska Western Iowa Health Care System, Omaha, NE

Introduction

Noncompressible truncal hemorrhage and brain injury currently account for most early mortality in warfighters on the battlefield. There is no effective treatment for noncompressible truncal hemorrhage, other than rapid evacuation to a surgical facility. The availability of an effective field treatment could increase the number of warfighters salvaged from this frequently-lethal scenario. Our intent was to develop a porcine model of noncompressible truncal hemorrhage so that we could study new treatments for this clinical problem.

Methods

Normovolemic normothermic domestic swine (barrows, 3 months old, 34-36 kg) were administered isoflurane anesthesia followed by line placement, cystotomy, and splenectomy, and then underwent one of three injury types through a midline incision: 1) central stellate injury, administered with x-shaped tines applied anterior to the suprahepatic inferior vena cava (N=6); 2) excision of a portal vein (PV) branch distal to the main PV trunk (N=5); or 3) near-transection of the left lateral lobe (LLL) of the liver at its base, which cut the hepatic vein (HV) and PV to this lobe (N=10). The midline incision was towel clipped immediately after injury, and animals were monitored for 60 min or until death. Resuscitation was performed with warm LR (max volume = 100 mL/kg), with a target MAP set at 80% of pre-injury MAP.

Results

The starting weight, MAP, hemoglobin, arterial pH, INR, and pre-injury blood loss did not differ among groups ($p > 0.05$, ANOVA). Select variables after injury are summarized in the Table. One type 3 pig required only 56% of the resuscitation fluid limit, otherwise all subjects received the 100 mL/kg maximum. Death occurred at 34±8 min in the type 2 pigs. Postmortem evaluation revealed that 2-3 HVs were transected by injury type 1 (central stellate), and that 1-2 PV branches plus 1 HV were transected by injury type 3 (LLL transection).

Conclusions

A goal of this work was to develop a model which would provide hemorrhage severe enough such that differential effects of future experimental therapies could be observed, but not so severe such that rapid death would preclude the ability to see an interventional effect. Hemorrhage from the central stellate injury was inadequate, while hemorrhage from excision of a proximal branch of the PV was too severe (i.e., the subjects died too quickly). Near-transection of the hepatic LLL at its base (type 3 injury), however, appeared to yield hemorrhage of appropriate severity, as indicated by the 40% 1-hour mortality and intermediate values for MAP, blood loss, and other variables. Our plan is to use this last injury model in the development of therapies for noncompressible truncal hemorrhage.

Table. Select variables at time of death or 1 hr post-injury.

Injury Type	Survival at 1 h, N (%)**	Final MAP, mm Hg (mean±sd)*	Blood loss, mL (mean±sd)*	Final Hb, g/dL (mean±sd)*	Final BE, mmol/L (mean±sd)	Final INR (mean±sd)#
1. Central	6/6 (100)	65 ± 24	1140 ± 684	8.3 ± 2.7	0.7 ± 1.5	1.1 ± 0.1
2. Excision PV branch	0/5 (0)	16 ± 4	3581 ± 353	1.1 ± 0.7	-6.4 ± 11.0	5.2 ± 4.4
3. LLL transect	6/10 (60)	28 ± 16	2852 ± 657	3.3 ± 2.0	-3.6 ± 7.3	3.1 ± 3.7

LLL = left lateral lobe of liver; PV = portal vein; MAP = mean arterial pressure; Hb = hemoglobin; BE = base excess; INR = international normalized ratio; **p < 0.05, Fisher Exact Test; *p < 0.05, ANOVA; #p < 0.05, Kruskal-Wallis nonparametric analysis of variance.

FIBRINOGEN/FIBRONECTIN COMPLEX FORMS STRONG FIBRIN POLYMER AND IS CHEMOTACTIC TO FIBROBLASTS AND ENDOTHELIAL CELLS *IN VITRO*

Ayman Ismail, Jennifer Calcaterra, Mark A. Carlson, Wilson Burgess and William H. Velander

Introduction: Plasma-derived fibrinogen (FI) and fibronectin (FN) are important components for hemostasis and wound repair. Past studies of normal plasma-derived fibrinogen (FI) have shown a constitutive presence of fibronectin (FN) which is a provisional matrix protein important in healing. While purifying FI from normal human plasma, we observed a room temperature stable interaction between a population of FI and FN. Previously, this FI:FN complex has only been isolated from plasma from rheumatoid arthritis patients. This study reports on the purification and characterization of the complex.

Materials and Methods: FI and the FI:FN complex was initially purified from human plasma from healthy individuals by common cryoprecipitation and ammonium sulfate fractionation methods. The resulting material was further fractionated by ion exchange chromatography using DEAE Sepharose Fast Flow resin. The FI:FN complex was disrupted by Gelatin Sepharose chromatography eluting with 6 M urea. SDS-PAGE gel electrophoresis and Western blot was used to identify proteins and their subpopulations. Relative sizes of pure FI, pure FN and the FI:FN complex were analyzed by size exclusion chromatography. The ability of the complex to form an insoluble fibrin clot was evaluated by thromboelastography. Biological activity of the FN component of the complex was tested with an *in vitro* fibroblast recruitment and adhesion assay.

Results and Discussion: Purified FI that was essentially FN-free did not interact with FN as measured by Biacore and other analysis. In the present study, we used sequence of ammonium sulfate fractionation and DEAE chromatography to isolate and purify a 1:1 stoichiometric complex of FI and FN from normal human plasma. The complex was stable at 4 to 37^{o}C and could be disrupted into the separate FI and FN components by Gelatin Sepharose affinity chromatography. When analyzed by SDS-PAGE, FI was found to consist of entirely of a heterodimeric γ/γ' FI species (γ/γ' FI) which represented about 10% of original fibrinogen in the starting normal plasma pool. Conversely, no γ'-chain containing FI was found in the remaining fibrinogen that was complex depleted. High pressure size exclusion chromatography (HPSEC) showed that the γ/γ' FI:FN complex structure was monolithic and distinct from its purified component γ/γ' FI and FN. The γ/γ' FI: FN had a compacted structure that was slightly smaller in size to γ'γ FI but larger than FN. HPSEC was also used to monitor *in vitro* reassembly of the disrupted complex: the γ/γ' FI and FN rapidly re-established the compacted complex. Surprisingly, the γ/γ' FI: FN had enhanced clotting kinetics and clot strength when measured by thromboelastography. The fibrin clots made from γ/γ' FI: FN showed a biological activity of fibroblast and EC recruitment and adhesion *in vitro* approximating or exceeding that of fibrin made from γ/γ FI and FN.

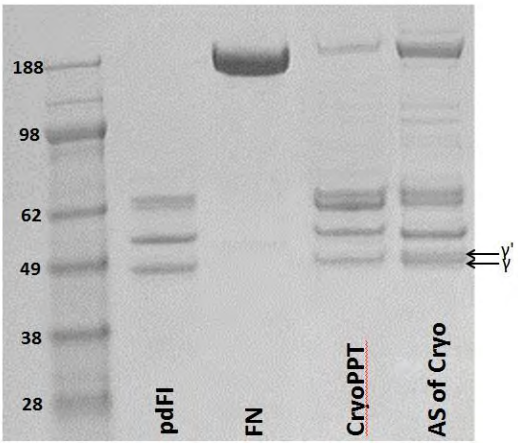

Figure 1. Gel evaluation of pdFI purified by ammonium sulfate fractionation. Samples were analyzed on 4-12% SDS-PAGE and stained with colloidal blue. Lane 1 is molecular weight marker. Lane 2 is human fibrinogen (Enzyme Research). Lane 3 is human fibronectin (Enzyme Research). Lane 4 is pdFI purified by cryoprecipitation. Lane 5 is pdFI purified by ammonium sulfate fractionation.

Conclusions: These results provide the basis for the advanced study of γ/γ' FI:FN for use in hemostasis and wound repair with potentially unique and biological properties and advantages of processing from normal plasma.

ACURO	Animal Care and Use Review Office
DEAE	diethylaminoethanol
EHD	electrohydrodynamics
ETCO2	end tidal carbon dioxide
FI	Factor I (fibrinogen)
FIIa	activated Factor II (thrombin)
FN	fibronectin
FS	fibrin sealant
FXIII	Factor XIII (cross---linking factor)
Hb	hemoglobin
HPC	hydroxypropylcellulose
HPSEC	High pressure size exclusion chromatography
IACUC	Institutional Animal Care and Use Committee
ISR	Institute of Surgical Research
IVC	inferior vena cava LFS
	Liquid Fibrin Sealant
LNK	LNKChemsolutions, LLC
LR	Lactated Ringers solution
MAP	mean arterial pressure
nhpp	normal human plasma pool
PCL	polycaprolactone
pd	plasma derived
PLA	polylactic acid
PT	protime
rFXIIIA2---a	activated recombinant Factor XIII
SBF	simulated body fluid
SDS PAGE	sodium dodecyl sulfate polyacrylamide gel electrophoresis
SEM	scanning electron microscopy
TEA	triethanolamine
TEG	thromboelastography
UNL	University of Nebraska—Lincoln
UNMC	University of Nebraska Medical Center

Grant Number: 10091006
PI: Carlson, Mark A.
Y2 Annual Report

Appendix H
Development of a swine noncompressible hemorrhage model (off-protocol studies during Y2Q1)

Note: the following studies were performed off-protocol (i.e., using a non-DoD protocol), and were not paid by DoD funds.

In order to obtain a working model of noncompressible hemorrhage for Task 8 ("Testing of dual foam in swine noncompressible model, laparotomy with 2˚ closure"; see Appendix B), various injury techniques were trialed in splenectomized normothermic normovolemic swine (N = 23) during September-December of 2012. The intent was to produce an intraabdominal injury in warm, resuscitated swine that would produce death by exsanguination in 30-60 min. The exsanguination could not occur too quickly, otherwise it would be difficult to measure the effect of any hemostatic device. Conversely, we wanted most of the hemorrhage to occur within the first 60 min (the "golden hour") in order to mimic a severe hemorrhagic injury, as might be experienced on the battlefield. The results of this experimentation with injury techniques are shown in Table H1.

Table H1. Results of various techniques of noncompressible hemorrhage in normothermic normovolemic swine.

No.	Injury	Outcome	Final MAP	Blood loss (mL)
1	Central liver laceration (HV x 2)	Survived	101	604
2	Central liver laceration (HV x 3)	Survived	63	688
3	Central liver laceration (HV x 3)	Survived	31	2362
4	Central liver laceration (HV x 3)	Survived	51	1537
5	Central liver laceration (HV x 4)	Survived	78	802
6	Central liver lac with PV branch injury	Death at 38 min	0	3289
7	Central liver laceration (HV x 3)	Survived	66	847
8	PV branch to LM hepatic lobe	Death at 44 min	0	3219
9	PV branch to LM hepatic lobe	Death at 26 min	0	3548
10	PV branch to LL hepatic lobe	Death at 38 min	0	4073
11	PV branch to LM hepatic lobe	Death at 24 min	0	3778
12	Small PV branch, LL lobe	Survived	68	947
13	Splenic vein transection	Survived	82	651
14	PV branch to LL hepatic lobe	Survived	37	2355
15	PV branches (2) to LL hepatic lobe	Death at 43 min	0	3649
16	PV branches (2) to LL hepatic lobe	Death at 15 min	0	3197
17	PV branch to LM hepatic lobe	Death at 40 min	0	2849
18	PV branch to LM hepatic lobe	Survived	51	2108
19	PV branch to LM hepatic lobe	Survived	28	2499
20	PV branch to LM hepatic lobe	Death at 26 min	0	4167
21	PV branch to LM hepatic lobe	Survived	36	2255
22	PV branch to LM hepatic lobe	Survived	42	2931
23	PV branch to LM hepatic lobe	Survived	31	2515

The midline incision was closed with towel clips immediately after injury in all subjects; no specific treatment (no laps, sponges, etc.) was administered in any subject. Postinjury observation period was 60 min in all subjects. Postinjury resuscitation fluid was limited to 100 mL/kg of warm LR. HV = hepatic vein (lacerated); PV = portal vein; LM = left medial; LL = left lateral.

A surprising finding was that a central liver laceration (liver clamp activated several times directly anterior to the IVC such that 2-4 hepatic veins were injured; see year 1 Annual Report) was not fatal; in fact, 4 of 6 subjects injured in this fashion survived 1 hr with <1 L of blood loss and final MAP >60. Postmortem examination of these subjects revealed that clot in these subjects (with pre-injury normovolemia) was sealing off the injury against the diaphragm (Figures H1-H2). One attempt at complete transection of the splenic vein transection produced <1 L of blood loss with no major instability, so the splenic vein technique was not pursued further.

Since the central hepatic laceration appeared to be an inadequate injury mechanism for the noncompressible hemorrhage model in normothermic normovolemic subjects, we progressed to portal vein injury. The results of our experimentation with PV injury was that hemitransection of the left lower hepatic lobe at its base seemed to produce a noncompressible injury model which met our criteria. This injury technique resulted in transection of one of the two major PV branches to the left lower lobe, the hepatic vein from the left lower lobe, and the branch of the hepatic artery to the left lower lobe (Figures H3-H7). Of the 9 subjects injured in this fashion, 3 exsanguinated prior to 60 min, and the final MAP in the surviving 6 subjects was 38 ± 8 mm Hg. The post-injury blood loss in the 9 subjects was 2861 ± 760 mL. We feel that this model, as shown in Figures H3-H7, will be adequate for use in Task 8.

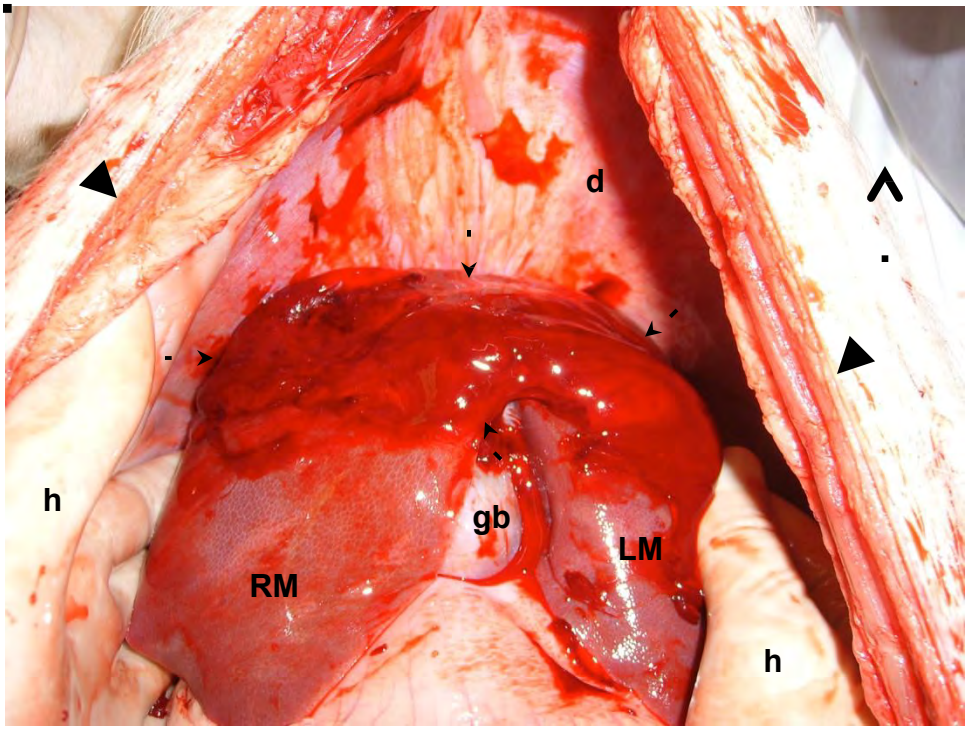

Figure H1: overhead view of liver *in vivo* from swine no. 4 (Table H1), immediately after the 60 min observation period. Subject is supine, with ventral midline incision that has been reopened. Large black arrow = cephalad; small black arrows = clot covering central liver injury; arrowheads = edge of incision; d = diaphragm; RM = right medial lobe; LM = left medial lobe; gb = gallbladder; h = surgeon hand.

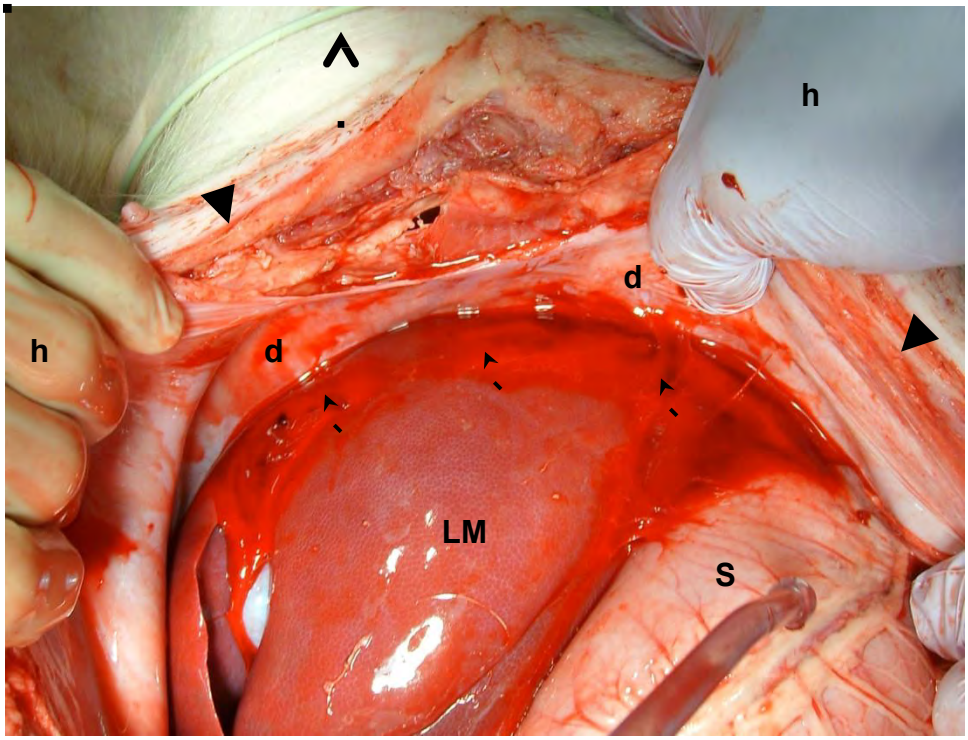

Figure H2: overhead view of liver *in vivo* from swine no. 5 (Table H1), immediately after the 60 min observation period. Subject is supine, with ventral midline incision that has been reopened. Large black arrow = cephalad; small black arrows = clot sealing liver against the diaphragm; arrowheads = edge of incision; d = diaphragm; LM = left medial lobe; S = stomach; h = surgeon hand.

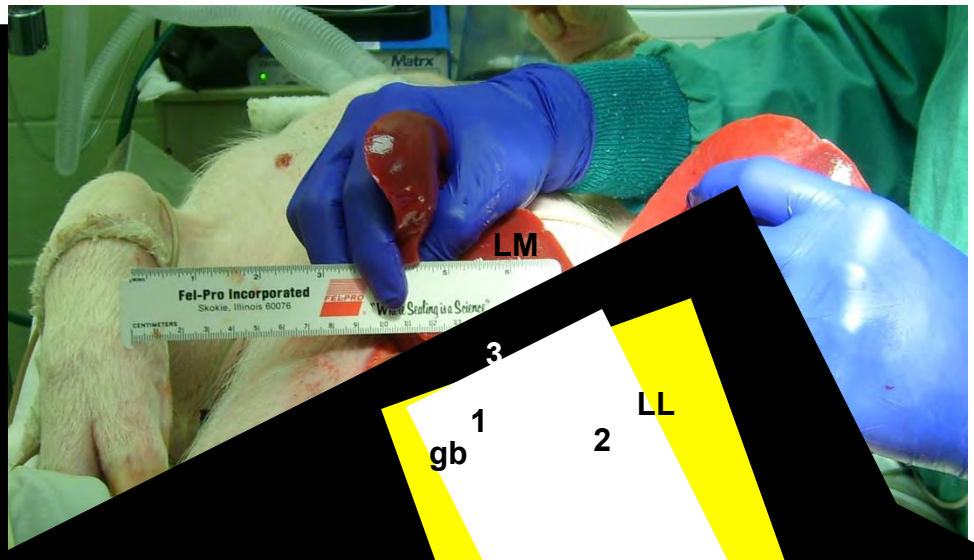

Figur … ly prior to injury; looking towa…
midli…
LM l…
Dash…

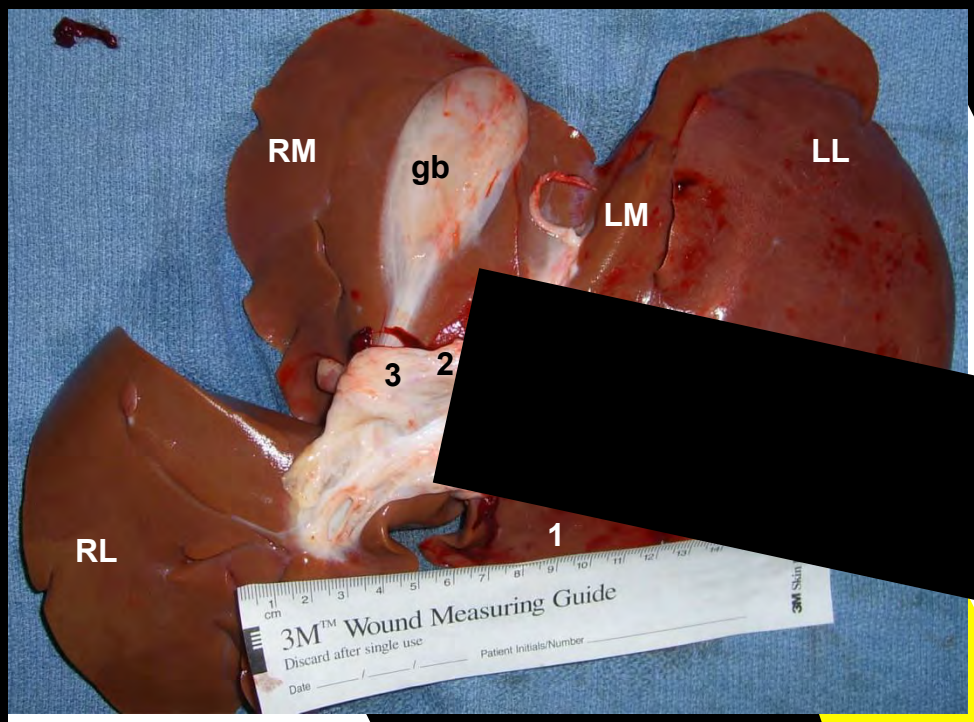

Figu… ex vivo of swine 22, inferior view… …ry was a partial transection
of t… …se; dashed yellow line indicates c… …e. RL = right lateral lobe;
RM… …l lobe; LM = left medial lobe; LL = l… …1st PV branch to LL lobe
(uni… …men of transected 2nd PV branch t… …4 = distal portion of cut
2nd… …rifice of cut hepatic vein to LL lobe.

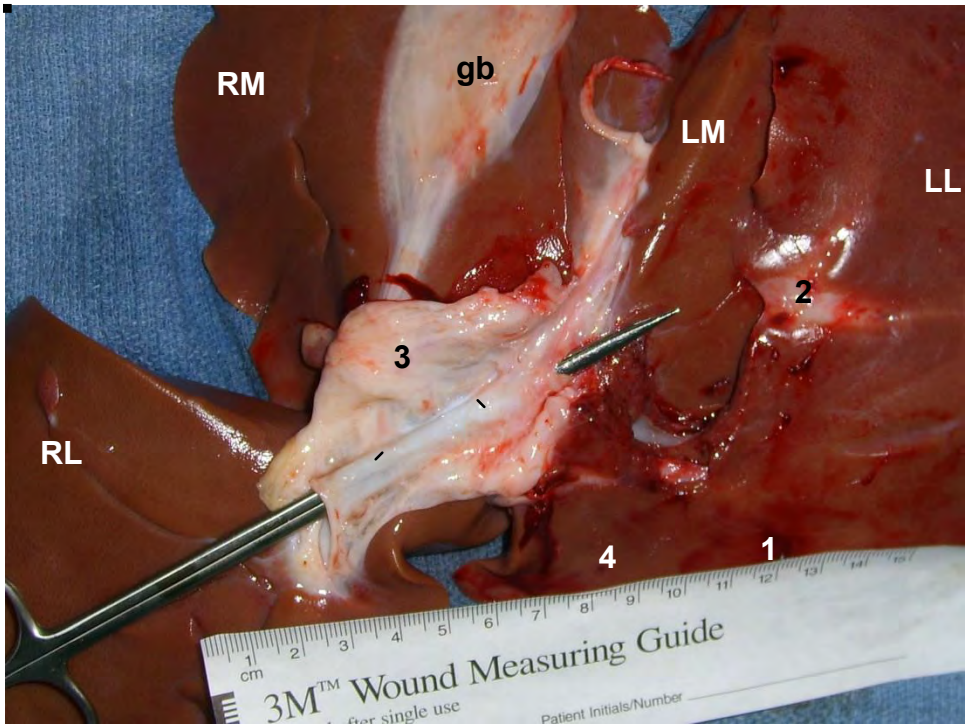

Figure H5. Liver ex vivo of swine 22, inferior view showing PV system & injury. This injury was a partial transection of the LL at its base. Scissors has been inserted in the orifice of the main PV, into the left main branch, and the tips are emerging through the cut proximal end of the 2nd branch to the LL lobe. RL = right lateral lobe; RM = right medial lobe; LL = left lateral lobe; 1 = 1st PV branch to LL lobe (uninjured); 2 = distal portion of cut 2nd PV branch to LL lobe; 3 = left main branch of PV; 4 = lumen of cut hepatic vein to LL lobe.

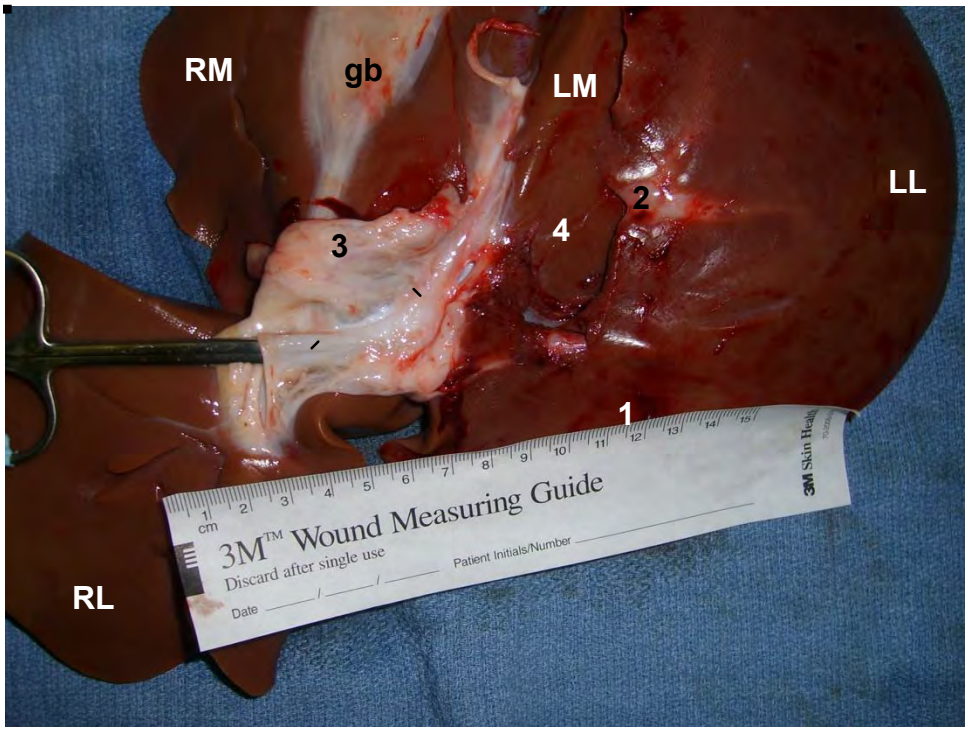

Figure H6. Liver ex vivo of swine 22, inferior view showing PV system & injury. Scissors has been inserted in the orifice of the main PV, into the left main branch, and then into the 1st branch to the LL lobe, which was not injured. RL = right lateral lobe; RM = right medial lobe; LL = left lateral lobe; 1 = 1st PV branch to LL lobe (uninjured); 2 = distal portion of cut 2nd PV branch to LL lobe; 3 = left main branch of PV; 4 = lumen of cut hepatic vein to LL lobe.

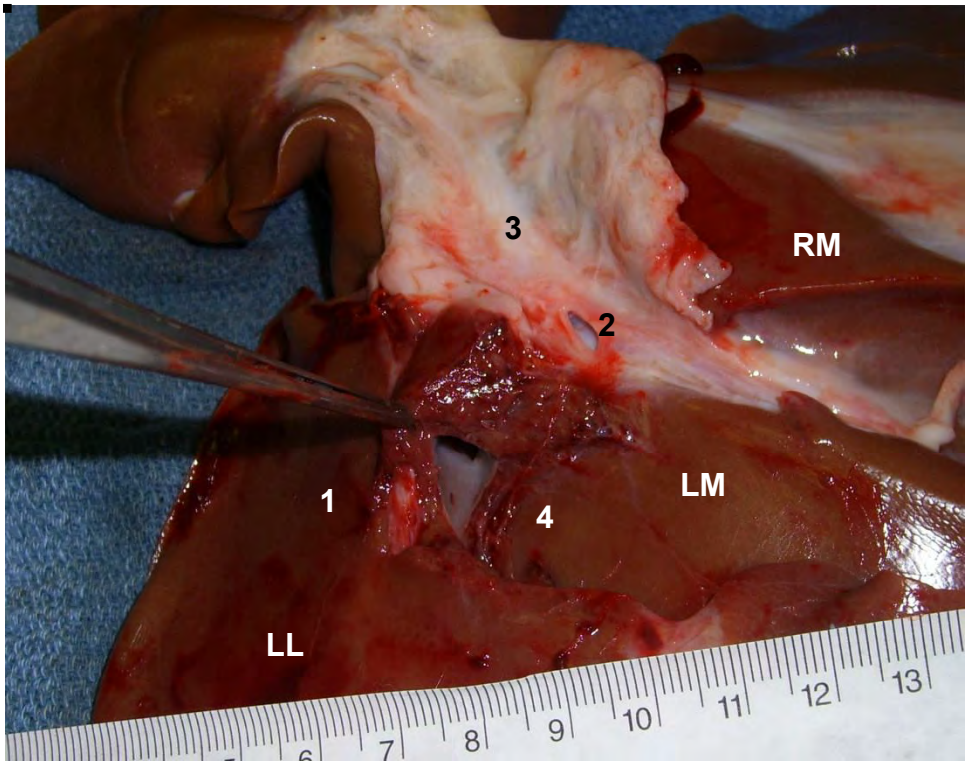

Figure H7. Swine 22; oblique inferior view, looking from left to right, demonstrating the proximal lumen of the transected hepatic vein to the LL lobe (4); 1 = 1st PV branch to LL lobe (uninjured); 2 = proximal orifice of cut 2nd PV branch to LL lobe; 3 = left main branch of PV.

Grant Number: 10091006
PI: Carlson, Mark A.
Y2 Quarterly Report

Appendix J
Initial evaluation of resorbable bandages in hypothermic coagulopathic swine (off-protocol studies during Y2Q1)

Note: the following studies were performed off-protocol (i.e., using a non-DoD protocol), and were not paid by DoD funds.

In order to determine whether the resorbable fibrin sealant bandages would be efficacious for Task 14 ("Final preclinical study of resorbable bandage in hypothermic coagulopathic swine"; see Appendix A), iterations of this bandage were tested in the hypothermic coagulopathic model (N = 10 swine) during June-September of 2012; see results in Table J1. The details of our technique with this model were described in the Y1 Annual Report.

Table J1. Results of hemostasis testing in the hypothermic coagulopathic (hemodiluted) model.

No.	Hepatic injury	Treatment	Outcome	Adherence	Blood loss (mL)
1	Central laceration	PCL macromesh with rFS	Death at 23 min	0	3295
2	Central laceration	PCL macromesh with rFS	Death at 15 min	0	2157
3	Central laceration	PLA micromesh, perforated, with rFS	Death at 26 min	0	4214
4	Lobar resection	PCL macromesh only	Death at 63 min	0	4522
5	Lobar resection	PCL macromesh with pdFS	Death at 50 min	++	3501
6	Lobar resection	PCL macromesh with pdFS	Survived	++	2346
7	Lobar resection	PCL macromesh with pdFS	Survived	0	3897
8	Lobar resection	PCL macromesh with pdFS	Survived	0	2698
9	Lobar resection	PCL macromesh with pdFS	Death at 53 min	0	4385
10	Lobar resection	PCL macromesh with pdFS	Survived	+	2080

rFS = recombinant fibrin sealant (rFI + rFIIa + rFXIIIa); pdFS = plasma derived fibrin sealant (pdFI + rFIIa + rFXIII). Total amount of FI given per treatment was 100 mg in all procedures; one treatment per subject. Adherence = degree of bandage adherence to the hepatic wound (0 = no adherence; + = minimal adherence; ++ = moderate adherence; but still bleeding; +++ = completely adherent & hemostatic).

Overall, the bandage performance with both injury types (central laceration or lobar resection) was poor, primarily due to poor bandage adherence to the hepatic wound. This resulted in high volumes of blood loss. Some animals survived to 1 hr, but his primarily was due to a tamponade effect of intraabdominal hemorrhage combined with a very low (but measurable) final arterial blood pressure.

Further iterations of the FS-supplemented resorbable bandage will be developed. We will need to focus on the adhesion phenomenon in this difficult-to-treat model of coagulopathic hemorrhage. Investigation in this area likely will require further off-protocol work so that we can arrive at a efficacious device to utilize in Task 14.

I. OVERVIEW
Date: Mar 21, 2013
Swine no: 130
Model: swine, planar resection x 1
Treatment: microfibrous macroporous PCL mesh with FS (pdFI + FN)
Personnel: Carlson, Yanala, Cavanaugh, Heimann, Hansen, Calcaterra, Noriega

---

II. PRE-INJURY PHASE

Start time: 10:15 AM
Swine sex: male
Date swine received from UNL Mead: 03/12/2013
Pre-procedure wt: 39.2 kg

Anesthetic Induction: Telazol (4.4 mg/kg), Ketamine (2.2 mg/kg), Xylazine (2.2 mg/kg), given as single IM shot
Anesthetic maintenance: 1.5% inhalational isoflurane

Lines/tubes/monitors/support
1. Endotracheal tube with ETCO2 monitor
2. EKG clips
3. Left ear vein angiocath (20g) for supplemental LR
4. Right carotid artery angiocath (20g), cutdown; for BP monitor
5. Right jugular vein angiocath (16g), cutdown; connected to rapid infusion pump
6. Transabdominal cystotomy for 16 Fr Foley catheter
7. Rectal temp probe
8. Pulse oximetry
9. Heating pad below subject

Initial VS
- HR: 86
- MAP: 96
- Temp: 39.0

Blood draw no. 1 (initial): 10:26 AM (ABG, hematocrit/hemoglobin, PT/PTT, qualitative fibrinogen)

Splenectomy time: 10:44 AM
Spleen wt: 274 gm
LR (22°C) infused after splenectomy: 825 mL at 150 mL/min

Pre-injury fluid data:
- Blood loss (spleen weight + phlebotomies + incidental): 274 + 20 + 15 = 299 mL
- LR (22°C) infused (spleen replacement + incidental): 825 + 125 = 950 mL

Pre-injury VS
- HR: 130
- MAP: 118
- Temp: 38.0

III. INJURY & TREATMENT PHASE

Time of resection10:51 AM
Injury type: planar hepatic resection. One resection-treatment sequence, on left lateral lobe of liver, distal portion of lobe resected (see Figures).
Treatment description: microfibrous macroporous PLA mesh, 4 x 8 cm multi-ply sheets; 2 sheet per resection. FS was sprayed onto each sheet of mesh immediately prior to application. Assistant manually compressed (pinched) base of each lobe during treatment to slow blood loss. Manual compression apposed bandages to face of wound for 5 min. After initial hold, hemostatic result was observed for several min, and then lobe was returned to abdomen, packed with several 4 x 4 cotton gauze and a blue towel, left still for an additional 5 min, and then re-inspected one final time before sacrifice and liver explantation.
Clotting factors: pdFI + FN, rFIIa. pdFI:FN ratio = ~2:1. No FXIIIa administered today.
Abdominal closure: none.
Resuscitation target MAP: 105
Resuscitation fluid: warm LR (3.9 L preset maximum, or 100 mL/kg)
Time resuscitation fluid began: 10:55 AM

Blood draw no. 2: (final): 11:07 AM (ABG, hematocrit/hemoglobin, PT/PTT, qualitative fibrinogen)

Final VS

- HR: NA
- MAP: ~100
- Temp: NA

Survival at 60 min? No
Target MAP attained? NA
Time of death: 11:09 AM
Cause of death: intentional exsanguination from supradiaphragmatic IVC transection.
Interval from first injury to death: 18 min

Post-treatment fluid data:

- Blood loss (intraabdominal suctioning + pads/gauze + phlebotomy): NA
- IV fluid given: LR (37°C): 755

IV. RESULTS OF TREATMENT/POSTMORTEM

Resection LL lobe: reasonable adherence; some bleeding through center of mesh noted after 5 min compression. After an additional 5 min of packing within the abdomen, however, hemostasis was complete.
Postmortem evaluation of liver ex vivo: bandage remained adherent (see Figures).
Ex vivo total liver wt: 888 gm.

Tissue harvested: bone marrow from femur.

V. COMMENTS

Very similar result to no. 129. Single planar resection in normovolemic non-coagulopathic swine treated with PCL macromesh + pdFI/FN-FS (without FXIIIa). Increased FN fraction (FI:FN = 2:1). Rough impression again is that the adhesion may have been better today compared to last week (when much less FN used), but as discussed before, this particular model is not well-suited to discriminate subtle differences in adhesion. The improved adhesion may have been secondary to the increased bandage-wound contact time, in that an additional 5 min of intraabdominal packing was employed after the initial 5 min of manual compression.

VI. PLAN

Consider another repeat procedure as above for next week. Alternatively, we can try alginate foam in noncompressible model.

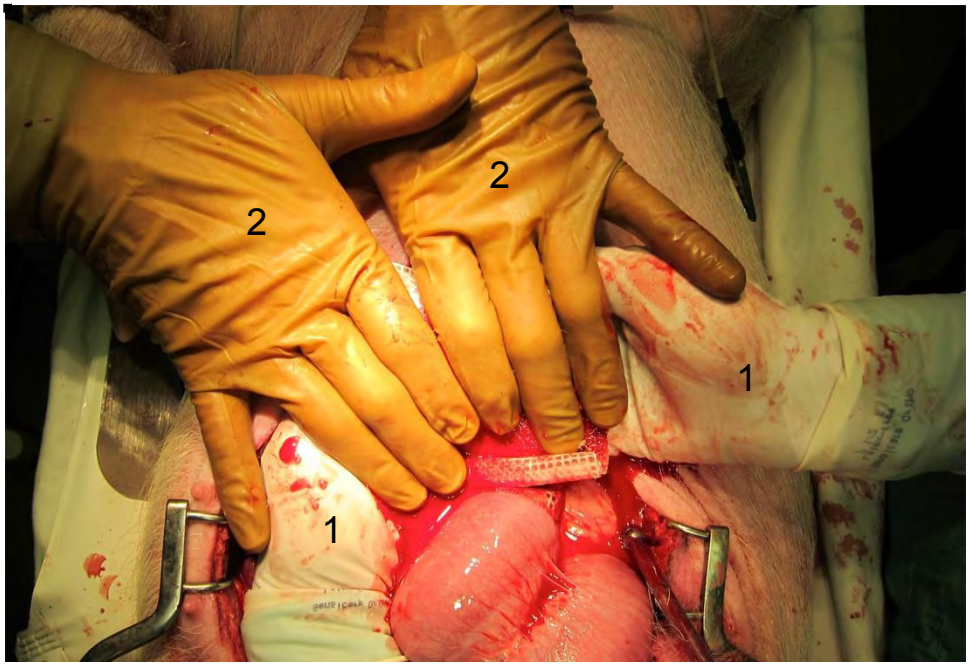

Fig. 1. Swine 130; *in vivo* view of compression during 5 min hold time. Hands with light-colored gloves (1) are applying a pincer-like manuever on the left lateral lobe, to decrease blood flow during the treatment phase, and also to provide counter-compression against the other set of hands. Hands with the dark-colored gloves (2) are providing top-down compression, keeping the PCL apposed to the wound surface. View is through open ventral midline incision; head is toward top of image.

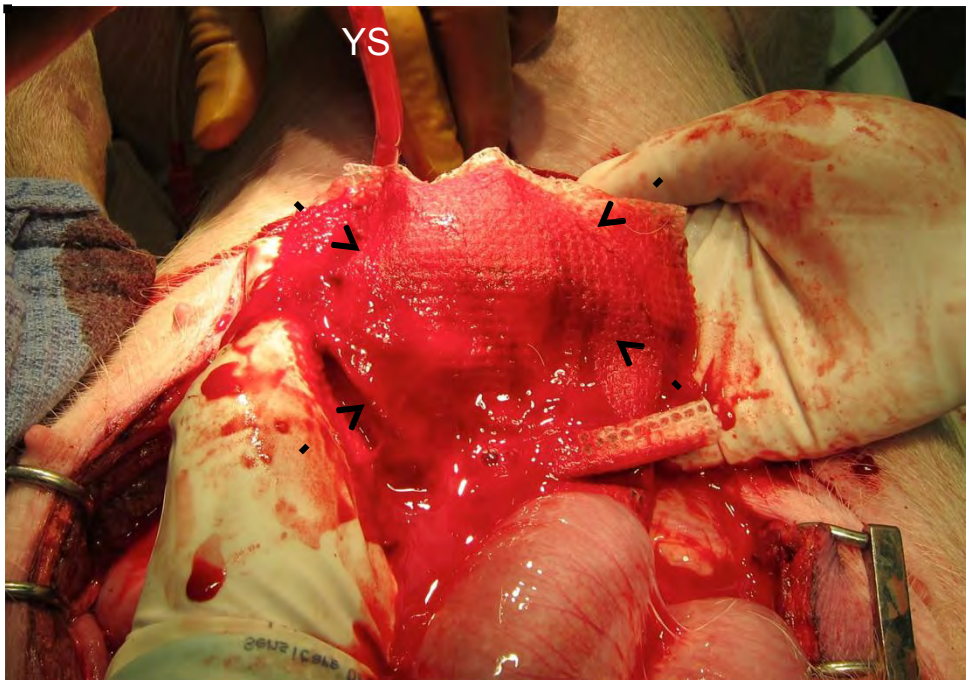

Fig. 2. Swine 130; *in vivo* view of resection site after treatment with PCL mesh (arrows). Resection of portion of left lateral lobe (see Fig. 4 below). View is through open ventral midline incision; head is toward top of image. Residual bleed through center of mesh. YS = Yankauer suction catheter.

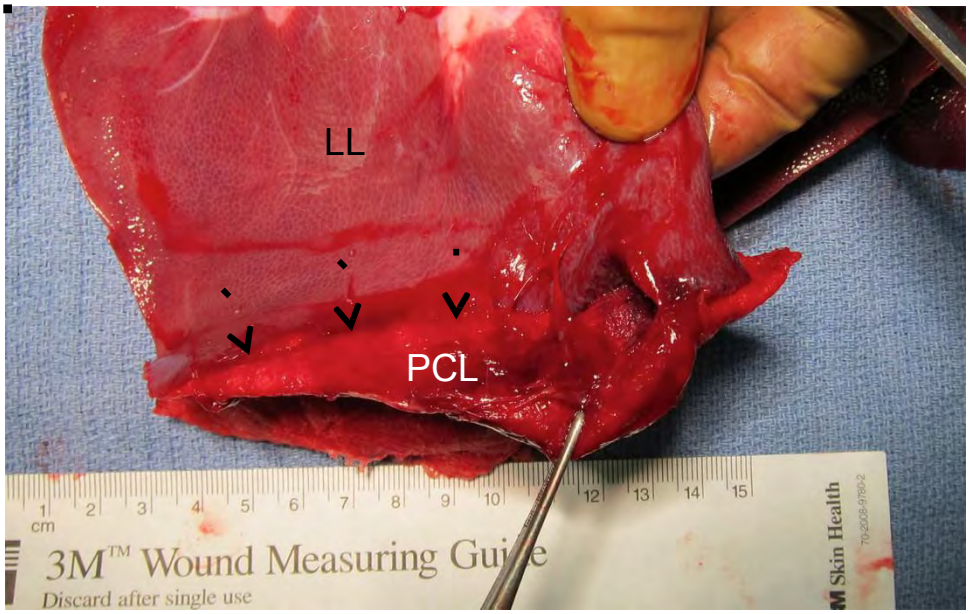

Fig. 3. Swine 130; *ex vivo* view of resection site, with PCL mesh still adherent (arrows). Mesh is being peeled forcibly off the liver with forceps. LL = base of left lateral lobe.

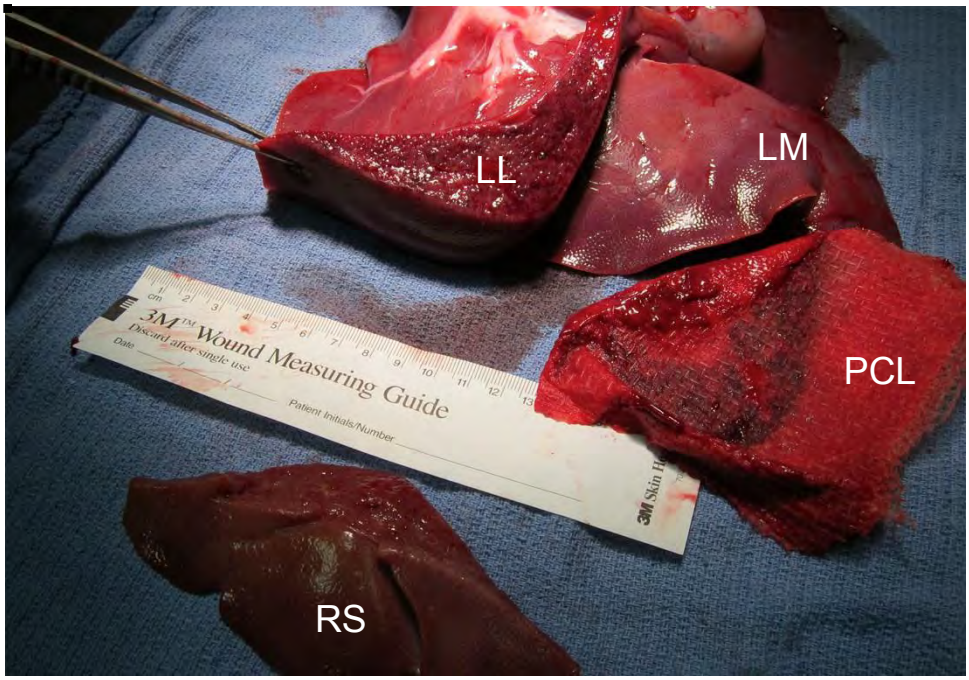

Fig. 4. *Ex vivo* views of liver and resection specimen. LL = left lateral lobe of liver (cut edge); LM = left medial lobe; RS = resection specimen.

I. OVERVIEW
Date: Mar 28, 2013
Swine no: 133
Model: swine, planar resection x 1
Treatment: microfibrous macroporous PCL mesh with FS (pdFI + FN)
Personnel: Carlson, Yanala, Heimann, Hansen, Calcaterra, Noriega

---

II. PRE-INJURY PHASE

Start time: 8:57 AM
Swine sex: male
Date swine received from UNL Mead: 03/22/2013
Pre-procedure wt: 35.2 kg

Anesthetic Induction: Telazol (4.4 mg/kg), Ketamine (2.2 mg/kg), Xylazine (2.2 mg/kg), given as single IM shot
Anesthetic maintenance: 1.5% inhalational isoflurane

Lines/tubes/monitors/support
1. Endotracheal tube with ETCO2 monitor
2. EKG clips
3. Left ear vein angiocath (20g) for supplemental LR
4. Right carotid artery angiocath (20g), cutdown; for BP monitor
5. Right jugular vein angiocath (16g), cutdown; connected to rapid infusion pump
6. Transabdominal cystotomy for 16 Fr Foley catheter
7. Rectal temp probe
8. Pulse oximetry
9. Heating pad below subject

Initial VS
- HR: 140
- MAP: 106
- Temp: 37.8

Blood draw no. 1 (initial): 9:08 AM (ABG, hematocrit/hemoglobin, PT/PTT, qualitative fibrinogen)

Splenectomy time: 9:27 AM
Spleen wt: 425 gm
LR (22°C) infused after splenectomy: 1275 mL at 150 mL/min

Pre-injury fluid data:
- Blood loss (spleen weight + phlebotomies + incidental): 425 + 20 + 18 = 463 mL
- LR (22°C) infused (spleen replacement + incidental): 1275 + 200 = 1475 mL

Pre-injury VS
- HR: 119
- MAP: 118
- Temp: 36.5

III. INJURY & TREATMENT PHASE

Time of resection10:51 AM
Injury type: planar hepatic resection. One resection-treatment sequence, on left lateral lobe of liver, distal portion of lobe resected (see Figures).
Treatment description: microfibrous macroporous PLA mesh, 4 x 8 cm multi-ply sheets; 2 sheet per resection. FS was sprayed onto each sheet of mesh immediately prior to application. Assistant manually compressed (pinched) base of each lobe during treatment to slow blood loss. Manual compression apposed bandages to face of wound for 5 min. After initial hold, hemostatic result was observed for several min, and then lobe was returned to abdomen, packed with several 4 x 4 cotton gauze and a blue towel, left still for an additional 5 min, and then re-inspected one final time before sacrifice and liver explantation.
Clotting factors: pdFI + FN, rFIIa, rFXIIIa. pdFI:FN ratio = ~2:1.
Abdominal closure: clipped loosely during 5 min cotton gauze packing.
Resuscitation target MAP: 95
Resuscitation fluid: warm LR (3.5 L preset maximum, or 100 mL/kg)
Time resuscitation fluid began: 9:42 AM

Blood draw no. 2: (final): 9:50 AM (ABG, hematocrit/hemoglobin, PT/PTT, qualitative fibrinogen)

Final VS: 9:50 AM

- HR: 117
- MAP: 85
- Temp: 35.7

Survival at 60 min? No (only observed ~10 min for bandage adhesion)
Target MAP attained? NA
Time of death: 9:57 AM
Cause of death: intentional exsanguination from supradiaphragmatic IVC transection.
Interval from first injury to death: 20 min

Post-treatment fluid data:

- Blood loss (intraabdominal suctioning + pads/gauze + phlebotomy): NA
- IV fluid given: LR (37°C): 1145 mL

IV. RESULTS OF TREATMENT/POSTMORTEM

Resection LL lobe: plus/minus adherence; some bleeding through center of mesh noted after 5 min compression. After an additional 5 min of packing within the abdomen, small amount oozing still remained.
Postmortem evaluation of liver ex vivo: bandage remained adherent (see Figures). Strips of PCL (1 cm wide) were peeled away with a hand-held spring gauge (see Figures); maximum force recorded on this gauze during these peel tests (total of three) was 20 centinewtons.
Ex vivo liver wt: 802 gm
Resection specimen: 59 gm
Tissue harvested: none.

V. COMMENTS

Single planar resection in normovolemic non-coagulopathic swine treated with PCL macromesh + pdFI/FN-FS;. FI:FN = 2:1. Today we utilized all three biologics (pdFI, rFIIa, rFXIIIa) plus FN. Could not really say whether adhesion was better today than what we have seen in the past. The force required for the manual peel-away assay (see Figures) of 1-cm bandage strips was relatively low (20-40 centinewtons). The Instron rep informed me that the sensitivity of the 5 N load cell (smallest they have) was in the range of 1/100 to 1/250 of the load cell rating, or 20-50 centinewtons. So using the 1-cm strip in a peel away assay, we really are at the limit of the sensitivity with a 5 N load cell. At this point I think we need to reconsider our options for quantification of bandage adhesion, because it appears that an Instron tensiometer with a 5 N load cell will not be sensitive enough.

Regarding the bandage adhesion itself, we probably should discuss our next steps, because the current formulation is not sticking all that well.

VI. PLAN

Repeat above with next swine (no. 134).

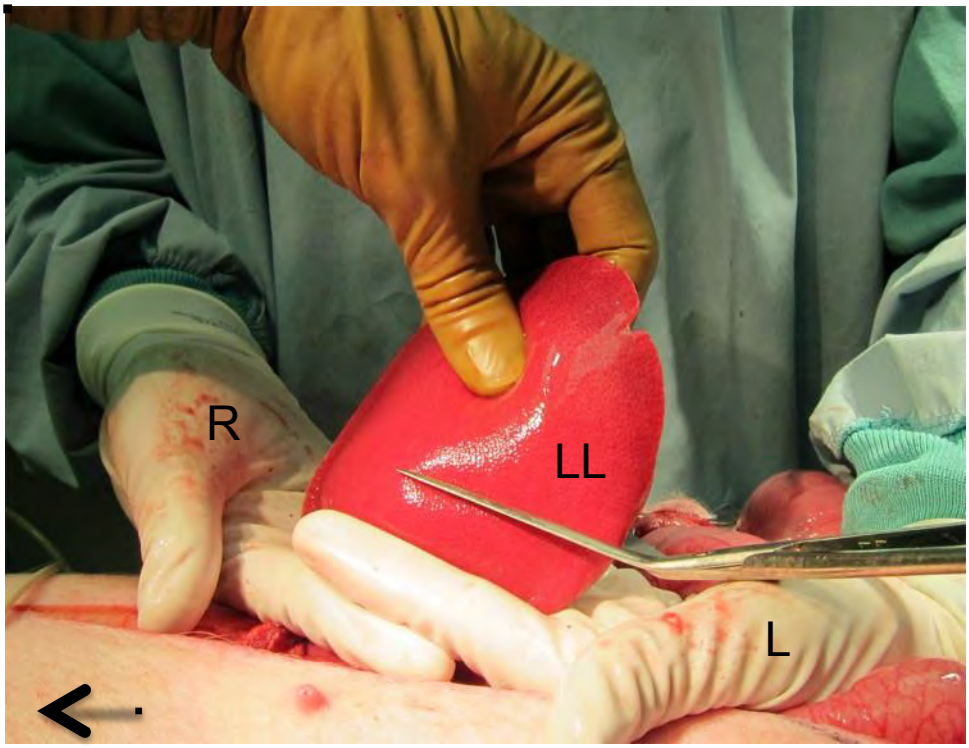

Figure 1, swine 133. Planar resection of liver. Distal portion of left lateral (LL) lobe is being pulled out of midline incision, and is about to be transected with the long scissors. Assistant's hands (R & L) will pinch the base to control hemorrhage during the bandage application. Arrow = cephalad.

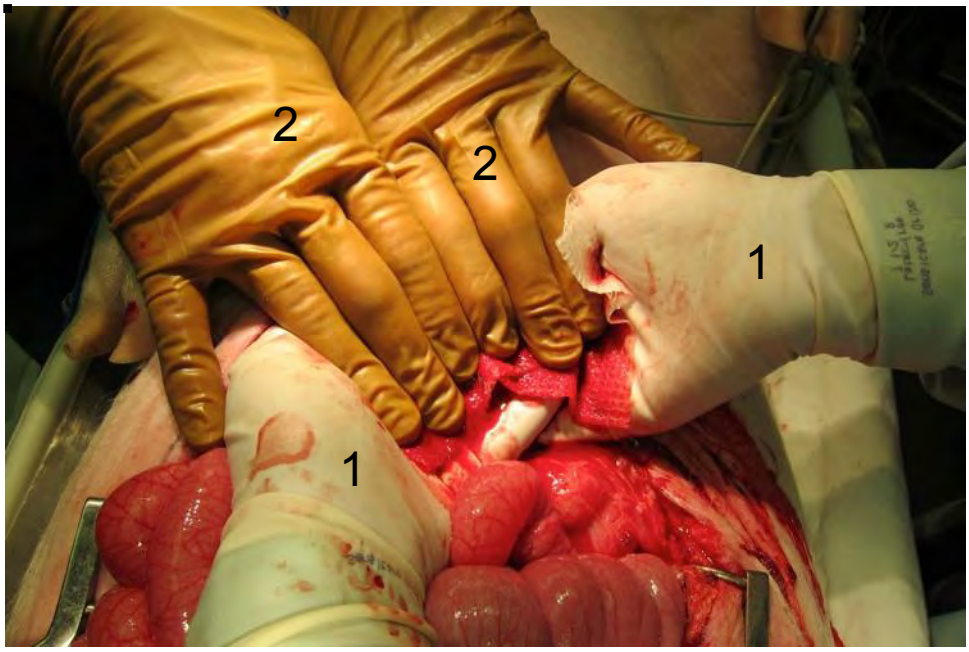

Figure 2, swine 133. Treatment phase after planar resection of liver. Assistant's hands (1) are pinching the base of the LL lobe; surgeon's hands (2) are compressing bandage (PCL + biologics) against wound face. Top = cephalad.

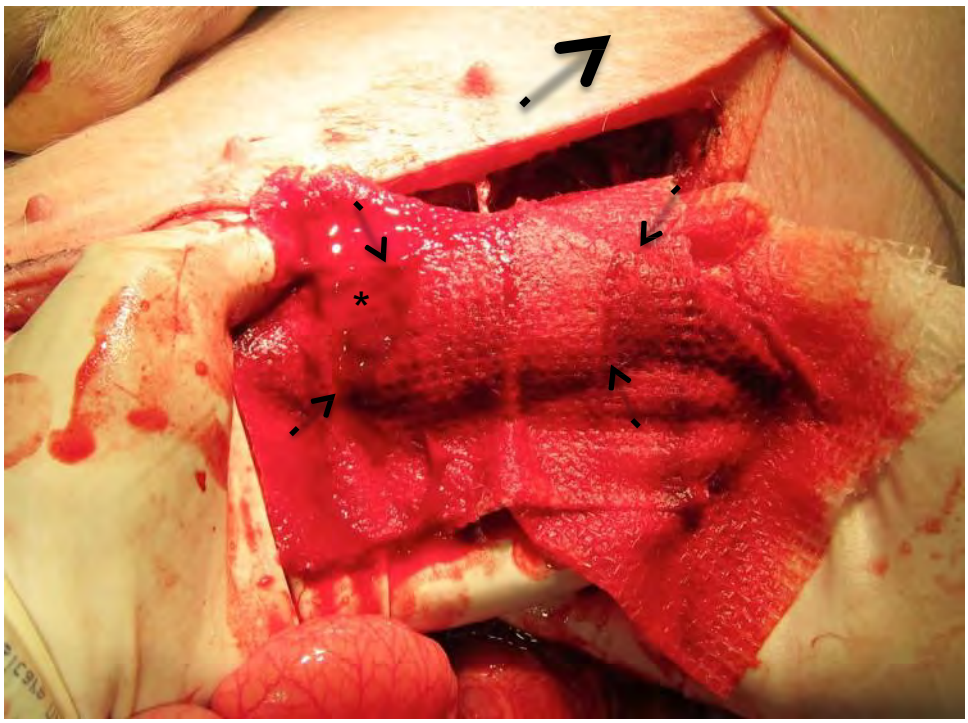

Figure 3, swine 133. Planar resection of distal portion of left lateral (LL) lobe, immediately after 5 min bandage (PCL + biologics) compression. Outline of wound edge visible through bandage (small arrows). Some residual hemorrhage is present (*). Large arrow = cephalad.

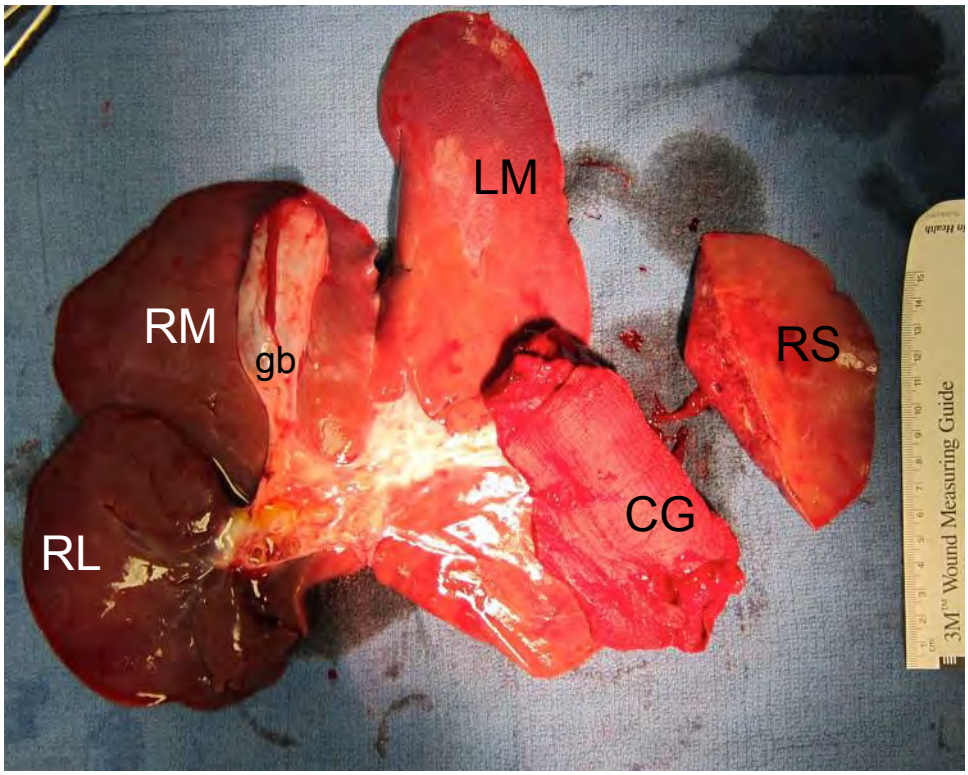

Figure 4, swine 133. Liver ex vivo, inferior aspect, showing resection specimen (RS) of LL lobe. The wound site is covered with cotton gauze (CG), with the PCL gauze underneath. RL = right lateral lobe; RM = right medial lobe; LM = left medial lobe; gb = gallbladder.

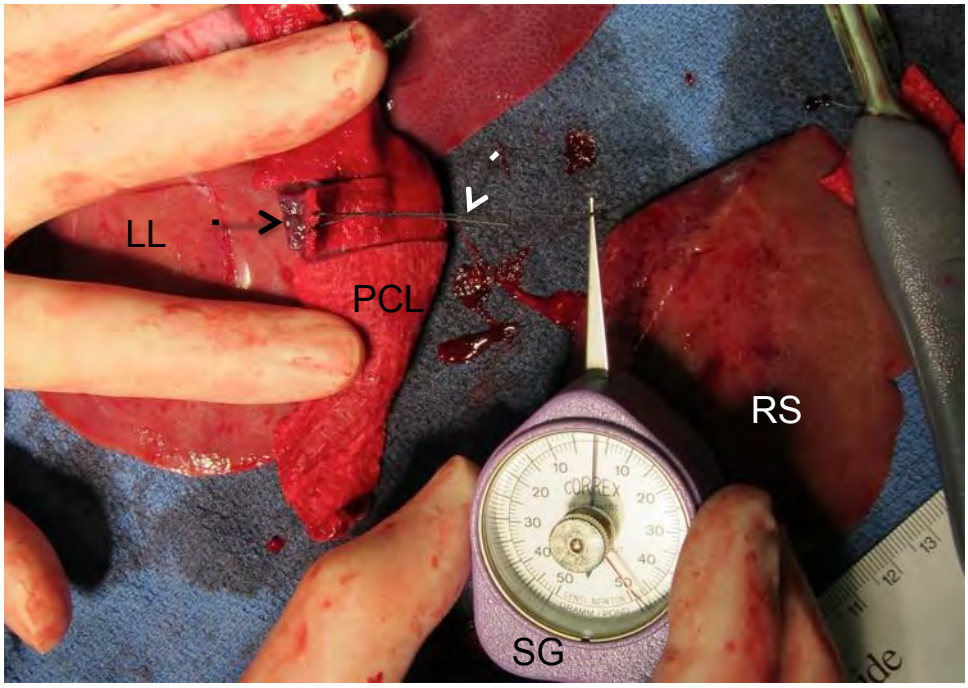

Figure 5, swine 133. “Peel” test of PCL bandage. A 1 cm strip (black arrow) of the PCL adherent to the wound site was scored with a scalpel. A silk suture loop (white arrow) was placed through the end of the PCL strip, and hooked to a hand-held spring gauge (SG). The strip subsequently was peeled away from the wound with tension on the spring gauge, in the direction of the black arrow. LL = left lateral lobe; RS = resection specimen.

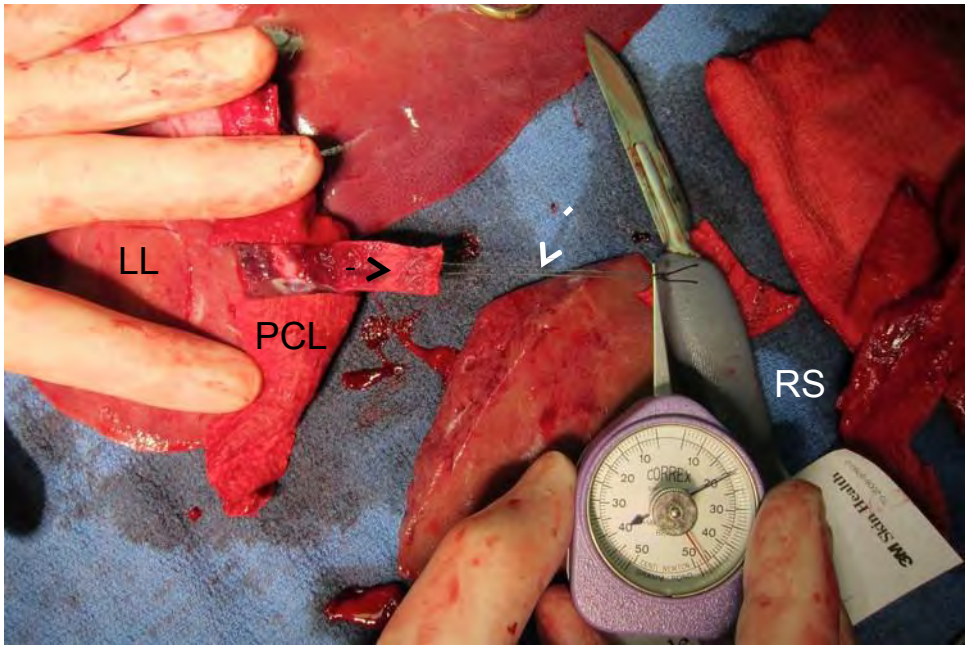

Figure 6, swine 133. Progression of peel test begun in Figure 5. Spring gauge is reading 20 centinewtons.

I. OVERVIEW
Date: Mar 28, 2013
Swine no: 134
Model: swine, planar resection x 1
Treatment: microfibrous macroporous PCL mesh with FS (pdFI + FN)
Personnel: Carlson, Yanala, Heimann, Hansen, Calcaterra, Noriega

---

II. PRE-INJURY PHASE

Start time: 10:27 AM
Swine sex: male
Date swine received from UNL Mead: 03/22/2013
Pre-procedure wt: 37.2 kg

Anesthetic Induction: Telazol (4.4 mg/kg), Ketamine (2.2 mg/kg), Xylazine (2.2 mg/kg), given as single IM shot
Anesthetic maintenance: 1.5% inhalational isoflurane

Lines/tubes/monitors/support
1. Endotracheal tube with ETCO2 monitor
2. EKG clips
3. Left ear vein angiocath (20g) for supplemental LR
4. Right carotid artery angiocath (20g), cutdown; for BP monitor
5. Right jugular vein angiocath (16g), cutdown; connected to rapid infusion pump
6. Transabdominal cystotomy for 16 Fr Foley catheter
7. Rectal temp probe
8. Pulse oximetry
9. Heating pad below subject

Initial VS
- HR: 138
- MAP: 120
- Temp: 38.4

Blood draw no. 1 (initial): 10:38 AM (ABG, hematocrit/hemoglobin, PT/PTT, qualitative fibrinogen)

Splenectomy time: 10:54 AM
Spleen wt: 281 gm
LR (22°C) infused after splenectomy: 840 mL at 150 mL/min

Pre-injury fluid data:
- Blood loss (spleen weight + phlebotomies + incidental): 281 + 20 + 108 = 409 mL
- LR (22°C) infused (spleen replacement + incidental): 840 + 150 = 990 mL

Pre-injury VS
- HR: 125
- MAP: 106
- Temp: 36.9

III. INJURY & TREATMENT PHASE

Time of resection: 11:03 AM
Injury type: planar hepatic resection. One resection-treatment sequence, on left lateral lobe of liver, distal portion of lobe resected (see Figures).
Treatment description: microfibrous macroporous PLA mesh, 4 x 8 cm multi-ply sheets; 2 sheet per resection. FS was sprayed onto each sheet of mesh immediately prior to application. Assistant manually compressed (pinched) base of each lobe during treatment to slow blood loss. Manual compression apposed bandages to face of wound for 5 min. After initial hold, hemostatic result was observed for several min, and then lobe was returned to abdomen, packed with several 4 x 4 cotton gauze and a blue towel, left still for an additional 5 min, and then re-inspected one final time before sacrifice and liver explantation.
Clotting factors: pdFI + FN, rFIIa, rFXIIIa. pdFI:FN ratio = ~2:1; total pdFI ~50 mg.
Abdominal closure: clipped loosely during 5 min cotton gauze packing.
Resuscitation target MAP: 85
Resuscitation fluid: warm LR (3.7 L preset maximum, or 100 mL/kg)
Time resuscitation fluid began: 11:08 AM

Blood draw no. 2: (final): 11:16 AM (ABG, hematocrit/hemoglobin, PT/PTT, qualitative fibrinogen)

Final VS: 11:16 AM

- HR: 120
- MAP: 83
- Temp: 36.5

Survival at 60 min? No (only observed ~10 min for bandage adhesion)
Target MAP attained? NA
Time of death: 11:20 AM
Cause of death: intentional exsanguination from supradiaphragmatic IVC transection.
Interval from first injury to death: 17 min

Post-treatment fluid data:

- Blood loss (intraabdominal suctioning + pads/gauze + phlebotomy): NA
- IV fluid given: LR (37°C): 425 mL

IV. RESULTS OF TREATMENT/POSTMORTEM

Resection LL lobe: plus/minus adherence; some bleeding through center of mesh and inferior edge noted after 5 min compression. After an additional 5 min of packing within the abdomen, small amount oozing still remained.
Postmortem evaluation of liver ex vivo: bandage remained adherent (see Figures). Strips of PCL (1 cm wide) were peeled away with a hand-held spring gauge (see Figures); maximum force recorded on this gauze during these peel tests (total of three) was 40 centinewtons (this was adhesion between the capsule and PCL, not the cut hepatic surface).
Ex vivo liver wt: 1010 gm
Resection specimen: 120 gm
Tissue harvested: none.

V. COMMENTS

Single planar resection in normovolemic non-coagulopathic swine treated with PCL macromesh + pdFI/FN-FS;. FI:FN = 2:1. Today we utilized all three biologics (pdFI, rFIIa, rFXIIIa) plus FN, with ~50 mg total of pdFI. Again, could not really say whether adhesion was better today than what we have seen in the past. The force required for the manual peel-away assay (see Figures) of 1-cm bandage strips was about the same as with swine 133 (20-40 centinewtons). Incidentally, the area to which the bandage stuck best was the intact liver capsule, not the cut liver parenchyma.

VI. PLAN

Recommend we discuss the next direction to take with this planar resection model. The foam/noncompressible model might be taken up if we have a new foam formulation available.

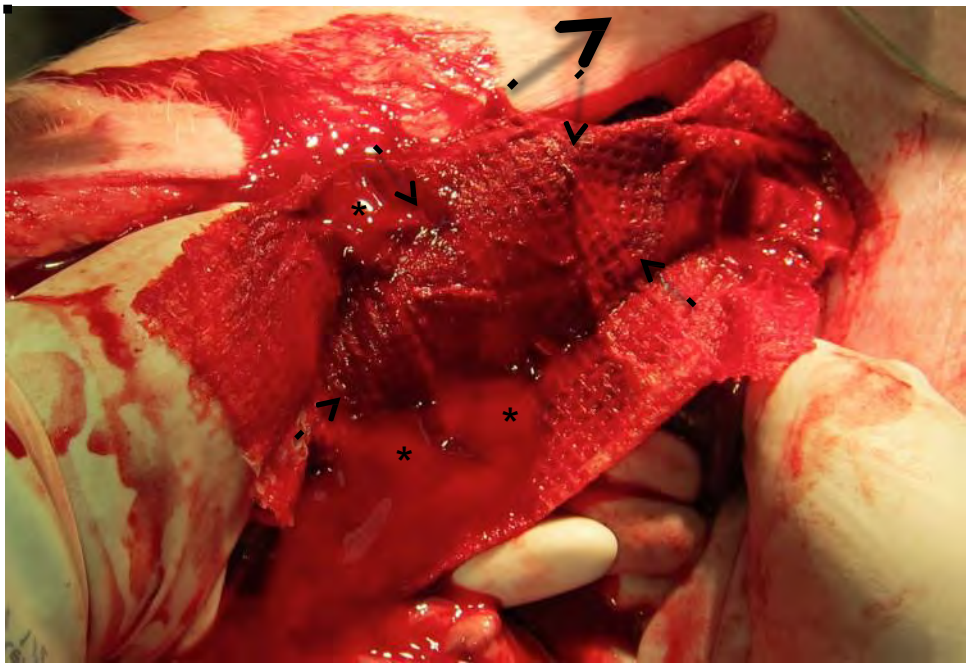

Figure 1, swine 134. Planar resection of distal portion of left lateral (LL) lobe, immediately after 5 min bandage (PCL + biologics) compression. Outline of wound edge visible through bandage (small arrows). Some areas of residual hemorrhage are present (*). Large arrow = cephalad.

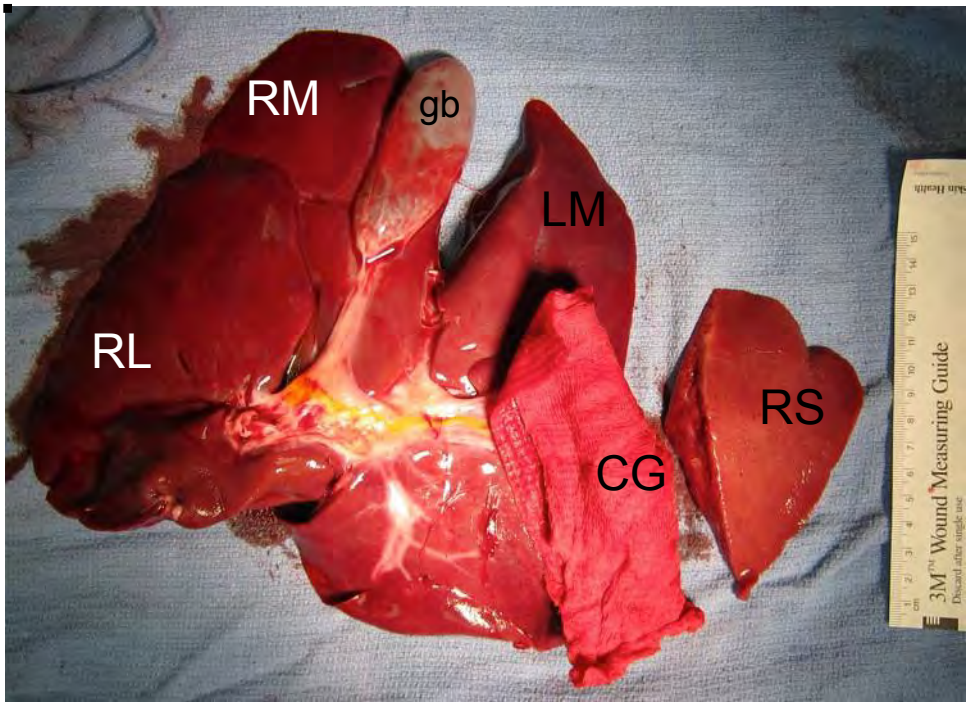

Figure 2, swine 134. Liver ex vivo, inferior aspect, showing resection specimen (RS) of LL lobe. The wound site is covered with cotton gauze (CG), with the PCL gauze underneath. RL = right lateral lobe; RM = right medial lobe; LM = left medial lobe; gb = gallbladder.

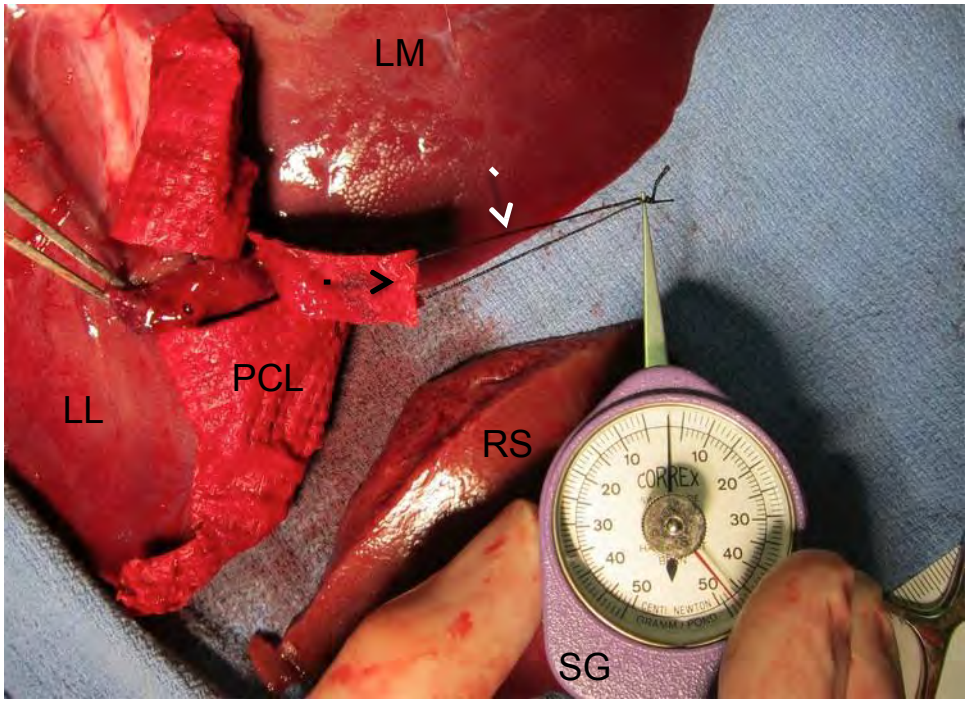

Figure 3, swine 134. “Peel” test of PCL bandage. A 1 cm strip (black arrow) of the PCL adherent to the wound site was scored with a scalpel. A silk suture loop (white arrow) was placed through the end of the PCL strip, and hooked to a hand-held spring gauge (SG). The strip subsequently was peeled away from the wound with tension on the spring gauge, in the direction of the black arrow. LL = left lateral lobe; RS = resection specimen.

I. OVERVIEW
Date: Apr 16, 2013
Swine no: 144
Model: swine, normothermic, normovolemic noncompressible hemorrhage; PV + HV injury
Treatment: Calcium alginate foam, no biologics
Personnel: Carlson, Yanala, Heimann, Hansen, Noriega

II. PRE-INJURY PHASE

Start time: 9:40 AM
Swine sex: male
Date swine received from UNL Mead: 04/12/2013
Pre-procedure wt: 34.6 kg

Anesthetic Induction: Telazol (4.4 mg/kg), Ketamine (2.2 mg/kg), Xylazine (2.2 mg/kg), given as single IM shot
Anesthetic maintenance: 1.0% inhalational isoflurane

Lines/tubes/monitors/support
1. Endotracheal tube with ETCO2 monitor
2. EKG clips
3. Left ear vein angiocath (20g) for supplemental LR
4. Right carotid artery angiocath (20g), cutdown; for BP monitor
5. Right jugular vein angiocath (16g), cutdown; connected to rapid infusion pump
6. Transabdominal cystotomy for 16 Fr Foley catheter
7. Rectal temp probe
8. Pulse oximetry
9. Heating pad below subject

Initial VS
- HR: 138
- MAP: 103
- Temp: 38.7

Blood draw no. 1 (initial): 9:50 AM (ABG, hematocrit/hemoglobin, PT/PTT, qualitative fibrinogen)

Splenectomy time: 10:08 AM
Spleen wt: 197 gm
LR (22°C) infused after splenectomy: 1000 mL at 150 mL/min

Pre-injury fluid data:
- Blood loss (spleen weight + phlebotomies + incidental): 197 + 20 + 66 = 283 mL
- LR (22°C) infused (spleen replacement + incidental): 1000 + 130 = 1130 mL

Pre-injury VS
- HR: 120
- MAP: 95
- Temp: 37.7

III. INJURY & TREATMENT PHASE

Time of injury: 10:21 AM
Injury type: portal/hepatic vein injury. An injury was made across the base of the left lateral lobe with a single cut of the scissors. Prior to the injury, the lower half of the ventral midline incision was closed with towel clips. The nozzle of the foam injector was inserted between these clips into the lower peritoneal cavity (see Figures).
Treatment description: calcium alginate foam, no biologics. This was applied with a creamer dispenser-based injection system which was supplemented with a calcium chloride solution via a syringe pump (see Figures).
Clotting factors: none.
Technique: with the lower half of the incision closed with towel clips and the nozzle in position, the target liver lobe was exteriorized through the upper half of the midline incision (see Figures). The injury then was created as described above. Immediately after injury, the injured liver lobe was dropped back into the abdomen, and the upper half of the incision was rapidly closed with towel clips. Injection of the foam began during this closure (within 30 s of injury). A small amount of foam (~50 mL) escaped from the abdomen during the injection. After injection (~1 min after injury), the nozzle was withdrawn and a final towel clip was placed in the space where the nozzle had been inserted.
Abdominal closure: "Semi-closed" technique, as described above
Resuscitation target MAP: 80
Resuscitation fluid: warm LR (3.4 L preset maximum, or 100 mL/kg)
Time resuscitation fluid began: 10:22 AM

IV. POST-TREATMENT PHASE

Blood draw no. 2 (15 min post-injury): 10:36 AM

15 min post-injury VS
- HR: 187
- MAP: 40
- Temp: 37.0

Blood draw no. 3: (30 min post-injury): 10:51 AM (ABG, hematocrit/hemoglobin, PT/PTT, qualitative fibrinogen)

Final (32 min) VS
- HR: 66
- MAP: 16
- Temp: 36.2

Survival at 60 min? No
Target MAP attained? Yes
Time of death: 10:55 AM
Cause of death: terminal hypotension, exsanguination from injury
Interval from injury to death: 34 min

Post-treatment fluid data:
- Blood loss (intraabdominal suctioning + pads/gauze + phlebotomy): 2996 + 380 + 40 = 3416 mL
- IV fluid given: LR (37°C): 1000 mL (jugular IV) + 50 mL ear vein = 3530 mL

V. RE-EXPLORATION/POST-MORTEM PHASE

Findings upon abdominal/chest exploration: abdomen grossly distended & tense. White foam mostly in the lower abdomen; some mixing with blood in the upper abdomen; ++clots.
Heart: red clot in right ventricle and right atrium, no evidence of foam (see Figures).
Number of hepatic veins lacerated: one, at the confluence of the veins to the LM & LL lobes (see Figures).
Portal vein injury: one complete transection (2nd branch of the PV to the left lateral lobe).
Other: stringy red clot extracted from cut orifice of HV (see Figures).
Ex vivo total liver wt: 846 gm

Tissue harvested: femur bone marrow.

V. COMMENTS

Test #2 of calcium alginate foam in the noncompressible model. System & technique worked OK. Foam appeared intact ~30 min after injection. Animal initially maintained relatively high MAP (>60), then crashed suddenly about 15 min after injury. Cardiac clot found at postmortem; this raises possibility that decompensation may have been in part due to embolism. But subject still had 3+ L blood loss at postmortem, which ultimately appeared to be the cause of death.

I don't think this subject had a foam embolism, as there was no gross evidence of foam in the heart. Whether foam was actually admixed into the cardiac clot is difficult to say. The next time we find clot, we will perform histology. I also asked Sandra & Mostafa whether we could add blue food coloring to the foam, to see if this helps to track the foam's spread.

I made the injury too proximal in this subject, resulting in a large rent at the confluence of the veins draining the LM & LL lobes. This likely produced more bleeding than expected with this model.

Note: determination of blood loss at postmortem is somewhat inexact because each subject continues to bleed from the injury after the abdomen is opened for inspection and blood evacuation. The blood loss that occurs during the evacuation process cannot really be attributed to the injury, because the conditions have changed (i.e., the tamponade effect is released after the abdomen is reopened). The blood loss occurring during the evacuation process may account for several hundred mL of the total blood loss. But this subject (#144) still had excessive injury-related blood loss which contributed to death.

Although not quantitated above, the foam contributed <50 mL to the measured blood loss. We quantify blood loss by weighing (1 gram = 1 mL), not measuring volume. So the actual contribution of the foam to the weight of blood loss is quite small.

VI. PLAN

Continue attempts with current iteration of Ca alginate foam.

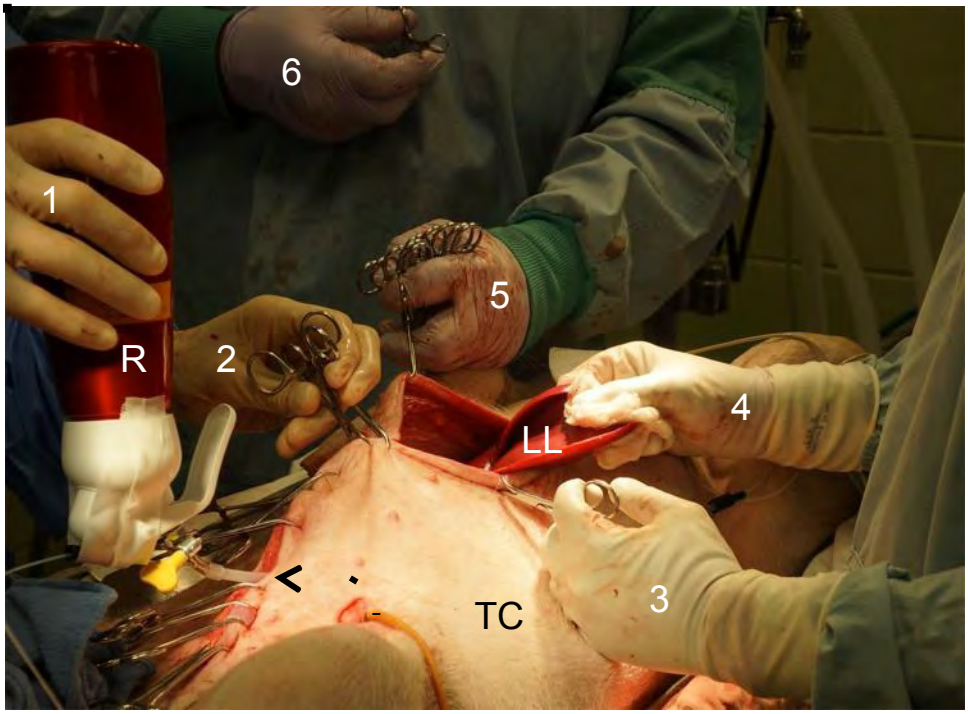

Fig. 1, Swine 144. Set-up prior to injury. Midline incision has been closed in the inferior portion with towel clips (hand #2). Reservoir (R) of foam application system is held by hand #1, with the nozzle inserted between clips and through the inferior portion of the incision (arrow), into the abdominal cavity. Hands #3 & 5 are splaying open the superior portion of the injury with towel clips, so that the left lateral lobe (LL, held by hand #4) can be exteriorized in preparation for the injury. Head is to the right of the image. TC = transabdominal cystostomy.

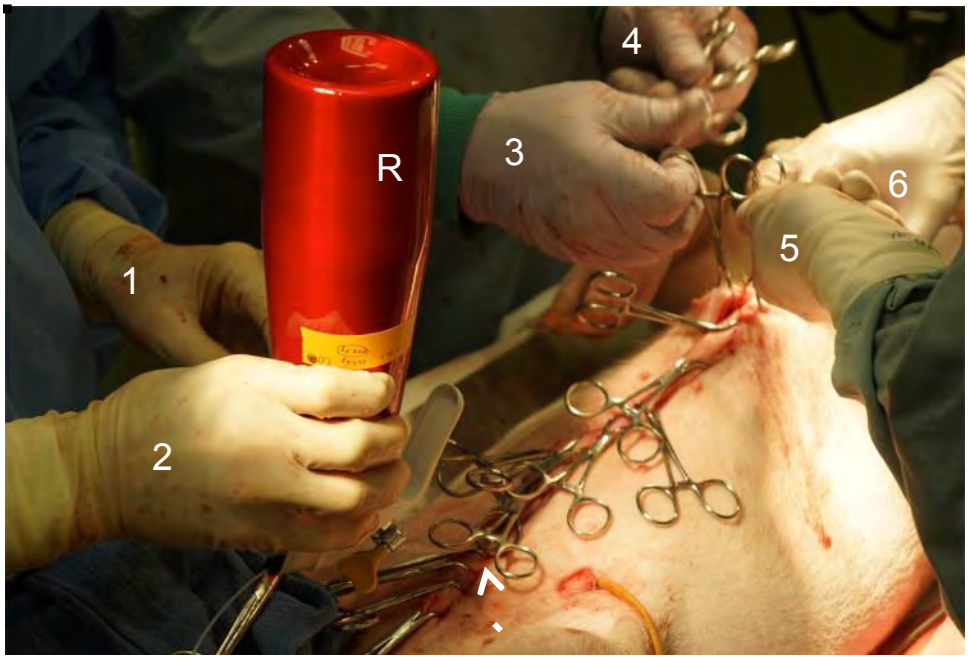

Fig. 2, Swine 144. Foam injection after injury. Hand #2 is holding the reservoir (R) and injecting foam into the abdomen; arrow indicates nozzle entering abdomen between clips. Hands 3-6 are closing the superior portion of the ventral midline incision with clips. Head is to the right of the image.

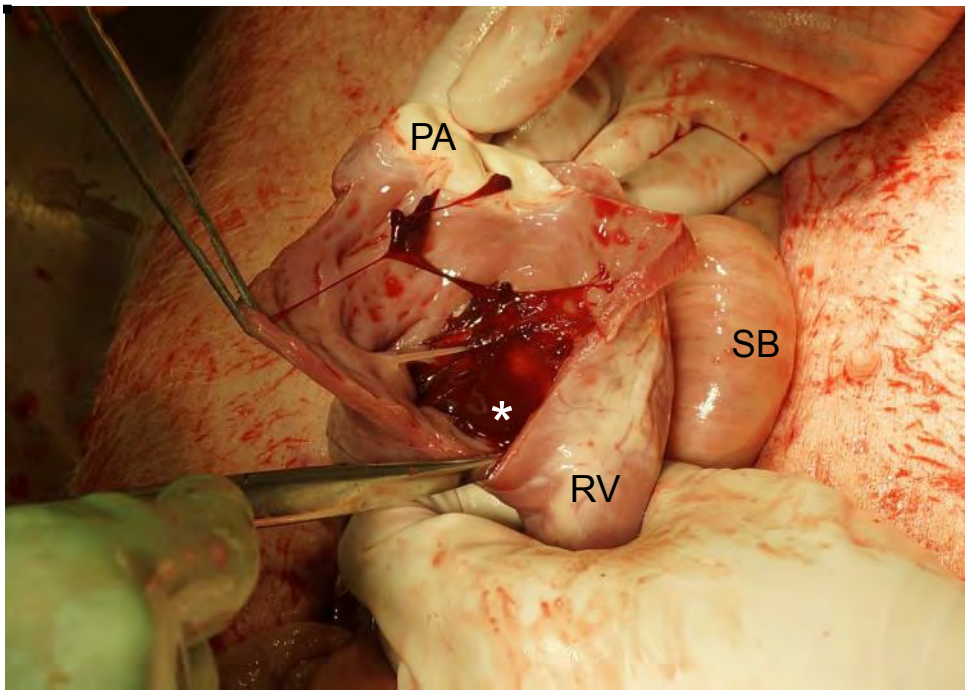

Fig. 3, Swine 144. Postmortem cardiac examination. Heart has been excised through a left anterior thoracotomy, and placed upon the abdomen for exam. There was clot (asterisk) present inside the right ventricle, but no foam. RV = right ventricle (external surface); PA = pulmonary artery; SB = small bowel.

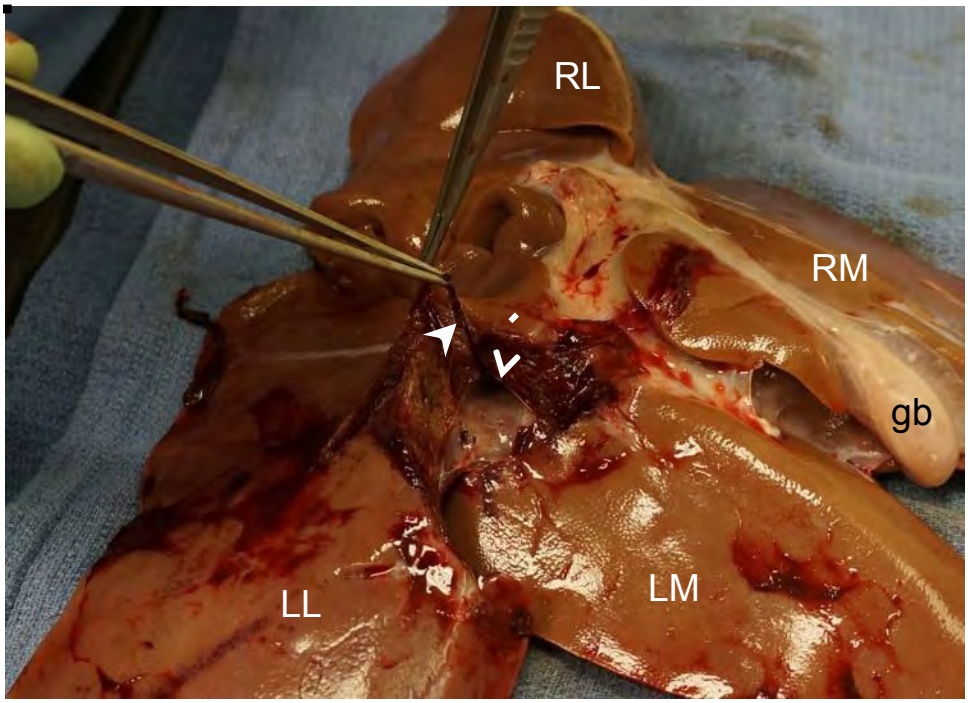

Fig. 4, Swine 144. Postmortem liver examination, inferior aspect, left lateral view. The injury was made too proximal, cutting into the confluence of the hepatic veins (arrow) draining the left lateral (LL) and left medial (LM) lobes. Forceps is pulling a clot (arrowhead) out of the transected vein.

I. OVERVIEW
Date: June 27, 2013
Swine no: 164
Model: swine, normothermic, normovolemic noncompressible hemorrhage; PV + HV injury
Treatment: Calcium alginate foam without dye; + FI/FII/FXIII
Personnel: Carlson, Yanala, Heimann, Hansen, Noriega, Calcaterra, Fatemi, Vanderslice, Ismail

---

II. PRE-INJURY PHASE

Start time: 9:35 AM
Swine sex: male
Date swine received from UNL Mead: 06/24/2013
Pre-procedure wt: 33.4 kg

Anesthetic Induction: Telazol (4.4 mg/kg), Ketamine (2.2 mg/kg), Xylazine (2.2 mg/kg), given as single IM shot
Anesthetic maintenance: 0.5-1.0% inhalational isoflurane

Lines/tubes/monitors/support
1. Endotracheal tube with ETCO2 monitor
2. EKG clips
3. Left ear vein angiocath (20g) for supplemental LR
4. Right carotid artery angiocath (20g), cutdown; for BP monitor
5. Right jugular vein angiocath (16g), cutdown; connected to rapid infusion pump
6. Transabdominal cystotomy for 16 Fr Foley catheter
7. Rectal temp probe
8. Pulse oximetry
9. Heating pad below subject

Initial VS
- HR: 81
- MAP: 108
- Temp: 39.1

Blood draw no. 1 (initial): 9:49 AM (ABG, hematocrit/hemoglobin, PT/PTT, qualitative fibrinogen)

Splenectomy time: 9:57 AM
Spleen wt: 258 gm
LR (22°C) infused after splenectomy: 775 mL at 150 mL/min

Pre-injury fluid data:
- Blood loss (spleen weight + phlebotomies + incidental): 258 + 20 + 75 = 353 mL
- LR (22°C) infused (spleen replacement + incidental): 775 + 50 = 825 mL

Pre-injury VS
- HR: 82
- MAP: 112
- Temp: 38.0

III. INJURY & TREATMENT PHASE

Time of injury: 10:11 AM
Injury type: portal/hepatic vein injury, cut across base of left lower lobe (i.e., the "standard" injury for the noncompressible model). The scissors were applied in the cleft between the LM & LL lobes. Prior to the injury, the lower half of the ventral midline incision was closed with towel clips. The nozzle of the foam injector was inserted between these clips into the lower peritoneal cavity.
Treatment description: calcium alginate foam without dye, but containing fibrinogen, thrombin, and Factor XIII. This was applied with a creamer dispenser-based injection system which was supplemented with a calcium chloride solution via a syringe pump.
Clotting factors: pdFI (252 mg)/rFII/rFXIII.
Technique: with the lower half of the incision closed with towel clips and the nozzle in position, the target liver lobe was exteriorized through the upper half of the midline incision. The injury then was created as described above. Immediately after injury, the injured liver lobe was dropped back into the abdomen, and the upper half of the incision was rapidly closed with towel clips. Injection of the foam began 30 sec after injury, after the abdomen had been completely closed with clips. After injection completed (~1 min after injury), the nozzle was withdrawn and a final towel clip was placed in the space where the nozzle had been inserted. Abdomen became distended during injection.
Abdominal closure: "fully-closed" technique, as described above
Resuscitation target MAP: 90
Resuscitation fluid: warm LR (3.3 L preset maximum, or 100 mL/kg)
Time resuscitation fluid began: 10:12 AM

IV. POST-TREATMENT PHASE

Blood draw no. 2 (15 min post-injury): 10:26 PM

15 min post-injury VS
- HR: 142
- MAP: 42
- Temp: 37.6

Blood draw no. 3: (31 min post-injury): 10:42 AM (ABG, hematocrit/hemoglobin, PT/PTT, qualitative fibrinogen)

Final (33 min) VS
- HR: na
- MAP: 10
- Temp: na

Survival at 60 min? No
Target MAP attained? No
Time of death: 10:44 PM
Cause of death: exsanguination from injury ± cardiac embolism (see Figures)
Interval from injury to death: 33 min

Post-treatment fluid data:

- Blood loss (intraabdominal suctioning + pads/gauze + phlebotomy): 1747 + 1715 + 40 = 3502 mL
- IV fluid given: LR (37°C): 3250 mL

V. RE-EXPLORATION/POST-MORTEM PHASE

Findings upon abdominal/chest exploration: abdomen grossly distended and tense/firm. Rush of air (smelling like butane) upon re-opening of incision. White foam forming a layer that covered the intestines (see Figures); no mixing with blood; ++clots and fresh blood underneath the foam. Volume of foam removed was ~500 mL. When we transected the suprahepatic IVC during the liver explantation, there was a long occluding clot present within the IVC (see Figures).
Heart: upon opening the RV, there was a large red thrombus (but no foam) within the RV (see Figures).
Number of hepatic veins lacerated: one, at base of LL lobe.
Portal vein injury: two (1st & 2nd PV branches to LL lobe; see Figures)
Other: none.
Ex vivo total liver wt: 797 gm

Tissue harvested: nasal membranes.

VI. COMMENTS

First subject with noncompressible injury treated with alginate foam + biologics. Subject died at 33 min with 3.5 L blood loss. Interestingly, there was a large amount of clot in the IVC and the RV, suggesting that cause of death was not simply exsanguination. The clots in the heart & IVC were well-formed, and I would assume that the clots were made early on after injury, when the animal was making good clot on it own. Of note, these clots did not contain any foam.

Central venous embolism appears like it will be a persistent issue in this model. I suspect that this complication would be an issue in any large animal model in which there is a major venous injury. We probably were not seeing it in the cold hemodiluted model, because those animals were never forming clot on their own. Recently we have had two central venous embolisms in warm normovolemic subjects that consisted solely of endogenous clot, without any foam. So incidentally, the foam treatment is not necessarily the culprit in the embolisms that we have been seeing.

Also, we retrieved only ~500 mL of foam from the abdomen at the postmortem exam. I think that we need a higher volume of foam present, maybe 2 L, if this treatment is going to show some effect.

VII. PLAN

Next two subjects will be on Tue July 2, 2013 starting at 8 AM. We will be using the noncompressible model again, with foam treatment. This will give us an additional 2 subjects that we can insert into the Y2Q3 Quarterly Report to TATRC, which is due on July 11th.

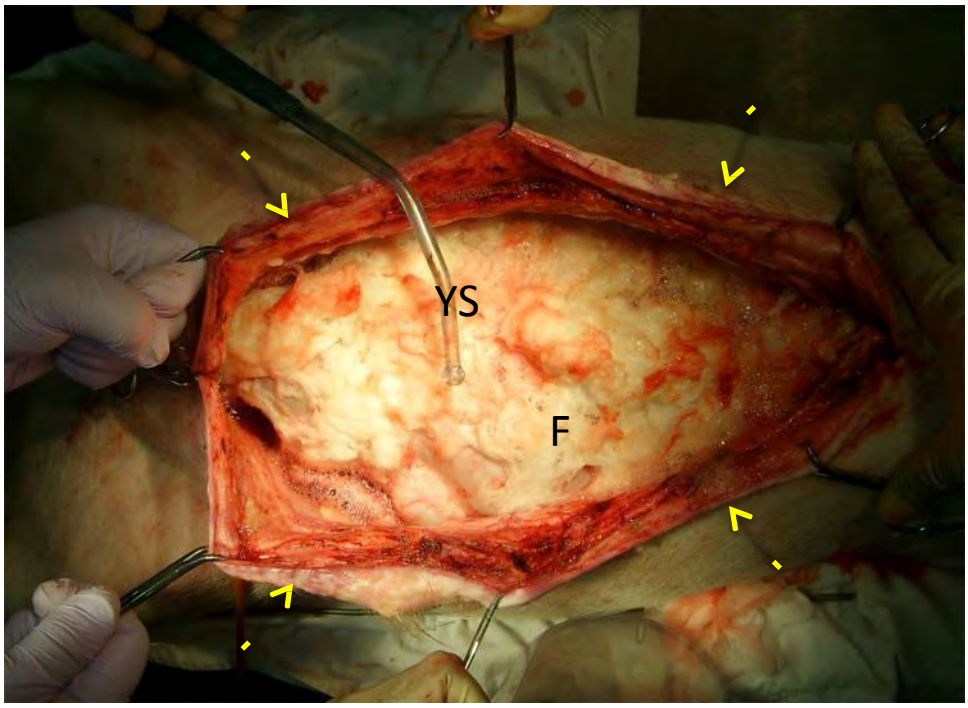

Figure 1, swine 164. Overhead view of the abdomen re-opened immediately after subject expired from hypotension. Cephalad is to the right. Arrows = margin of incision, stretched open. F = calcium alginate foam covering the intestines. YS = Yankaur suction tip.

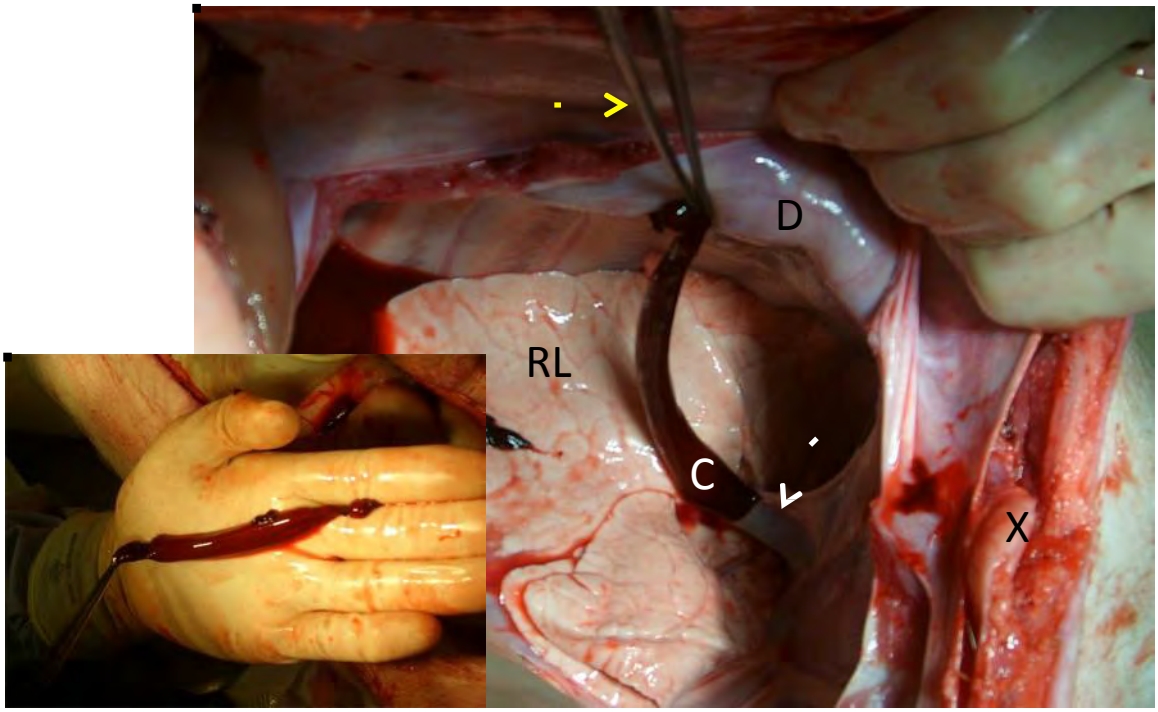

Figure 2, swine 164. View of the right chest at autopsy, showing a long tubular clot (C) being extracted from the intrathoracic inferior vena cava (white arrow) using a forceps (yellow arrow). RL = right lung; D = diaphragm; X = xiphoid process. Cephalad is to the right. Inset: extracted clot in palm of hand.

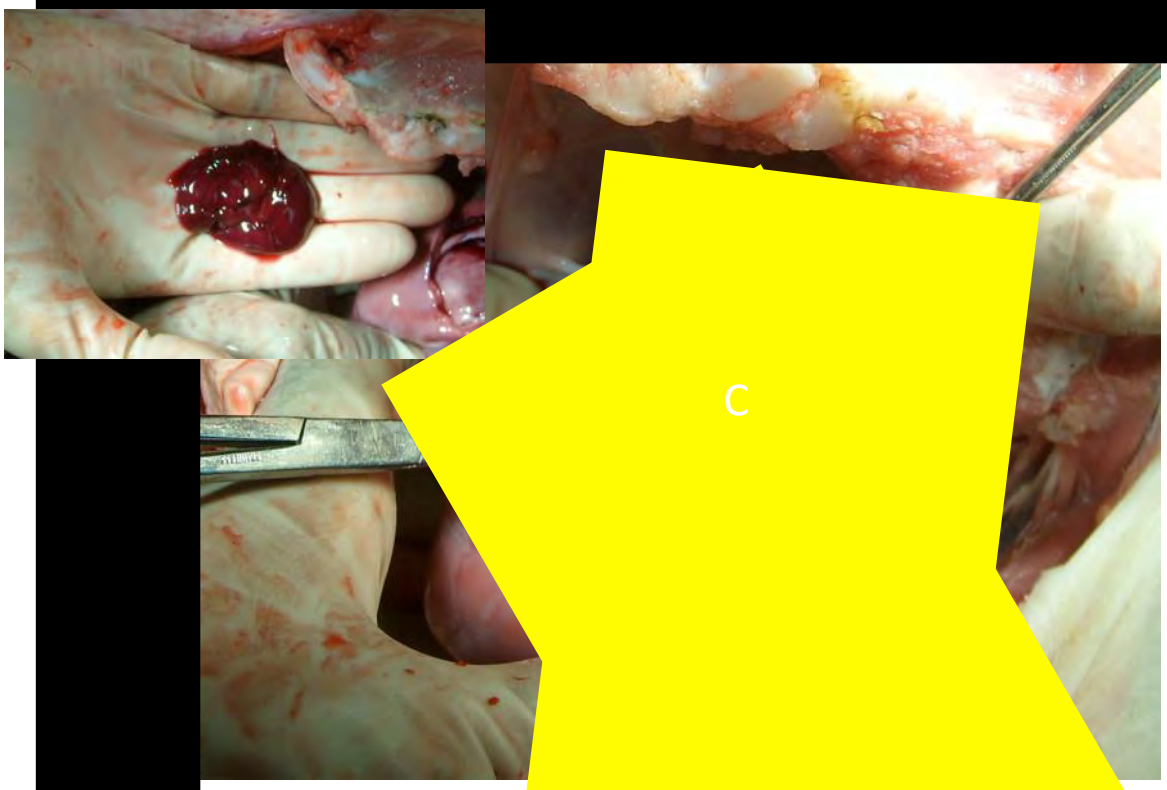

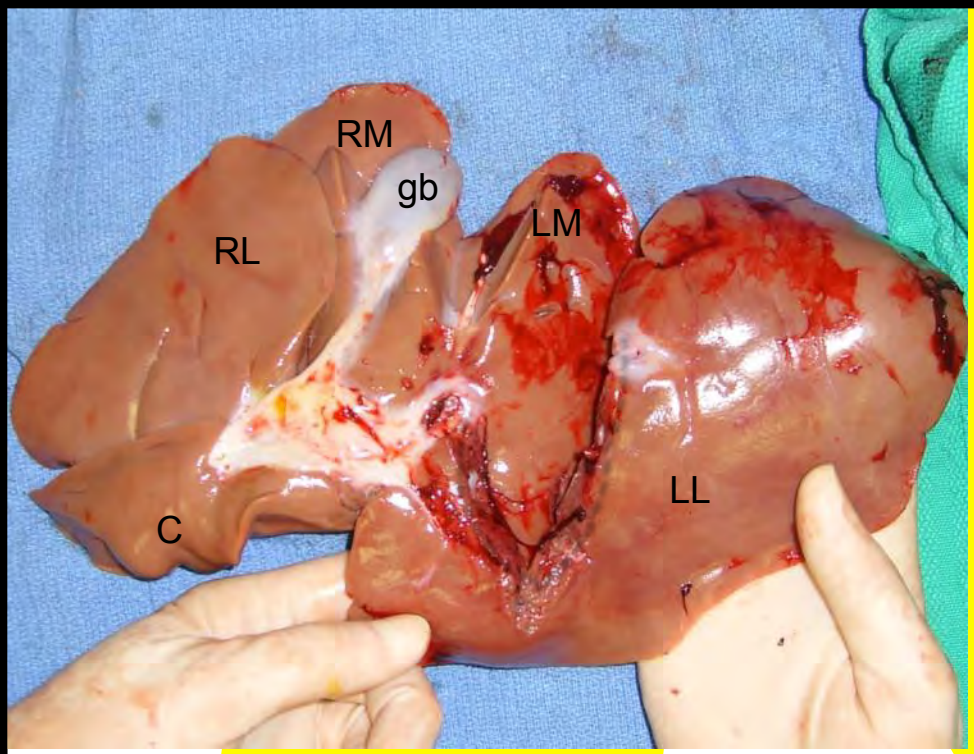

ine 164. Liver ex vivo (inferior aspect). Standard injury was made at base of LL lobe. C = be; RL = right lateral lobe; RM = right medial lobe; LM = left medial lobe; LL = left lateral gallbladder. Dotted blue line = outline of injury created in base of LL lobe.

2013 DEFENSE UNIVERSITY RESEARCH INSTRUMENTATION PROGRAM (DURIP)
PA-AFOSR-2013-0001

NARRATIVE

Proposal Summary

This 2013 DURIP submission proposes the purchase of an Instron model 5943 tensiometer (system price = $58,020). This instrument will support research in an active DoD project which studies hemostasis of severe exsanguinating injuries (project title: "Technologies for Hemostasis and Stabilization of the Acute Traumatic Wound;" award number: W81XWH-11-1-0836). Acquisition of this instrument will allow the project's PI (Mark A. Carlson) to study adhesion phenomena at the bandage-wound interface. This data will facilitate the design of a fibrin sealant bandage to treat hemorrhage from solid organ injury in a coagulopathic subject, thus allowing the PI to fulfill the Statement of Work for Specific Aim 2 of this project. In addition, the PI has some planned work on resorbable hernia mesh which will be the basis of a future DoD submission. In addition, the work enabled as a result of this DURIP would promote education of trainees in research areas that are of interest to the DoD. Since the proposed instrument would impact both the DoD-funded work and work intended for future DoD funding, and also educate trainees in DoD priority areas, the PI is pleased to submit this DURIP for acquisition of a tensiometer.

This proposal is intended for the following DoD program/division: Biochemistry (Stephanie A. McElhinny, Ph.D., Program Manager), Life Sciences Division, U.S. Army Research Office. The impact, importance and priority, education potential, and cost realism of this DURIP submission are described in the following four sections.

I. Impact

Two types of impact. The impact of the acquisition of the tensiometer described in this DURIP proposal will have two major types: (1) enhancement of the PI's research that currently is funded by the DoD; and (2) enhancement of capabilities in the PI's laboratory, which will facilitate research that is relevant to DoD areas of interest, and which will enhance the PI's ability to obtain future DoD funding.

The first impact type: the PI's funded DoD project. The first major type of impact regards a project currently funded by the DoD. The PI on this funded DoD project and the present DURIP proposal are the same. The details of the funded DoD project are as follows:

- Title: "Technologies for Hemostasis and Stabilization of the Acute Traumatic Wound"
- Principal Investigator: Mark A. Carlson
- Award/Contract No.: W81XWH-11-1-0836
- USAMRMC No.: 10091006
- Start Date: September 26, 2011
- End Date: October 25, 2015

- Duration: 4 years
- Total Funding: $5,033,983

There also are six Co-Investigators on this project: William Velander, PhD (a biomolecular engineer with expertise in clotting proteins); Gustavo Larsen, PhD (a materials engineer with expertise in synthetic polymers); Wilson Burgess, PhD (a biochemist); Jason Johanning, MD (a vascular surgeon); Iraklis Pipinos, MD (a vascular surgeon), and Grant Bochicchio, MD (a trauma surgeon). As mentioned above, the work of this funded DoD project primarily involves swine and benchtop experiments; no human subjects were intended for this project.

Objective of the PI's funded DoD project. The objective of the above funded project is to develop therapies for severe exsanguinating hemorrhage in the warfighter injured on the battlefield. The project is preclinical, utilizing porcine models. There are two types of hemorrhage addressed in this project by two separate Specific Aims: noncompressible truncal hemorrhage (Aim 1), in which the first-responder has no effective method of direct control [1-3]; and hemorrhage in a hypothermic hemodiluted (i.e., coagulopathic) subject (Aim 2), a condition commonly encountered in the severely injured subject who undergoes fluid resuscitation, evacuation, and emergent operation by a Forward Surgical Team [4, 5]. Research on both of these hemorrhage types have been identified as priorities by the United States Army, as discussed below under section II. The tensiometer proposed by this DURIP will provide data that will enhance the work performed under Specific Aim 2 (hemorrhage in the hypothermic hemodiluted subject). For reference, Aim 2 of the above funded project has been reproduced below:

> "Specific Aim 2. A hemostatic device consisting of a nano-engineered, low-density, nonexpanding synthetic mesh combined with human fibrin sealant components will be developed to treat experimental compressible traumatic hemorrhage under coagulopathic conditions. This device will be usable by someone with minimal training." [reproduced from USAMRMC No. 10091006]

Mechanism of the first impact type. The mechanism by which acquisition of the proposed tensiometer will impact the above funded project will be collection of *ex vivo* data that will facilitate the completion of the project's Statement of Work (SoW; reproduced in Table 1) that covers Specific Aim 2. For Aim 2, the SoW specified delivery of a resorbable bandage containing fibrin sealant for the treatment of hemorrhage in the hypothermic hemodiluted (i.e., coagulopathic) subject (see Table 1). During performance of the preclinical experiments specified by Aim 2, however, it became apparent that bandage prototype developed for this project would not be effective in treating coagulopathic hemorrhage in the swine model (discussed in detail below). This unforeseen failure of the bandage prototype necessitated planning for alternative prototypes. After extensive discussion, the PI and his Co-Investigators concluded that development and testing of new bandage prototypes directly in the swine model would be a slow and costly endeavor. Such experimentation would require a major revision to the SoW; furthermore, there likely would be insufficient funds within the project to study the required number of subjects (estimated to be more than 100) if swine were utilized as the primary mode of bandage testing. Therefore, an alternative method of bandage development was

conceived which would require *ex vivo* testing of bandage-tissue adhesion with a tensiometer (detailed below), thereby minimizing the number of swine needed. The PI and his Co-Investigators believe that the data obtained with the proposed tensiometer will guide the design of a new bandage prototype that will be able to treat coagulopathic hemorrhage, thus allowing the investigators to fulfill the project's SoW. Prior to discussing the proposed tensiometer experiments, more background details (including a description of the experimental animal model) will be provided below.

Table 1. Statement of Work (SoW) for the funded DoD project ("Technologies for Hemostasis and Stabilization of the Acute Traumatic Wound"). The relevant tasks for Specific Aim 2 are numbers 12-15 (high-lighted in yellow).

No.	Task description	Site	Year	Aim
1	Purification/generation of pd-FI and rFXIIIA2-a	UNL	1-3	1
2	Generation of ultrafine particles for tamponade carrier foam	LNK	1-3	1
3	Testing of candidate tamponade carrier & FS foams	LNK & UNL	1-2	1
4	Testing of single foams in swine (tamponade carrier & FS foams separately)	UNMC	2-3	1
5	Development & engineering of dual foam candidate devices	LNK & UNL	1-2	1
6	Testing of dual foam in swine	UNMC	2-3	1
7	Engineering of firm foams from alginate and alginate derivatives	LNK	2-3	1
8	Testing of dual foam in swine noncompressible model (laparotomy with 2° closure)	UNMC	3-4	1
9	Delivery of candidate field-ready dual foam device	UNL & LNK	3	1
10	Testing of dual foam in swine noncompressible model (closed penetrating wound)	UMM	3	1
11	Delivery of report on final recommended product description for dual foam device for treatment of noncompressible hemorrhage	LNK, UNL, UNMC, UMM	4	1
12	Delivery of resorbable bandage for final preclinical study in hypothermic coagulopathic model	LNK	1	2
13	Delivery of fibrin sealant for final preclinical study in hypothermic coagulopathic model	UNL	1	2
14	Final preclinical study of resorbable bandage in for hypothermic coagulopathic model (swine)	UNMC	1	2
15	Delivery of report on final recommended product description for resorbable fibrin sealant bandage for treatment of compressible coagulopathic hemorrhage	LNK, UNL, UNMC	2	2

The porcine model of hypothermic hemodiluted hemorrhage. This model, utilized in Specific Aim 2 of the funded DoD project as described above, was developed in the latter 1990's [6], and now is a standard for studying difficult-to-treat coagulopathic hemorrhage. In brief, the anesthetized domestic swine subject (3 months old, ~35 kg) undergoes an exchange of 60% if its blood volume (~1.5 L) with cold iso-osmolar fluid; this exchange induces hypothermia and depletion/dilution of endogenous clotting factors such that the subject develops a profound hypocoagulable (coagulopathic) state, demonstrable with coagulation testing. In other words, the subject is unable to form clot if a bleeding injury is incurred. The actual injury that is created in this model is a central liver laceration performed with a specialized scissoring clamp (Figure 1).

Untreated, the swine subjects in this manner expire from exsanguination in less than one hour. Treatment of this hemorrhage in this porcine model is extremely difficult, and has only been successful with application of large amounts of exogenous clotting factors [6, 7], which are not readily available. This porcine model of coagulopathic hemorrhage is intended to replicate the analogous clinical scenario in a severely injured trauma patient/warfighter who is hypothermic, hemodiluted, and unable to clot on their own, and who therefore has an unacceptably high mortality rate [4, 5].

Initial bandage prototype. The bandage prototype intended for the above model consisted of a matrix constructed from a synthetic polymer (polylactic acid, or PLA) which carried activated clotting proteins. The PLA matrix was electrospun with fiber diameter and pore size that were engineered at the nanoscale level [8, 9], and treated with a surfactant to increase the hydrophilicity of the fiber surface. Immediately prior to treatment, the PLA matrix was wetted with specific amounts of three clotting factors: (a) fibrinogen, or Factor I; (b) activated thrombin, or Factor IIa; and (c) activated Factor XIII (cross-linking factor). These three factors (along with added calcium ion) provide a "minimum" combination of coagulation factors which produces a rapid and strong clot [10-12]. Clinically, this combination of clotting factors is know as fibrin sealant or fibrin glue [10-12]. Extensive *in vitro* work, primarily with thromboelastography (TEG), was done to optimize the relative amounts of each factor in the bandage formula [10, 12]. That is, TEG was utilized to maximize clotting speed and strength while using the minimum amount of clotting proteins.

Failure of the prototype during* in vivo *testing. Initial testing of the above bandage prototype on the standardized central liver injury in the porcine hypothermic hemodiluted model (N = 5 swine) resulted in hemostatic failure in all cases (i.e., each subject bled to death within an hour). The details of this testing have been documented in the project's Quarterly Reports (available upon request). The porcine experimentation for this Aim of the project subsequently was halted in favor of discussion and planning among the project's Investigators. The basic mechanism of bandage failure in each of the five subjects was a lack of adhesion between the bandage prototype and the liver injury (see Figure 2). Without adhesion at the bandage-wound interface, it is virtually impossible to obtain hemostasis. The unpublished observations of the PI's group on the coagulopathic liver injury have indicated that without bandage adhesion, ongoing flow of blood simply will push the bandage away from the wound, even after long periods of manual compression. Unfortunately, analysis of *in vitro* clotting efficacy with TEG does not provide any information on the ability of a clotting formulation to adhere to tissue [13], so the extensive preliminary optimization studies done for this project [10] were not able to predict the *in vivo* failure of the bandage prototype.

Utility of the tensiometer. The advantage of having a tensiometer with respect to the above research problem is that the tensiometer would allow intensive study of adhesion at the bandage-tissue interface. Using discarded fresh liver obtained either from other porcine protocols at the Investigators' institution or from a local slaughterhouse, the tensiometer can be used to determine the ultimate tensile strength (UTS) of the bandage-tissue interface for multiple iterations of the fibrin sealant bandage. In other words, the strength of adhesion of the bandage to liver tissue can be tested in a large number of samples without the need for increasing the number of swine approved for use in the funded DoD project. Importantly, the bandage adhesion strength in these *ex vivo* experiments would be entirely dependent on bandage factors; since the liver tissue utilized would be *ex vivo*, there would be no contribution of endogenous porcine clotting factors. This distinction is highly relevant to coagulopathic liver injury model, in which

endogenous clotting is dysfunctional (i.e., almost nonexistent). In this injury scenario, the fibrin sealant component of the bandage has to "glue" the bandage to the wound in order for bandage adhesion and hemostasis to result. The data from this *ex vivo* tensile testing will guide the development of an improved hemostatic bandage that can be taken back and tested in the porcine coagulopathic liver injury model. This pathway should allow the Investigators to fulfill the SoW for Specific Aim 2 in their funded DoD project.

Proposed experiments utilizing the tensiometer (funded DoD project). As described in the preceding paragraph, acquisition of the tensiometer will permit the Investigators to undertake a large amount of *ex vivo* tensile testing. Iterations of the fibrin sealant bandage can be tested with adequate replicates such that statistical comparison of UTS values will be possible. Since more than one bandage characteristic ("factor") will require evaluation, a factorial design [14] will be utilized for the set-up of the tensile testing experimentation. The mean UTS values then can be compared across groups with ANOVA, which should determine whether individual factors have a significant effect on UTS, and whether there are factor interaction effects on UTS. The factors of bandage configuration to be tested will include clotting factor concentration, polymer type, polymer fiber diameter, and bandage pore size (a total of six factors). In order to keep the number of experiments manageable, only two levels of each factor will be utilized (e.g., a low *vs.* high value of fibrinogen). For six factors at two levels per factor, the number of experiments would be $2^6 = 64$. As an illustration of this strategy, a sample factorial design using just three factors (fibrinogen, Factor XIIIa, and fiber thickness) at two levels each ($2^3 = 8$ experiments) is shown in Table 2. If the tensile data from the factorial design produces a promising finding (e.g., strong adhesion with high fibrinogen concentration interacting with a large pore size), then additional experiments could be performed that would focus on these factors. If necessary, the PI will request a no-cost extension for his funded DoD project if the tensiometer experiments and subsequent animal testing cannot be completed prior to the project's end (October, 2015).

Table 2. Sample factorial design using three factor (FI concentration, FXIIIa concentration, and fiber thickness) at two levels per factor.

Exp No.	[FI]	[FXIIIa]	fiber
1	low	low	thin
2	low	low	thick
3	high	low	thin
4	high	low	thick
5	low	high	thin
6	low	high	thick
7	high	high	thin
8	high	high	thick

FI = fibrinogen; FXIIIa = activated Factor XIII. Relative values of factor indicated (low, high, etc.); specific values for each factor to be used in the actual experiments will be determined later.

The second impact type: development of a resorbable hernia mesh. In addition to the primary impact on the funded DoD project described above, the acquisition of a tensiometer by

the PI and his collaborators would have a secondary impact on project currently in the planning stages: the development of an economical, next-generation resorbable hernia mesh. The PI of this DURIP submission and his collaborators (working through LNK Chemsolutions, a small Nebraska business) submitted an SBIR grant to the NSF in June of 2013, entitled "Synthetic Resorbable Hernia Mesh Material" (NSF Proposal Number 1346030; PI = Ruben Spretz). The utility of the tensiometer in this planned project would be to generate data that would facilitate the optimization of the *in vivo* degradation rate of the hernia mesh. A critical characteristic of resorbable hernia mesh is the rate at which the mesh loses tensile strength *in vivo* [15]. If the mesh loses tensile strength too quickly, then its utility as a tissue replacement is limited; if the mesh degrades too slowly, then the risk of mesh-associated complications (e.g., infection, erosion) may be increased [16]. Furthermore, different clinical scenarios will require hernia mesh with different degradation characteristics. Of note, a novel aspect of the above NSF proposal is the development of a resorbable hernia mesh which would have an externally-adjustable rate of degradation; this feature would be controlled with an external low-energy power source. This would permit the clinician to adjust the strength and degradation rate of the hernia mesh after it had been implanted, depending on the needs of the clinical situation.

Proposed experiments utilizing the tensiometer (NSF proposal). The acquisition of the tensiometer described in this DURIP proposal would allow collection of UTS data that would help the investigators to carry out the Specific Aims of the NSF proposal. Specifically, the UTS data will enable the investigators to fine-tune the construction of their resorbable hernia mesh such that the desired mesh degradation rate is achieved. Determination of mesh degradation kinetics can be accomplished with tensile testing of mesh materials which have been incubated in a simulated body fluid environment [17]. The prototype hernia mesh which was designed according to the *in vitro* testing subsequently will be tested in an animal model of abdominal wall replacement. This experimental design will minimize the animal requirements for developing a resorbable hernia mesh in the NSF proposal. It is relevant to note that the investigators on this NSF proposal intend to proceed with the hernia mesh experimentation at some level even if the proposal is not funded. In addition, this work likely will be the basis of a future submission for DoD funding, since the work is relevant to a DoD area of interest (discussed under section II below).

Description of the proposed tensiometer. The tensiometer specified for purchase in this DURIP proposal is an Instron Model 5943 Material Testing System (www.instron.com). In addition to the tensiometer unit, the system includes a computer with software, two load cells (10 N and 1 kN), pneumatic grips for non-slip gripping of wet tissue samples, and a sample submersion (BioPuls) bath, which eliminates the confounding effect of drying during tensile testing of wet specimens. The quoted price for the entire system, which includes installation, calibration, and training, is $58,020 (which is the total amount requested in this DURIP proposal). Of note, an Instron representative brought this system to the PI's laboratory on August 8, 2013 for a demonstration. During this demo, the system performed satisfactorily on the applications specified in this DURIP proposal. Specifically, the Instron unit was capable of measuring wet specimen forces of less than 1 grams force, with good precision. As a result of this demo, the Instron model 5943 tensiometer was identified as the target of this submission.

Interface of the proposed instrumentation with facilities. The Research Service of the Omaha VA Medical Center currently has two Instron tensiometers under the supervision of Dennis Chakkalakal, a colleague and collaborator of the PI's. The PI used one of Dr. Chakkalakal's instruments (an Instron 1011) to generate tensile strength data on a recent study of

murine incisional healing [18]. The two Instron units presently at the PI's facility, however, do not have the sensitivity necessary to measure bandage-wound adhesion forces which, for an adhesion area of 0.5 cm^2, will be mostly <20 grams force (unpublished observations). As mentioned above, the Instron 5943 tensiometer was sensitive enough to measure these low forces with good precision. The existing units also do not have submersion baths or pneumatic grips. So the proposed addition of the Instron 5943 tensiometer to the Research Service will complement the existing instrumentation by providing the ability to measure low forces in submerged tissue specimens with pneumatic grips (i.e., exactly what is needed for the experiments outlined above); these tasks cannot be achieved with the current instrumentation. In addition, the Omaha VAMC has local expertise with Dr. Chakkalakal, with whom the PI can consult regarding technical aspects of tensile testing. So the instrumentation described in this DURIP proposal will mesh well with the PI's facility.

Ongoing or proposed support facilitated by the instrumentation. As described above, the acquisition of the tensiometer will enhance the PI's work on hemostasis that currently is funded by a DoD grant (total amount = $5.03 M). In addition, the tensiometer would be used to collect data on resorbable hernia mesh for an NSF SBIR grant (total Phase I amount = $150,000) that currently is under review. The latter data also would be used to submit for a future DoD grant in the field of biomaterials and hernia surgery.

Special circumstances regarding the instrumentation. The Instron 5943 is small and light enough such that it may occupy any reasonably stable benchtop. No special installation, plumbing, or electronic requirements exist, other than having a surface that is not subject to shaking or severe vibrations. The instrument is portable from room to room with modest effort. The estimated useful life of the instrument is at least 10 years (www.instron.com). For reference, the 1011 Instron that the Omaha VA owns is 23 years old, and still functions well.

II. Importance and Priority

Overview. As discussed in section I, the acquisition of the tensiometer described in this DURIP proposal will impact (i) the PI's ongoing, funded DoD project on hemostasis and (ii) the PI's proposed research on resorbable hernia mesh. The importance of these two research areas to the DoD and the priority that the DoD has placed on these areas is discussed below. Of note, the PI had a telephone consultation with Dr. Stephanie A. McElhinny on September 25, 2013, and some of the following aspects of the importance and priority of this DURIP proposal were discussed.

Importance and priority of the PI's funded DoD project. The DoD, and particularly the Army, has had heightened interested in the science and applications of hemostasis since the Vietnam War [19-21]. Since the 1990's, the DoD has placed particular emphasis on two vexing problems in hemostasis: (1) noncompressible truncal hemorrhage [1-3, 22, 23] and (2) coagulopathic hemorrhage [4, 5, 22, 23], sometimes know as the coagulopathy of trauma, and described as a component of the "fatal triad of trauma," i.e., hypothermia, acidosis, and coagulopathy [24, 25]. As described above, the PI's funded DoD project has an Aim devoted to each of these two hemostasis problems; the tensiometer would heavily impact the performance of that Aim (no. 2) which deals with coagulopathic hemorrhage. So the DoD has demonstrated an ongoing interest in research on the control of severe hemorrhage. With regard to the Army Research Office, the work of the PI's funded DoD project is aligned with the ARO's research priorities (per the 2012-2017 ARO BAA) in that the PI and Co-Investigators will be dissecting

the adhesion phenomena at the wound-bandage interface, and then use this information to engineer an improved version of the fibrin sealant bandage for injury treatment in the coagulopathic patient. That is, the data from this work will illuminate interactions at the interface between a biologic and a synthetic surface, which is relevant to the following ARO statement of priority (yellow high-lights were added for this DURIP proposal):

> "Of particular interest are studies exploring the controlled organization of biomolecules at the nanoscale, the integration of biomolecules with synthetic materials or systems, and innovative approaches for supporting biological activity outside of the cellular environment and in non-aqueous conditions." [ARO BAA For Basic and Applied Research, 15 May 2012 – 31 March 2017; 8.1 Biochemistry, p. 40]

In Aim 2 of the funded DoD project, the PI and his Co-Investigators intend to develop a synthetic nano-engineered bandage containing biomolecules (i.e., clotting factors) that will successfully integrate with and adhere to an injured tissue interface. This goal fits the ARO priority excerpted above.

Importance and priority of the PI's proposed research project. Research into biomaterial applications also has been a longstanding interest of the DoD, particularly as it relates to stabilization and reconstruction of the injured warfighter (refer to the Broad Agency Announcements released by the US Army Medical Research and Material Command in recent years, e.g., BAA 11-1, BAA 12-1, and BAA 13-1). Resorbable hernia mesh is an important component in the surgeon's armamentarium for the treatment of contaminated abdominal wall defects and other acute tissue loss in trauma patients, including the injured warfighter [26-28]. So the PI's proposal on resorbable hernia mesh currently under review at the NSF will be relevant to the longstanding interest of the DoD in biomaterials for tissue replacement. The work that comes out of this NSF proposal should form the basis for a future DoD proposal on abdominal wall biomaterials. With regard to the ARO, the PI's proposed work on resorbable hernia mesh is aligned with the ARO's research priorities in that this work will advance the field of biomaterials with novel designs in resorbable hernia mesh that ultimately will give the army surgeon better options when faced with severe traumatic injuries and tissue loss. Two statements of priority from the 2012 ARO BAA which support this conclusion are as follows (yellow high-lights were added for this DURIP proposal):

> (i) "The results of fundamental research supported by this division are expected to enable the creation of new technologies for optimizing warfighters' physical and cognitive performance capabilities, for protecting warfighters, and for creating new Army capabilities in the areas of biomaterials, energy, logistics, and intelligence." [8.0 Life Sciences, p. 39]

> (ii) "materials enhancement theory (e.g., developing a robust understanding of the interrelationships between materials processes and compositions and the range of properties that can be attained by them, particularly in terms of developing new materials theory capable of predicting such processing-property relationships and identifying novel mechanisms for enhancing specific toughness, engineering and synthesizing new materials containing unique and specifically designed chemical and biological

functionalities and activities while maintaining, and preferably enhancing, requisite mechanical properties)." [9.2 Mechanical Behavior of Materials, p. 43]

The second high-lighted passage is particularly relevant to the NSF proposal goal in which a resorbable hernia mesh will be engineered whose strength and degradation can be modified in the postoperative period, using an external low-energy power source. So the intended work of the NSF proposal also is supported by the stated ARO priorities.

III. Education Potential

The education potential that would be engendered by the acquisition of the tensiometer in this DURIP proposal would include the education of medical students, graduate students, and postdoctoral associates in the research areas impacted by the instrument, as described in section I. Specifically, all planned work utilizing the proposed tensiometer in the PI's laboratory will be carried out by a graduate student and/or postdoctoral associate. The personnel currently on the PI's funded DoD project include four graduate students and two postdoctoral associates. In addition to these personnel, the PI routinely has 1-2 medical students working in his laboratory during the summer months. One of the goals of PI's funded project and his planned project with hernia mesh will be to train these personnel in the areas of research that are of interest to the DoD. These areas include severe hemorrhagic injury, interactions of biomolecules with synthetic materials, nanoengineered materials, and biomaterials, as described in section II. Specifically in regard to this DURIP proposal, the PI estimates that over the initial four years after acquisition of the tensiometer, 4-6 trainees will become competent in the performance of tensile testing and the associated experimental design and data analysis. So funding of this DURIP proposal will promote the education of trainees in areas of research that are of interest to the DoD.

IV. Cost Realism

The PI obtained two competitive quotes for tensiometer systems for the purpose of this DURIP, one from Instron and the other from MTS (www.mts.com). Both quotes described comprehensive systems appropriate for the type of testing described in this proposal, and both quotes had a total price in the mid-$50K range. As described in section I, the PI was able to obtain an on-site demonstration for the Instron system, but there was not enough time prior to the DURIP due date to get a similar demonstration from MTS. Since the Instron system performed well at the demo, and since the two quotes were close in price, the PI decided to go with the Instron quote. So the cost of the Instron system appears to be competitive with the other major manufacturer of these devices. Any costs related to the instrument after its acquisition (e.g., supplies, routine maintenance, repairs, etc.) will be absorbed by the PI.

Literature Cited

1. Holcomb JB, McMullin NR, Pearse L, Caruso J, Wade CE, Oetjen-Gerdes L, et al. Causes of death in U.S. Special Operations Forces in the global war on terrorism: 2001-2004. *Ann Surg* 2007; 245(6): 986-91.
2. Kelly JF, Ritenour AE, McLaughlin DF, Bagg KA, Apodaca AN, Mallak CT, et al. Injury severity and causes of death from Operation Iraqi Freedom and Operation Enduring Freedom: 2003-2004 versus 2006. *J Trauma* 2008; 64(2 Suppl): S21-6; discussion S6-7.
3. Owens BD, Kragh JF, Jr., Wenke JC, Macaitis J, Wade CE, Holcomb JB. Combat wounds in operation Iraqi Freedom and operation Enduring Freedom. *J Trauma* 2008; 64(2): 295-9.
4. Eddy VA, Morris Jr JA, Cullinane DC. Hypothermia, coagulopathy, and acidosis. *Surg Clin N Am* 2000; 80(3): 845-54.
5. Thorsen K, Ringdal K, Strand K, Soreide E, Hagemo J, Soreide K. Clinical and cellular effects of hypothermia, acidosis and coagulopathy in major injury. *Br J Surg* 2011; 98(7): 894-907.
6. Holcomb JB, Pusateri AE, Harris RA, Reid TJ, Beall LD, Hess JR, et al. Dry fibrin sealant dressings reduce blood loss, resuscitation volume, and improve survival in hypothermic coagulopathic swine with grade V liver injuries. *J Trauma* 1999; 47(2): 233-40; discussion 40-2.
7. Delgado AV, Kheirabadi BS, Fruchterman TM, Scherer M, Cortez D, Wade CE, et al. A novel biologic hemostatic dressing (fibrin patch) reduces blood loss and resuscitation volume and improves survival in hypothermic, coagulopathic Swine with grade V liver injury. *J Trauma* 2008; 64(1): 75-80.
8. Larsen G, Velarde-Ortiz R, Minchow K, Barrero A, Loscertales IG. A method for making inorganic and hybrid (organic/inorganic) fibers and vesicles with diameters in the submicrometer and micrometer range via sol-gel chemistry and electrically forced liquid jets. *J Am Chem Soc* 2003; 125(5): 1154-5.
9. Loscertales IG, Barrero A, Marquez M, Spretz R, Velarde-Ortiz R, Larsen G. Electrically forced coaxial nanojets for one-step hollow nanofiber design. *J Am Chem Soc* 2004; 126(17): 5376-7.
10. Calcaterra J. Recombinant Factors For Hemostasis [PhD Thesis]. Lincoln: University of Nebraska–Lincoln; 2010.
11. Carlson MA, Calcaterra J, Johanning JM, Pipinos II, Cordes CM, Velander WH. A Totally Recombinant Human Fibrin Sealant. *J Surg Res* 2013, published online September 26, doi: 10.1016/j.jss.2013.09.039.
12. Calcaterra J, Van Cott KE, Butler SP, Gil GC, Germano M, van Veen HA, et al. Recombinant Human Fibrinogen That Produces Thick Fibrin Fibers with Increased Wound Adhesion and Clot Density. *Biomacromolecules* 2013; 14(1): 169-78.
13. Chandler WL. The thromboelastography and the thromboelastograph technique. *Semin Thromb Hemost* 1995; 21 Suppl 4: 1-6.
14. Freedman D. Statistical models: theory and practice: Cambridge University Press; 2009. ISBN 0521112435.
15. Bringman S, Conze J, Cuccurullo D, Deprest J, Junge K, Klosterhalfen B, et al. Hernia repair: the search for ideal meshes. *Hernia* 2010; 14(1): 81-7.

16. Amid PK. Classification of biomaterials and their related complications in abdominal wall hernia surgery. *Hernia* 1997; 1: 15-21.
17. Stamboulis A, Hench L, Boccaccini A. Mechanical properties of biodegradable polymer sutures coated with bioactive glass. *J Mater Sci Mater Med* 2002; 13(9): 843-8.
18. Carlson MA, Chakkalakal D. Tensile properties of the murine ventral vertical midline incision. *PLoS ONE* 2011; 6(9): e24212.
19. Pearl JP, McNally MP, Perdue PW. Femoral vessel injuries in modern warfare since Vietnam. *Mil Med* 2003; 168(9): 733.
20. Pilcher DB. Penetrating injuries of the liver in Vietnam. *Ann Surg* 1969; 170(5): 793.
21. Heisterkamp III CA, Simmons RL, Vernick J, Matsumoto T. Solid organ injuries in Vietnam: emergency hemostasis with n-butyl cyanoacrylate adhesive. *Arch Surg* 1970; 100(1): 109.
22. United States Army Institute of Surgical Research. Tactical Combat Casualty Care (TCCC) First Responder Conference, Tampa, FL. September, 2008.
23. United States Army Medical Research and Materiel Command. 2011 Broad Agency Announcment for Extramural Medical Research (USAMRMC BAA 11-1). http://wwwusamraaarmymil/pages/baa_paa/BAA_11_1/BAA 11-1pdf.
24. Ferrara A, MacArthur JD, Wright HK, Modlin IM, McMillen MA. Hypothermia and acidosis worsen coagulopathy in the patient requiring massive transfusion. *Am J Surg* 1990; 160(5): 515-8.
25. Moore EE. Staged laparotomy for the hypothermia, acidosis, and coagulopathy syndrome. *Am J Surg* 1996; 172(5): 405-10.
26. Jernigan TW, Fabian TC, Croce MA, Moore N, Pritchard FE, Minard G, et al. Staged management of giant abdominal wall defects: acute and long-term results. *Ann Surg* 2003; 238(3): 349-55; discussion 55-7.
27. Bellows CF, Alder A, Helton WS. Abdominal wall reconstruction using biological tissue grafts: present status and future opportunities. *Exp Rev Med Dev* 2006; 3(5): 657-75.
28. Latifi R, Leppaniemi A. Complex abdominal wall defects and enterocutaneous fistulae in the era of biological mesh: did we make any real progress? *World J Surg* 2012; 36(3): 495-6.

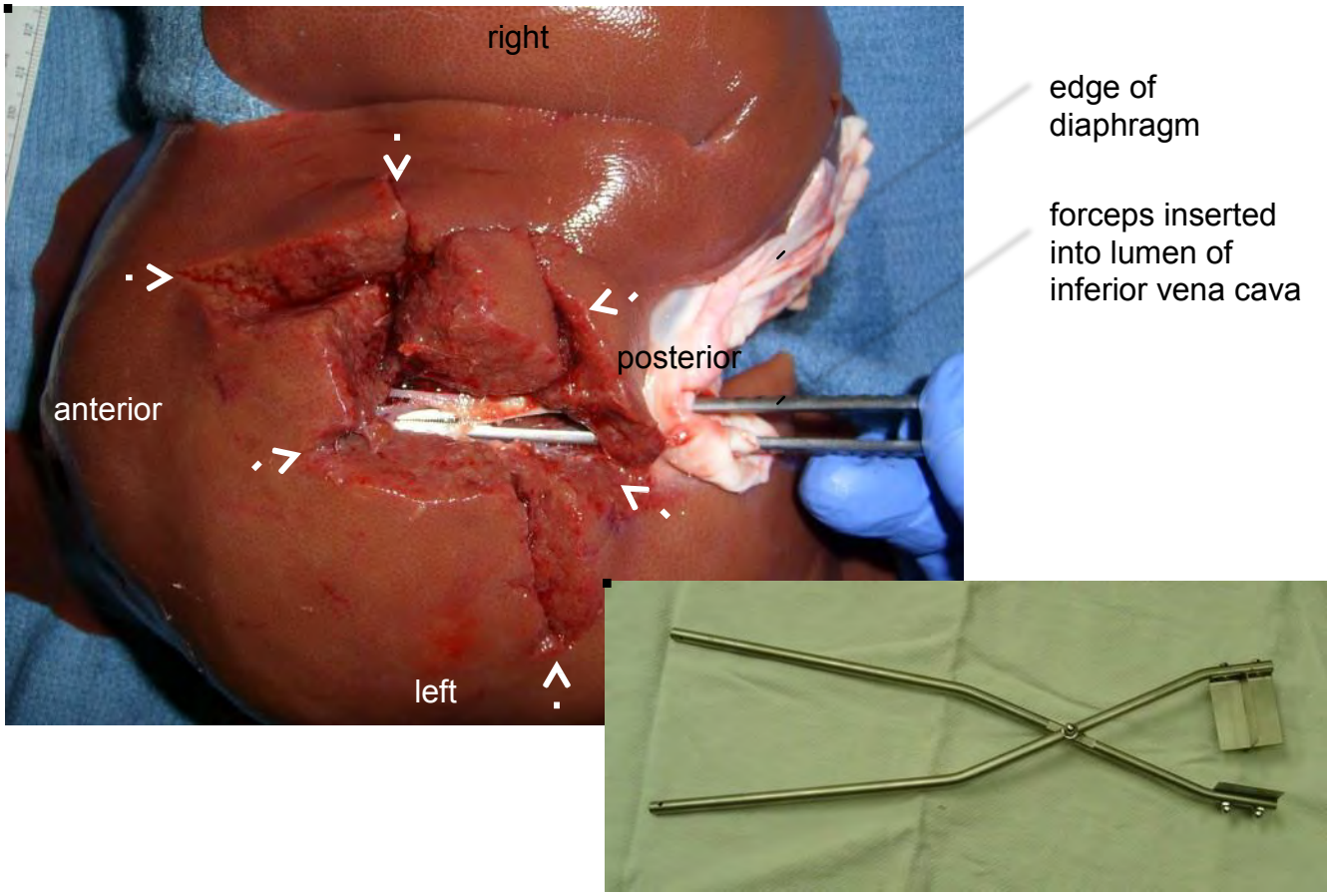

Figure 1. *Ex vivo* appearance of porcine liver after central injury. Superior or diaphragmatic aspect, showing dome of liver. The injury defect (arrows) was created with two adjacent applications of a customized liver injury clamp (lower right inset). Forceps visible within the injury indicate that the hepatic veins that drain into the intrahepatic vena cava were lacerated; this was an intended outcome of this injury. Scale (cm) at upper left.

This injury was created in a hypothermic hemodiluted pig, as described in the text. Without any treatment other than intravenous fluid administration (limited to 100 mL/kg), a coagulopathic subject with this injury will expire from exsanguination in less than one hour, as this subject did.

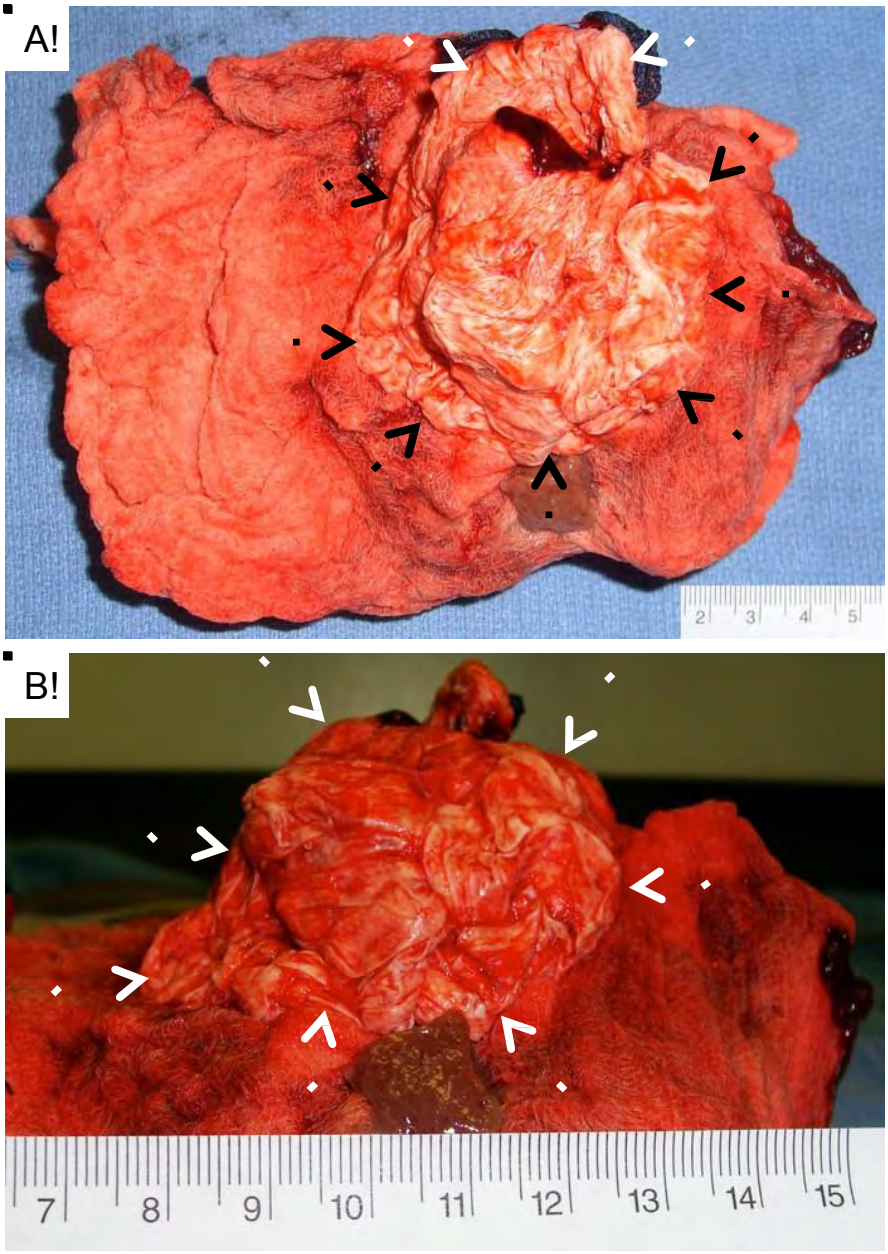

Figure 2. A failed dressing, shown *ex vivo*. A hypothermic hemodiluted (coagulopathic) pig underwent a laparotomy, and then a central liver injury similar to that shown in Figure 1 was created. The injury was treated immediately with a fibrin sealant bandage (i.e., a polylactic acid polymer wet with fibrinogen, activated thrombin, activated Factor XIII, and ionized calcium). The dressing was held firmly against the injury site with manual compression for 5 min. After this compression, the subject's laparotomy incision was closed. Despite high-volume fluid resuscitation, the subject expired in <30 min from exsanguination. All of the blood loss came from the liver injury; the peritoneal cavity contained >3 L of nonclotted blood. At postmortem examination, the fibrin sealant bandage (arrows) was observed to have formed a cast or plug of the wound defect, but there absolutely no adhesion between the bandage and the wound surface. Blood was flowing freely around the bandage. The bandage was removed intact from the subject's abdomen, and placed on a table for photography. The outcome in this swine represented a complete failure of this iteration of the fibrin sealant bandage. Scale in cm.

(A) Overhead view; arrows indicate the cast formed by the bandage (formed inside the cavitary liver injury).
(B) Side view, showing the 3D effect of the bandage cast.

BIOENGINEERING STRONGER FIBRIN SEALANTS: HETERO-DIMERIC γ/γ' FIBRINOGEN FROM NORMAL HUMAN PLASMA FORMS A ROOM TEMPERATURE STABLE COMPLEX WITH FIBRONECTIN

Ayman Ismail,[1] M.A. Carlson,[2] W.H. Burgess,[3] and W.H. Velander[1]

[1] Department of Chemical & Biomolecular Engineering, University of Nebraska---Lincoln, [2] University of Nebraska Medical Center, [3] LNK ChemsoluXons LLC.

IntroducXon

Plasma---derived fibrinogen (FI) and fibronecIn (FN) are important components for hemostasis and wound repair. FI and FN are both complex mulI domain proteins that are capable of binding a variety of plasma proteins and cellular surfaces. FI is cleaved by thrombin to generate fibrin which leads to the formaIon of an insoluble clot to achieve hemostasis. Ten percent of FI is the γ' hetero---dimeric subpopulaIon (γ/γ') and has several unique funcIonal aPributes arising from its 25 addiIonal amino acids on the carboxyl terminal of the gamma chain. FibronecIn is incorporated into the clot and serves to promote the aPachment and migraIon of cells to iniIate healing and regeneraIon.

FibronecIn is found as a consItuIve contaminant in FI preparaIons at 1---14%. Earlier studies showed that heparin could induce the formaIon of a cold---insoluble precipitate of fibrinogen and cold---insoluble globulin of plasma which is now known as FN. These studies showed that the binding of FI to FN was strong at 4°C but weak at 22°C and the Aα chain of fibrin/fibrinogen is required for this interacIon.

While purifying FI from normal human plasma, we observed a room temperature stable interacIon between a populaIon of FI and FN. Previously, this FI:FN complex has only been isolated from plasma from rheumatoid arthrIs palents. This study reports on the purificaIon and characterizaIon of the complex.

Methods

- FI and the FI:FN complex purificaIon and disrupIon:
  - IniIally purified from human plasma from healthy individuals by common cryoprecipitaIon and ammonium sulfate fracIonaIon methods.
  - Further fracIonated by ion exchange chromatography (DEAE Sepharose Fast Flow)
  - FI:FN complex disrupted by GelaIn Sepharose chromatography eluIng with 6 M urea
- *in vitro* tesIng :
  - SDS---PAGE gel electrophoresis and Western blot were used to idenIfy proteins and their subpopulaIons
  - High pressure size exclusion chromatography (HPSEC) was used to examine relaIve sizes of pure FI, pure FN and FI:FN complex.
  - Biacore was used to determine the binding characterisIcs of pure FI, pure FN and the FI:FN complex components
  - Thromboelastography was used to evaluate the ability of the FI:FN complex to form an insoluble fibrin clot.
  - Fibroblast recruitment and adhesion assay was used to test the biological acIvity of the FN component of the FI:FN complex.

Contact: W.H. Velander, wvelander2@unl.edu

Research was supported by a grant from the DoD

Results

We used a sequence of ammonium sulfate fracIonaIon and DEAE chromatography to isolate and purify a 1:1 stoichiometric complex of FI and FN from normal human plasma. The complex was stable at 4 to 37°C and could be disrupted into the separate FI and FN components by GelaIn Sepharose affinity chromatography. When analyzed by SDS---PAGE, FI was found to consist of enIrely of a heterodimeric γ/γ' FI species (Figure 1) which represented about 10% of original fibrinogen in the starIng normal plasma pool. Conversely, no γ'---chain containing FI was found in the remaining fibrinogen that was complex depleted.

SDS---PAGE

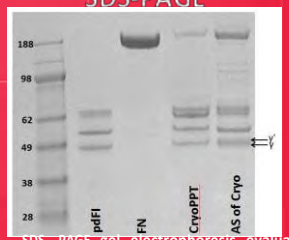

Figure 1. SDS---PAGE gel electrophoresis evaluaXon of FI purified by ammonium sulfate fracXonaXon. Lane 1: MW marker, Lane 2: FI (ERL), Lane 3: FN (ERL), Lane 4: FI:FN complex purified by ammonium sulfate fracXonaXon.

HPSEC showed that the γ/γ' FI:FN complex structure was monolithic and disInct from its purified component γ/γ' FI and FN (Figure 2). The γ/γ' FI: FN had a compacted structure that was slightly smaller in size to γ/γ' FI but larger than FN. HPSEC was also used to monitor *in vitro* reassembly of the disrupted complex: the γ/γ' FI and FN rapidly re---established the compacted complex. From 4 to 37°C, the solubility of γ/γ' FI:FN was considerably greater than γ/γ FI.

RelaXve Size of FI:FN Complex

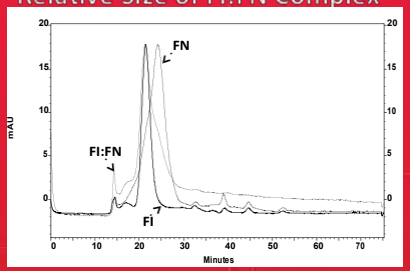

Figure 2. HPSEC evaluaXon of relaXve sizes of FI, FN and the FI:FN complex.

The γ/γ' FI: FN had enhanced clocng kineIcs and clot strength when measured by thromboelastography (Figure 3A). The fibrin clots made from γ/γ' FI: FN showed a biological acIvity of fibroblast and EC recruitment and adhesion *in vitro* approximaIng or exceeding that of fibrin made from γ/γ FI and FN (Figure 3B).

Biological AcXvity of FI:FN Complex

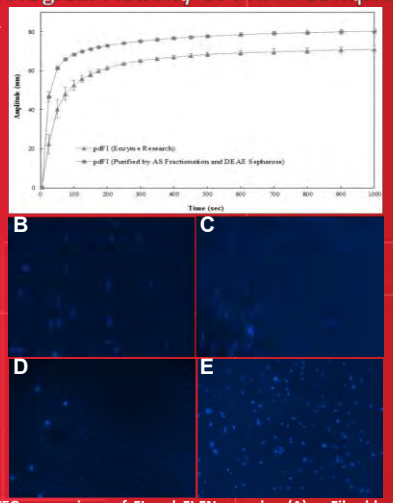

Figure 3. TEG comparison of FI and FI:FN complex (A). Fibroblast adhesion to polypropylene (B) and clots made with pure FI + pure FN (C), pure FI (D) and FI:FN complex.

Conclusions

1. A room temperature stable FI:FN complex exists in healthy human plasma.
2. The FI:FN complex consists enIrely of the γ/γ' FI subspecies.
3. The FI:FN complex similar in size to pure FI.
4. The FI:FN complex creates a stronger clot than pure FI.
5. Fibroblasts adhere bePer to clots formed by the FI:FN complex than pure FI.

These results provide the basis for the advanced study of the γ/γ' FI:FN for use in hemostasis and wound repair with potenIally unique and biological properIes and advantages of processing from normal plasma.